Identifying Xenobiotic Transporter Involvement in Complex Drug-Drug Interactions

by
Jasleen Sodhi

DISSERTATION
Submitted in partial satisfaction of the requirements for degree of
DOCTOR OF PHILOSOPHY

in

Pharmaceutical Sciences and Pharmacogenomics

in the

GRADUATE DIVISION
of the
UNIVERSITY OF CALIFORNIA, SAN FRANCISCO

Approved:

DocuSigned by:
Leslie Z. Benet
336FEDB181AF457...

Leslie Z. Benet
Chair

DocuSigned by:
Kathleen M. Giacomini

Kathleen M. Giacomini

DocuSigned by:
Adam Renslo
FBDB6299FCD244B...

Adam Renslo

Committee Members

ACKNOWLEDGEMENTS

Although the completion of a thesis dissertation typically represents the culmination of an individual achievement, none of the scientific advancements in the following pages would have been possible without the support of my mentors, family, friends and community. The gratitude I feel is beyond what can be expressed in this dedication.

This incredible experience can be entirely attributed to the unconditional support from my mentor Dr. Leslie Benet. Les has taught me that scientific boundaries are meant to be pushed and that basic assumptions should always be questioned, without which advancement within the field is not possible. His enthusiasm for understanding what has not yet been explained and his courage to challenge scientific dogma, all with the biggest smile and infectious laugh is inspiring and has given me the confidence to forge ahead. Thank you Les for being a great teacher, supporter, and friend.

Thank you to my mother Neetu Sodhi for her boundless love and support, who always welcomed me home with laughs, love and lots of delicious food to keep me happy and focused every week. You are the strongest woman I know, and every day I strive to be more like you. My brother Raj Sodhi is one of the smartest people I have ever known and I am lucky to call him my best friend. Thank you for providing me with encouragement and tons of fun over the past five years. Thank you to my father Ravi Sodhi for his fortitude and support. My grandfather Kuldip S. Sodhi taught me the importance of hard work and dedication from a very young age, and together with my grandmother Harminder K. Sodhi, have lovingly supported me in every way possible. To my grandmother Surinder K. Bakshi who taught me the importance of being a hard-working and independent woman, thank you for all your love, and to my grandfather Jagdish S.

Bakshi for watching over me. Thank you to my grandmother Bhupinder K. Bedi whose strength and love has always encouraged me since I was a young girl. To my grand-uncle Dr. Jaswant S. Uppal, who is the original Dr. Jas of the family; thank you for inspiring me to follow in your footsteps. I am fortunate to be a part of a family that fiercly supports one another despite any distance between us; thank you to the Ghais in San Diego, the Holdens and Bawas in California, the Bindras of California, Texas and Wyoming, and to all of my family in India.

Being a member of the Benet Lab family is an incredible honor, and a special thank you goes to Frances Peterson for ensuring that each member of this family is connected, supported, and loved. Your kindness is sincerely appreciated and has made my experience a wonderful one. Thank you to Dr. Hideaki Okochi and Alan Wolfe for the support and scientific discussions that have made me a better scientist. Thank you to all of my Benet lab colleagues for the memories, especially Dr. Christine Bowman, Dr. Rosa Chan, Shufang Liu, Dr. Hong-Jaan Wang, Shuaibing Liu, Wendy Kou, Dr. Yue Zhang, Dr. Ivan Kozachenko, Dr. Annette Chu, Caroline Huang, and Tsubasa Kameyama.

I would like to sincerely thank Dr. Deanna Kroetz for being a wonderful mentor even before I was a UCSF student; I would not have decided to pursue a PhD degree if it were not for her encouragement. A special thank you goes to Dr. Beau Norgeot and Julia Cluceru for their support and friendship, and for making UCSF feel like a home since the very first day. Drs. Kathy Giacomini and Adam Renslo, members of my thesis committee, provided me with incredible scientific guidance and encouragement. I would also like to thank Drs. Michelle Arkin, Nadav Ahituv, Laura Bull for their guidance and helpful discussions. Thank you to Dr. Janne Backman

from the University of Helsinki, Finland for the interesting scientific discussions that helped me advance my thesis research.

To all my mentors and friends at Genentech, thank you for the years of support, encouragement and collaborations. In particular, I would like to thank my mentor Dr. Jason Halladay for developing my interest and skills as a drug metabolism scientist, and for continuing to be a collaborator and friend. Drs. Cyrus Khojasteh, Jane Kenny and Marcel Hop further encouraged me to take this step and continuously supported me on many levels throughout the PhD. In addition, I would like to thank Jonathan Cheong, Emile Plise, Dr. Laurent Salphati, Jason Boggs, Jim Driscoll, Susan Wong, Dr. Ryan Takahashi, and Dr. Joseph Ware for encouraging me, teaching me, and supporting me as a new scientist in the field. There are more people to thank, more than I can include here, including all of my close friends that have been nothing but supportive.

I am grateful for the opportunity to do the science that I love.

CONTRIBUTIONS

Portions of Chapter 1 include contributions from “How Transporters Have Changed Basic Pharmacokinetic Understanding” published in September 2019, which was executed, analyzed and written by Leslie Benet with contributions from Jasleen Sodhi and Christine Bowman.

Chapter 2 is modified from “Volume of Distribution is Unaffected by Metabolic Drug-Drug Interactions” as it was accepted in the journal Clinical Pharmacokinetics in July 2020. Jasleen Sodhi and Leslie Benet contributed to the study design, which was executed and analyzed by Jasleen Sodhi and Caroline Huang. Jasleen Sodhi wrote the manuscript with contributions from Leslie Benet.

Chapter 3 is modified from “A Simple Methodology to Differentiate Changes in Bioavailability From Changes in Clearance Following Oral Dosing of Metabolized Drugs” as it was published in Clinical Pharmacology and Therapeutics in August 2020. Jasleen Sodhi and Leslie Benet contributed to the study design, performed the research, and analyzed the data. Jasleen Sodhi wrote the manuscript with contributions from Leslie Benet.

Chapter 4 is modified from “The Necessity of Using Changes in Absorption Time to Implicate Transporter Involvement in Oral Drug-Drug Interactions” as it was published in the AAPS Journal in August 2020. Jasleen Sodhi and Leslie Benet contributed to the study design, which was executed and analyzed by Jasleen Sodhi. Jasleen Sodhi wrote the manuscript with contributions from Leslie Benet.

Chapter 5 is modified from a manuscript entitled “Intestinal Efflux Transporters P-gp and BCRP Are Not Clinically Relevant in Apixaban Disposition” as it was published in Pharmaceutical Research in September 2020. Jasleen Sodhi and Leslie Benet contributed to the study design,

which was executed and analyzed by Jasleen Sodhi with contributions from Shuaibing Liu. Jasleen Sodhi wrote the manuscript with contributions from Leslie Benet.

Chapter 6 is modified from "Challenging the Relevance of Unbound Tissue-to-Blood Partition Coefficient (Kp_{uu}) on Prediction of Drug-Drug Interactions" as it was published in Pharmaceutical Research in March 2020. Jasleen Sodhi and Leslie Benet contributed to the study design, which was executed and analyzed by Jasleen Sodhi with contributions from Shuaibing Liu. Jasleen Sodhi wrote the manuscript with contributions from Leslie Benet and Shuaibing Liu.

Chapter 7 is modified from "Are There Any Experimental Perfusion Data that Preferentially Support the Dispersion and Parallel-Tube Models over the Well-Stirred Model of Organ Elimination?" as it was published in Drug Metabolism Disposition in July 2020. Jasleen Sodhi, Hong-Jaan Wang and Leslie Benet contributed to the study design and the analysis. Jasleen Sodhi and Leslie Benet wrote the manuscript with contributions from Hong-Jaan Wang.

Identifying Xenobiotic Transporter Involvement in Complex Drug-Drug Interactions

Jasleen K. Sodhi

ABSTRACT

Complex drug-drug interactions are defined as those in which both metabolic enzymes and xenobiotic transporters are implicated as clinically significant determinants of drug disposition. Both metabolic enzymes and xenobiotic transporters have the potential to contribute to clearance pathways (i.e. metabolic, renal or biliary elimination) and bioavailability-related processes (i.e. drug absorption, intestinal metabolism, or first pass hepatic elimination). Transporters have the unique ability to influence the distribution of drug throughout the body, in addition to influencing intestinal drug absorption or drug clearance via renal or biliary routes. Thus, characterization of the contributions of metabolic enzymes and xenobiotic transporters is crucial in anticipating any potential alterations in drug exposure due to a drug-drug interaction, pharmacogenomic or disease state variance of activity or expression of relevant metabolic enzymes or transporters.

Predictions of drug-drug interactions are routinely conducted based on results of *in vitro* metabolic enzyme or xenobiotic transporter inhibition studies. However, translating such results to clinical significance continues to challenge the field, particularly for transporter-mediated interactions since the susceptibility of a drug to transporters *in vitro* does not always translate to clinically significant *in vivo* involvement and due to a lack of specific and clinically validated index substrates, inhibitors and inducers for major xenobiotic transporters. The objective of this

research was to provide a framework for recognizing transporter involvement in clinical drug-drug interactions, grounded in basic pharmacokinetic theory.

Since xenobiotic transporters can allow (or disallow) substrates access to various tissues throughout the body, it was recognized that significant xenobiotic transporter interactions are accompanied by changes in volume of distribution, in addition to potential changes in clearance, which can result in counterintuitive changes in mean residence time and terminal half-life. Metabolic interactions are not expected to result in any volume of distribution changes and this hypothesis was extensively evaluated via examination of 72 intravenous metabolic drug-drug interaction studies with clinically recommended index substrates and inhibitors. The results indicate that volume of distribution is almost always unchanged in strictly metabolic interactions with marked exposure changes, resulting in changes in mean residence time and half-life that are equal but opposite to clearance changes, further highlighting that volume and clearance are indeed independent parameters.

Understanding that metabolic interactions do not result in volume of distribution changes can allow for estimation of bioavailability changes in oral drug-drug interactions, where the extent of change in apparent volume of distribution will reflect changes in bioavailability alone due to unchanged volume of distribution. Such estimates of changes in bioavailability can subsequently be utilized to differentiate changes in clearance alone from measures of apparent clearance following oral dosing. This approach can also be utilized to predict if an overall exposure change for oral drug-drug interactions is primarily due to changes in systemic clearance versus bioavailability.

To identify clinically significant intestinal transporter interactions, it was demonstrated that alteration of intestinal transporter activity or expression will result in significant changes in absorption rate, and such changes should always be used to implicate transporter involvement *in vivo*. Inhibition of apical efflux transporters result in decreased absorption time, as efflux transporter-mediated drug cycling between the enterocyte and gut lumen is prevented, while efflux transporter induction results in prolonged absorption time, as reflected in values of mean absorption time and time to maximum concentration.

Analyses of clinical data, such as examining changes in volume of distribution following intravenous dosing, changes in absorption rate following oral dosing, and examining the relationship between clearance changes and half-life and mean residence time changes, can confirm transporter involvement of purported complex drug-drug interactions. Such an approach was utilized to critically evaluate the purported clinical significance of the efflux transporters P-glycoprotein (P-gp) and Breast Cancer Resistance Protein (BCRP) in the disposition of apixaban, as has been indicated throughout the literature and even on the apixaban FDA label. Rational examination of all published apixaban clinical drug-drug interaction studies, using the proposed basic clinical pharmacokinetic methodologies, does not support the clinical significance of the efflux transporters P-gp nor BCRP in apixaban disposition. In fact, inhibition or induction of intestinal metabolism via cytochrome P450 3A4 (CYP3A4) can account for all exposure changes of clinically significant drug-drug interactions, and lack of intestinal CYP3A4 inhibition can explain all studies with no exposure changes.

Understanding the utility and limitations of experimental systems, as well as the inherent assumptions of the pharmacokinetic equations utilized to translate such results, is crucial in

translating *in vitro* or *in situ* experimental information to an *in vivo* prediction of drug disposition. For instance, there is limited benefit to using measurements of unbound liver-to-blood partitioning (Kp_{uu}) to improve predictions of drug-drug interactions, as DDIs can adequately be predicted by the Extended Clearance Model without any measurements of intracellular drug concentrations, a difficult task hindered by experimental variability. Further, the recognition that Kp_{uu} has inherently assumed the well-stirred model implies that such approaches cannot account for the nuances of intracellular drug distribution. Finally, recognition that clearance calculations based on extraction ratio have inherently assumed the well-stirred model further highlights the importance of understanding the assumptions inherent in basic pharmacokinetic relationships that are universally utilized to characterize clinical drug disposition.

TABLE OF CONTENTS

LIST OF FIGURES

LIST OF TABLES

CHAPTER 1. CHALLENGES IN THE PREDICTION OF XENOBIOTIC TRANSPORTER INVOLVEMENT IN COMPLEX DRUG-DRUG INTERACTIONS

Drug exposure, or the integrated measurement of drug concentrations over time, is considered the driving force for pharmacodynamic outcomes, such as the therapeutic efficacy or potential toxicity of a drug. Drug exposure (*AUC*) is inversely proportional to clearance (*CL*), a measure of the body's ability to remove drug, and directly proportional to bioavailability (*F*), the fraction of an extravascular dose that reaches systemic circulation intact:

$$AUC = \frac{F \cdot Dose}{CL}$$

Thus, *CL* and *F* are critical determinants of safe and efficacious dosing regimens. In drug-drug interactions, any alterations in *AUC* can lead to a loss of efficacy or safety of a victim drug, therefore, anticipation of the potential of a drug combination to alter *AUC* requires consideration of how both *CL* and *F* change. Predictions of *CL* changes are routinely conducted in drug discovery efforts, however, following oral dosing changes in extent of absorption or first pass extraction due to a drug-drug interaction may also result in significant *AUC* changes. Such *F* changes are often underemphasized as an important contributor in drug-drug interaction related exposure changes as compared to *CL* changes.

Drug disposition is reliant on the action of metabolic enzymes and xenobiotic transporters, both of which can influence the clearance and bioavailability of drug. Metabolic enzymes can contribute to the systemic elimination of drug while xenobiotic transporters can

influence both the distribution of drug throughout the body as well as its elimination via renal or biliary routes. Enzymes and transporters are expressed throughout the body including the intestine, thus having the potential to contribute to both clearance and bioavailability. Characterization of the contribution of enzymes and transporters to bioavailability and clearance pathways is crucial in anticipating any potential alterations in drug exposure due to a drug-drug interaction, pharmacogenomic or disease state variance of activity or expression of relevant metabolic enzymes or transporters. In this context, complex drug-drug interactions are defined as those in which both metabolic enzymes and xenobiotic transporters are implicated as clinically significant determinants of drug disposition.

Prediction of Metabolic- and Transporter-Mediated Drug-Drug Interaction Potential

In Vitro Prediction Methodologies

In order to predict metabolic- versus transporter-mediated clearance or drug-drug interaction potential, a number of *in vitro* studies are routinely performed in drug discovery and development efforts. For victim drugs, *in vitro* metabolic stability studies with human liver microsomes or hepatocytes can assess the potential for metabolic elimination, while the potential for transporter-mediated uptake or efflux can be evaluated using hepatocytes or transporter-overexpressing cell lines. To assess the metabolic inhibitory potential of a drug-of-interest, *in vitro* inhibition studies are routinely conducted against the major cytochrome P450 (CYP) isoforms to assess the reversible or time-dependent inhibition potential of new chemical entities. In addition, inhibitory studies with transporter probe substrates in hepatocytes or transporter-overexpressing cell lines can be performed to assess inhibitory potential against the

major xenobiotic transporters. Many important recommendations relating to evaluating metabolism-mediated and transporter-mediated drug interactions are been summarized by a Guidance prepared by the Food and Drug Administration (FDA) [1].

Biopharmaceutics Drug Disposition Classification System

The purported clinical involvement of transporters and/or enzymes is often based on results of the above mentioned *in vitro* investigations. However, it is further possible to contextualize such *in vitro* results to clinical significance, to allow for anticipation of which drugs may be susceptible to transporters *in vivo*, by utilizing the Biopharmaceutics Drug Disposition Classification System (BDDCS) [2]. BDDCS is a simple drug classification system based on permeability rate and solubility that can predict various drug disposition characteristics, such as major route of elimination and the clinically significant involvement of transporters (**Figure 1.1**).

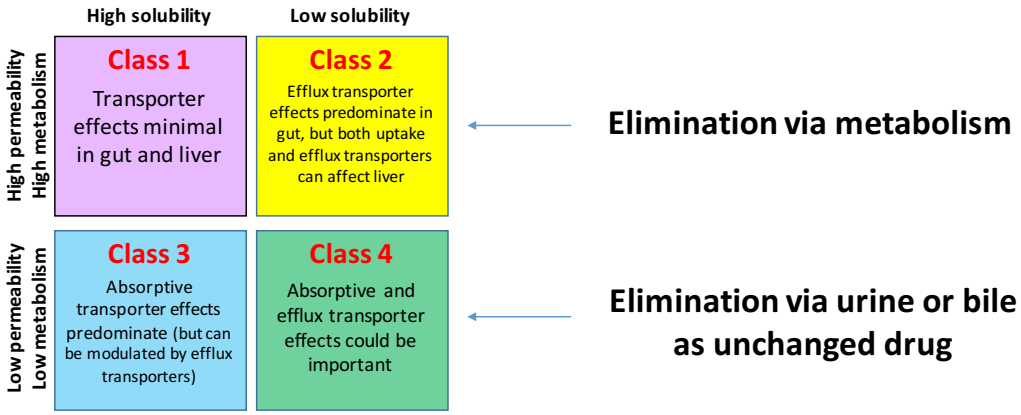

Figure 1.1: Transporter effects following oral dosing and major route of elimination predicted by the Biopharmaceutics Drug Disposition Classification System (BDDCS)

Due to the high solubility and rapid membrane permeability of BDDCS Class 1 drugs, it is theorized that these drugs can rapidly cross biological membranes at concentrations high enough to either saturate active transport, or render any transporter-mediated component to be only a minimal part of total membrane passage. Thus, the clinically significant involvement of transporters *in vivo* may be negligible, even if demonstrated to be a substrate in *in vitro* studies. The primarily metabolized BDDCS Class 2 drugs are also highly permeable, however due to their low solubility it is thought that (in some cases) the lower soluble concentrations available for passive diffusion may either be incapable of saturating transporters or passive membrane passage does not outweigh the active process. BDDCS Class 3 and 4 have unfavorable membrane permeability characteristics and thus rely on transporters to cross membranes, and this theory is supported by the fact that Class 3 and 4 drugs are primarily eliminated in the urine or bile (i.e. transporter-dependent processes) rather than being metabolized. Thus, results of *in vitro* predictions of elimination pathways (metabolism- versus transporter-mediated) can be considered in tandem with BDDCS theory in order to make conclusions on the clinical relevance of *in vitro* results.

Current Limitations in the Prediction of Transporter-Mediated Drug-Drug Interactions

Predictions of strictly metabolic interactions are considered reasonable to anticipate from *in vitro* studies [1] due to a strong understanding by the field of metabolizing enzymes that are commonly implicated in drug metabolism, that is further bolstered by well-characterized clinical specificities of routinely used metabolic inhibitors and inducers [3]. However, validation of transporter-mediated drug-drug interactions continues to pose significant challenges. Although regulatory agencies have recommended transporter substrates and inhibitors, there remains a

need for additional validated clinical transporter index substrates and inhibitors [3] and routinely-used inhibitors are often not specific and may have inhibitory potential towards both enzymes and transporters [4]. For example, rifampin is a commonly used *in vitro* and clinical inhibitor of several organic anion transporting polypeptide (OATP) transporters, however it also has the potential to inhibit CYP3A4 [3, 5, 6]. Upon multiple dosing, rifampin can strongly induce the expression of the efflux transporter P-glycoprotein (P-gp) and hepatic and intestinal CYP3A4, in addition to a number of other CYP isoforms [3, 5]. Rifampin has also been demonstrated to induce the efflux transporter Breast Cancer Resistance Protein (BCRP) *in vitro* [7], although the clinical relevance has not yet been established [7, 8]. In fact, the FDA has noted that improved *in vitro* experimental methodologies are required to evaluate the induction potential of P-gp and additional transporters, and pointed out that any such recommendations have been excluded from the most recent drug-drug interaction guidance [1]. Further complicating the situation is that additional xenobiotic transporters are continuously emerging and are suggested to be clinically relevant by the field [9], such as the hepatic uptake transporter organic anion transporter 2 (OAT2) [10] and the renal uptake transporter OATP4C1 [11], for which specific *in vitro* and *in vivo* index substrates and inhibitors will need to be identified and/or validated. Thus, significant advancement in *in vitro* methodologies to predict transporter interactions is required by the field.

In complex drug-drug interactions, those in which both metabolic enzymes and transporters have been implicated, prediction of exposure changes following oral dosing requires estimating how enzymes and transporters will affect both systemic clearance and bioavailability. Accurate estimation of the contribution of enzymes versus transporters is a difficult task, is

further complicated by the potential for enzyme-transporter interplay, and is a current area of significant efforts by the field [12, 13]. Due to the limitations of tools to detect and predict transporter-mediated interactions, it is of concern that a number of clinical investigations (and even approved drug labeling) have concluded that drug-drug interactions are transporter mediated based only on *in vitro* interaction potential and an observed change in *AUC*. This highlights the need for advancement of clinical pharmacokinetic theory to identify hallmarks of transporter involvement in interactions in which xenobiotic transporters are purported to be clinically significant determinants of drug disposition.

Clinically Significant Transporter Interactions Result in Changes in Volume of Distribution

Xenobiotic transporters can allow or restrict drug access to various tissues throughout the body. Therefore, it has been recognized that the function of transporters can influence a drug's volume of distribution (V_{ss}) [14]. Thus, significant xenobiotic transporter interactions are accompanied by changes in V_{ss}, in addition to potential changes in transporter-mediated *CL* [14, 15]. Drug half-life and mean residence time (*MRT*) are dependent parameters that reflect the influence of both *CL* and V_{ss}:

$$MRT = \frac{V_{ss} \,/\, F}{CL \,/\, F}$$

Therefore, it is expected that in drug-drug interactions in which volume is unaffected (i.e. strictly metabolic interactions), changes in *CL* will be accompanied by changes in *MRT* and half-life that are of similar magnitude, but opposite in direction. This hypothesis will be extensively addressed

in Chapter 2. For transporter drug-drug interactions, it is possible that changes in both *CL* and V_{ss} can result in counterintuitive changes in *MRT* and half-life. For instance, a reduction in drug *CL* that is accompanied by a shorter half-life, due to an even larger reduction in V_{ss}.

Our laboratory has very recently thoroughly documented the expected changes in pharmacokinetic parameters for interactions involving purely metabolic enzymes [16] versus xenobiotic transporters [15]. For a number of clinically significant transporter drug-drug interactions with the transporter substrates atorvastatin, rosuvastatin, pitavastatin and glyburide and the inhibitor rifampin (single dose), the magnitude of *MRT* and half-life changes are not predicted by changes in *CL* alone due to significant reduction in V_{ss} [15]. For atorvastatin [17] and rosuvastatin [18], decreased *CL* is associated with shorter *MRT* and half-life (rather than an increase that would be intuitively expected) due to an even larger decrease in V_{ss}. For pitavastatin [19] and glyburide [20], similar changes in *CL* and V_{ss} resulted in essentially unchanged *MRT* and half-life.

Conclusions: Thesis Aims

This thesis aims to provide a framework for recognizing transporter involvement in clinical drug-drug interaction studies, grounded in basic pharmacokinetic theory. The second chapter of this thesis extensively evaluates the hypothesis that in strictly metabolic interactions, volume of distribution remains unchanged. The analysis proceeded by examining 72 intravenous metabolic drug-drug interaction studies with clinically recommended index substrates and inhibitors of the major CYP isoforms. The results indicate that volume of distribution is largely unchanged in significant drug-drug interactions with marked changes in exposure. Further examination of

these results highlights that in metabolic drug-drug interactions, changes in *CL* result in changes in *MRT* or terminal half-life that are equal but opposite in direction, as would be expected for an interaction in which volume does not change, and further highlights that volume and clearance are indeed independent parameters.

With recognition that volume remains unchanged in strictly metabolic drug-drug interactions (based on the findings of Chapter 2), Chapter 3 further applies this knowledge in a methodology that allows for discrimination of bioavailability changes from clearance changes following oral dosing of metabolic DDIs. Since volume will remain unchanged in such interactions, changes in apparent volume of distribution at steady state (V_{ss}/F) can provide estimates of changes in bioavailability alone. The estimated bioavailability change can subsequently be utilized to predict changes in *CL* from observed changes in apparent clearance (CL/F). This approach can also be utilized to predict if an overall exposure change in an oral drug-drug interaction is primarily due to a change in systemic clearance or/and due to a change in bioavailability.

Chapter 4 describes another methodology that was developed to identify clinically significant intestinal transporter interactions. It was demonstrated that clinically relevant alteration of intestinal transporter activity or expression will result in significant changes in absorption rate, and such changes should always be used to implicate transporter involvement *in vivo*. Inhibition of efflux transporters results in decreased absorption time, as efflux transporter-mediated drug cycling between the enterocyte and the gut lumen is prevented, while efflux transporter induction results in prolonged absorption time, as reflected in values of mean absorption time and time to maximum concentration.

Chapter 5 demonstrates how the pharmacokinetic methodologies presented in Chapters 2-4 can be practically implemented to identify evidence of transporter involvement in purported complex-drug-drug interactions of apixaban. Throughout the literature and even on FDA approval documentation, apixaban has been implicated as a drug that is susceptible to the efflux transporters P-gp and BCRP [21], based only on *in vitro* results [22, 23]. However, we would suspect that the clinical significance may be questionable due to the BDDCS Class 1 designation of apixaban. The published apixaban clinical data were analyzed by examining the changes in volume of distribution following intravenous dosing (based on Chapter 2), changes in absorption rate following oral dosing (based on Chapter 4), and examining the relationship between clearance changes and half-life and *MRT* changes (based on Chapter 2). Further, the clearance versus bioavailability differentiation methodology presented in Chapter 3 was utilized to predict the major site of interaction for all orally dosed drug-drug interactions. The results of this analysis indicated that inhibition or induction of intestinal CYP3A4 metabolism can account for all exposure changes observed with clinically significant drug-drug interactions, and lack of intestinal CYP3A4 inhibition can explain all studies with no exposure changes.

Chapters 6 and 7 highlight the importance of understanding the limitations of *in vitro* or *in situ* systems, as well as the inherent assumptions of the pharmacokinetic equations utilized to translate such results. In Chapter 6 the unbound liver-to-blood partitioning coefficient (Kp_{uu}) is derived from first principles, highlighting that the relationship is based on the well-stirred model, which cannot account for the nuances of intracellular drug distribution. Although it has been suggested by the International Transporter Consortium that Kp_{uu} may improve drug-drug interaction predictions [24], simulations show that utilization of Kp_{uu} changes may not correlate

with changes in systemic or intraorgan drug exposure, and thus may mislead an investigator. It has been recently recognized that clearance calculations based on extraction ratio have inherently assumed the well-stirred model [25], thus all clearance calculations are model-dependent when drug concentrations entering and exiting an organ at steady-state are utilized. Chapter 7 critically reviews previously published isolated perfused rat liver studies for high clearance metabolized drugs for evidence of hepatic disposition model preference, concluding that the well-stirred model can describe all well-designed perfusion studies. The consequence of this analysis is our contention that the field has inappropriately interpreted a number of experimental studies by accepting models of the liver that are not consistent with the experimental data. Both Chapters 6 and 7 highlight the importance of understanding the assumptions inherent in the basic pharmacokinetic relationships that are universally utilized to characterize clinical drug disposition.

In summary, this thesis advances the clinical pharmacokinetic methodologies required to analyze complex drug-drug interaction studies, and in particular provides tools for clinical scientists to recognize clinically significant involvement of xenobiotic transporters. It further points out the importance of understanding the limitations of experimental systems, as well as the inherent assumptions of the pharmacokinetic equations utilized to translate *in vitro* or *in situ* results, in the successful prediction of *in vivo* drug disposition.

References

1. U.S. Food and Drug Administration, Center for Drug Evaluation and Research. In vitro drug interaction studies – cytochrome P450 enzyme- and transporter- mediated drug interactions guidance for industry. Silver Spring, MD; 2020.
2. Wu C-Y, Benet LZ. Predicting drug disposition via application of BCS: transport / absorption / elimination interplay and development of a biopharmaceutics drug disposition classification system. *Pharm Res*. 2005;22(1):11-23.
3. Tornio A, Filppula AM, Niemi M, Backman JT. Clinical studies on drug-drug interactions involving metabolism and transport: methodology, pitfalls and interpretation. *Clin Pharmacol Ther*. 2019;105(6):1345-1361.
4. Cheong J, Halladay JS, Plise E, Sodhi JK, Salphati L. The effects of drug metabolizing enzymes inhibitors on hepatic efflux and uptake transporters. *Drug Metab Lett*. 2017;11(2):111-118.
5. Niemi M, Backman JT, Fromm MF, Neuvonen PJ, Kivistö KT. Pharmacokinetic interactions with rifampicin. *Clin Pharmacokinet.* 2003;42(9):819-850.
6. Kajosaari LI, Laitila J, Neuvonen PJ, Backman JT. Metabolism of repaglinide by CYP2C8 and CYP3A4 in vitro: effect of fibrates and rifampicin. *Basic Clin Pharmacol Toxicol.* 2005;97:249-256.
7. Lemmen J, Tozakidis IEP, Galla H-J. Pregnane X receptor upregulates ABC-transporter Abcg2 and Abcb1 at the blood-brain barrier. *Brain Res.* 2013;1491:1-13.

8. Goreczyca L, Aleksunes LM. Transcription factor-mediated regulation of the BCRP/ABCG2 efflux transporter: a review across tissues and species. *Expert Opin Drug Metab Toxicol.* 2020;16(3):239-253.
9. Zamek-Gliszczynski MJ, Taub ME, Chothe PP, Chu X, Giacomini KM, Kim RB, Ray AS, Stocker SL, Unadkat JD, Wittwer MB, Xia C, Yee S-W, Zhang L, Zhang Y, International Transporter Consortium. Transporters in drug development: 2018 ITC recommendations for transporters of emerging clinical importance. *Clin Pharmacol Ther*. 2018;104(5):890-899.
10. Kimoto E, Mathialagan S, Tylaska L, Niosi M, Lin J, Carlo AA, Tess DA, Varma MVS. Organic anion transporter 2-mediated hepatic uptake contributes to the clearance of high-permeability-low-molecular-weight acid and zwitterion drugs: evaluation using 25 drugs. *J Pharmacol Exp Ther*. 2018;367(2):322-334.
11. Sato T, Mishima E, Mano N, Abe T, Yamaguchi H. Potential drug interactions mediated by renal organic anion transporter OATP4C1. *J Pharmacol Exp Ther*. 2017;362(2):271-277.
12. Alluri RV, Li R, Varma MVS. Transporter-enzyme interplay and the hepatic drug clearance: what have we learned so far? *Expert Opin Drug Metab Toxicol*. 2020;16(5):387-401.
13. Varma MV, El-Kattan AF. Transporter-enzyme interplay: deconvoluting effects of hepatic transporters and enzymes on drug disposition using static and dynamic mechanistic models. *J Clin Pharmacol*. 2016;56:S99-S109.

14. Grover A, Benet LZ. Effects of drug transporters on volume of distribution. *AAPS J*. 2009;11(2):250-261.
15. Benet LZ, Bowman CM, Sodhi JK. How transporters have changed basic pharmacokinetic understanding. *AAPS J*. 2019;21(6):103.
16. Benet LZ, Bowman CM, Koleske ML, Rinaldi CL, Sodhi JK. Understanding drug-drug interaction and pharmacogenomic changes in pharmacokinetics for metabolized drugs. *J Pharmacokinet Pharmacodyn*. 2019;46(2):155-163.
17. Lau YY, Huang Y, Frassetto L, Benet LZ. Effect of OATP1B transporter inhibition on the pharmacokinetics of atorvastatin in healthy volunteers. *Clin Pharmacol Ther.* 2007;81(2):194-204.
18. Wu H-F, Hristeva N, Chang J, Liang X, Li R, Frassetto L, Benet LZ. Rosuvastatin pharmacokinetics in Asian and White subjects wild type for both OATP1B1 and BCRP under control and inhibited conditions. *J Pharm Sci.* 2017;106(9):2751-2757.
19. Prueksaritanont T, Chu X, Evers R, Klopfer SO, Caro L, Kothare PA, Dempsey C, Rasmussen S, Houle R, Chan G, Cai X, Valesky R, Fraser IP, Stoch SA. Pitavastatin is a more sensitive and selective organic anion-transporting polypeptide 1B clinical probe than rosuvastatin. *Br J Clin Pharmacol*. 2014;78(3):587-598.
20. Zheng HX, Huang Y, Frassetto LA, Benet LZ. Elucidating rifampin's inducing and inhibiting effects on glyburide pharmacokinetics and blood glucose in healthy volunteers: unmasking the differential effects of enzyme induction and transporter inhibition for a drug and its primary metabolite. *Clin Pharmacol Ther*. 2009;85(1):78-85.

21. ELIQUIS (apixaban) [package insert]. Princeton, NJ: Bristol-Myers Squibb Company; 2012.

22. Jacqueroux E, Mercier C, Margelidon-Cozzolino V, Hodin S, Bertoletti L, Delavenne X. In vitro assessment of P-gp and BCRP transporter-mediated drug-drug interactions of riociguat with direct oral anticoagulants. *Fundam Clin Pharmacol*. 2020;34(1):109-119.

23. Zhang D, He K, Herbst JJ, Kolb J, Shou W, Wang L, Balimane PV, Han Y-H, Gan J, Frost CE, Humphreys WG. Characterization of efflux transporters involved in distribution and disposition of apixaban. *Drug Metab Dispos*. 2013;41(4):827-835.

24. Chu X, Korzekwa K, Elsby R, Fenner K, Galetin A, Lai Y, Matsson P, Moss A, Nagar S, Rosania GR, Bai JPF, Polli JW, Sugiyama Y, Brouwer KLR, International Transporter Consortium. Intracellular drug concentrations and transporters: measurement, modeling, and implications for the liver. *Clin Pharmacol Ther*. 2013;94(1):126-141.

25. Benet LZ, Liu S, Wolfe AR. The universally unrecognized assumption in predicting drug clearance and organ extraction ratio. *Clin Pharmacol Ther*. 2018;103(3):521-525.

CHAPTER 2: VOLUME OF DISTRIBUTION IS UNAFFECTED BY METABOLIC DRUG-DRUG INTERACTIONS[*]

Abstract

It has been recognized that significant transporter interactions result in volume of distribution changes in addition to potential changes in clearance (*CL*). For drugs that are not clinically significant transporter substrates, it is expected that drug-drug interactions (DDIs) would not result in any changes in volume of distribution. An evaluation of this hypothesis proceeded via an extensive analysis of published intravenous (IV) metabolic DDIs, based on clinically recommended index substrates and inhibitors of major cytochrome P450 (CYP) isoforms. Seventy-two metabolic drug interaction studies were identified where volume of distribution at steady state (V_{ss}) values were available for the CYP index substrates caffeine (CYP1A2), metoprolol (CYP2D6), midazolam (CYP3A4), theophylline (CYP1A2), and tolbutamide (CYP2C9). Changes in exposure (*AUC)* up to 5.1-fold were observed, however ratios of V_{ss} changes have a range of 0.70 – 1.26, with one outlier displaying a V_{ss} ratio of 0.57. These results support the widely-held founding tenant of pharmacokinetics that *CL* and V_{ss} are independent parameters. Knowledge that V_{ss} is unchanged in metabolic DDIs can be helpful in discriminating changes in *CL* from changes in bioavailability (*F*) when only oral dosing data are available. Since V_{ss} remains unchanged for IV metabolic DDIs, following oral dosing changes in V_{ss}/F will reflect changes in *F* alone. This estimation of *F* change can subsequently be utilized to assess changes

[*]Modified from the publication: Sodhi JK, Huang CH, Benet LZ. Volume of distribution is unaffected by metabolic drug-drug interactions. *Clin Pharmacokinet.* 2020; [E-pub ahead of print, July 28, 2020].

in *CL* alone from calculations of *CL*/*F*. Utilization of this simple methodology for orally dosed drugs will have a significant impact on how DDIs are interpreted from drug development and regulatory perspectives.

Introduction

Volume of distribution in pharmacokinetics (PK) is the theoretical volume in which a drug must distribute to relate the observed systemic drug concentrations to the amount of drug present in the body. It is a non-physiologic volume that reflects the degree of tissue distribution of drug. It has been recognized that xenobiotic transporters can influence the volume of distribution of drugs by allowing or restricting drug access to various tissues throughout the body [1], and therefore significant transporter drug interactions may result in changes in volume of distribution in addition to potential changes in clearance [2]. For drugs that are not clinically significant transporter substrates, it is expected that drug-drug interactions (DDIs) would not result in any changes in steady-state volume of distribution (V_{ss}). Knowledge that V_{ss} is unchanged in metabolic DDIs can be helpful in implicating transporter involvement in complex DDIs as well as in facilitating the discrimination of changes in clearance from changes in bioavailability when only oral dosing data are available. Here we present a comprehensive evaluation of the hypothesis that V_{ss} remains unchanged in metabolic drug interaction studies.

Methods

Literature Search Strategy and Inclusion / Exclusion Criteria

Based on a recent compilation of recommended clinical index substrates of major drug metabolizing enzymes and cytochrome P450 (CYP) isoforms [3], a comprehensive literature search identified caffeine (CYP1A2), metoprolol (CYP2D6), midazolam (CYP3A4), theophylline (CYP1A2) and tolbutamide (CYP2C9) as index substrates for which intravenous (IV) dosing drug interaction data were available. Oral drug interaction studies of these index substrates were

excluded from the analysis to avoid the confounding impact that changes in bioavailability (F) would have on apparent volume of distribution (V_{ss}/F). Due to the large number of IV interaction studies for the probe substrate midazolam, the scope of the analysis was further refined to primarily include DDIs involving index inhibitors with known clinical inhibitory specificities against the various CYP isoforms and xenobiotic transporters, again based on the recent recommendations of Tornio et al. [3]. If additional victim-perpetrator combinations were investigated in these studies, these interaction data were also included in the analysis and information regarding the *in vivo* substrate or inhibitory specificities of these drugs were referenced from the literature [4-10]. Since V_{ss} is not often reported by clinical investigators, estimation of this parameter often proceeded via digitization and non-compartmental analysis of published pharmacokinetic profiles. If V_{ss} was not reported, studies were excluded if (1) pharmacokinetic profiles were not reported and/or were difficult to reliably digitize, or if (2) resulting estimates of *AUC* were greater than 25% different from reported values. The latter aspect will be further discussed in the next section.

This analysis focuses on DDI studies conducted with the same subjects in the control and treatment arms, and as such, four midazolam studies with a parallel study design were excluded. However, some studies included in this analysis conducted the DDI investigation (within the same person) in multiple populations, for example, with respect to pharmacogenomic variance of drug metabolizing enzymes or in healthy versus disease state subjects. Thus, we also analyze changes in V_{ss} of victim drug only between these populations to investigate the inherent potential of V_{ss} to change between different individuals.

The specificities of all substrates and inhibitors are summarized, and in addition, the Biopharmaceutics Drug Disposition Classification System (BDDCS) is listed. This simple system classifies drugs based on solubility and permeability and can anticipate when metabolism versus transporter-mediated processes (such as renal and biliary elimination) are the major route of drug elimination [11].

Data Analyses

Thirty-one published DDI studies were examined and changes in exposure (*AUC*), clearance (*CL*), V_{ss}, mean residence time (*MRT*) and terminal half-life ($t_{1/2,z}$) were calculated and reported as ratios of interaction/control. When individual PK data were reported, the ratios of the parameters-of-interest were calculated for each individual and the average of this ratio for all subjects was reported (and indicated in tables with a footnote). Although the initial volume of distribution in the central compartment (V_1) and terminal volume of distribution (V_z) are commonly reported in clinical pharmacokinetic studies, our primary analysis was based on changes in V_{ss} as it is a non-compartmental parameter that represents the whole-body volume of distribution, theoretically is independent of elimination measures [12], and is not associated with a particular compartment or phase of the PK curve (as is the case for V_1 and V_z for drugs that display multi-compartment kinetics). Methods of each paper were carefully reviewed to ensure reported V_{ss} was appropriately calculated. For investigations in which V_{ss} could not be determined, data for V_z were reported with the understanding that V_z changes will only reflect the same degree of change as V_{ss} if the victim drug follows a one compartment model or if the distribution phase minimally affects measures of *AUC* and *AUMC* (area under the moment curve).

For investigations that did not explicitly report all parameters-of-interest, the parameter was either (1) back-calculated from reported data or (2) estimated by digitization of reported plasma-concentration time profiles. Clearance and *AUC* could be calculated from one another if only one of the two parameters were reported by using known dose and the equation: *CL* = *Dose* / *AUC*. Similarly, *CL* can be used to calculate either V_{ss} or *MRT* (if one of the two parameters were reported) using the following relationship [12]:

$$V_{ss} = CL \cdot MRT$$

If *MRT* values were not reported, *MRT* was calculated via non-compartmental methods using the following relationship:

$$MRT = \frac{AUMC}{AUC} - MIT$$

where *MIT* is mean input time. For IV bolus doses, *MIT* is zero. For IV infusions, *MIT* is defined as half of the length of the dosing infusion time (τ), i.e. *MIT* = τ / 2. For investigations that did not report V_{ss} (or any of the other pharmacokinetic parameters of interest), plasma concentration-time profiles were digitized using WebPlotDigitizer Version 4.2 (Ankit Rohatgi, San Francisco, CA, USA) and non-compartmental analysis was conducted with WinNonlin Professional Edition Version 2.1 (Pharsight, Mountain View, CA, USA). Digitized *AUC* values were compared to reported *AUC* values and studies were excluded if reported average *AUC* values were greater than 25% different from digitized values. All pharmacokinetic ratios calculated from digitization

of published concentration-time profiles are specifically indicated in the data tables with a footnote. Published values of pharmacokinetic parameters were reported in priority, with digitization/reanalysis of reported average concentration-time profiles utilized only to supplement unreported data. Each value in the data tables is annotated based on calculation methods (published versus digitized, individual versus average PK data used for ratios, equations used or assumptions made).

The average absolute differences in *AUC* and V_{ss} were compared to one another for all 72 DDIs, as well as the subset of DDIs with greater than 30% *AUC* change (i.e. ratios outside of the range of 0.77 and 1.30, n=49), which could be considered a potentially clinically significant interaction. To account for interactions resulting in a decrease in *AUC*, such as potential enzyme induction, the inverse for all ratios less than unity was utilized in calculation of average absolute *AUC* and V_{ss} changes. Box plot representations of the data were generated to allow visual depiction of any differences in degree of change in these two parameters, which indicate the median, 25^{th} and 75^{th} percentiles, range from minimum to maximum values, and depict each individual point. To investigate if the classic trend of *CL* changes being equal (but opposite in magnitude) to half-life and *MRT* changes in these metabolic DDIs, the relationship between changes in half-life and *MRT* were compared to the inverse of the change in *CL*.

Results

Relevant information on the specificity of all substrates analyzed are outlined in **Table 2.1** and the inhibitory specificities of the perpetrator drugs included in this analysis are listed in **Table 2.2**. The comprehensive literature search identified DDI studies for the following index substrates

where V_{ss} measurements were available: caffeine [13], metoprolol [14], midazolam [15-24], theophylline [25-37], and tolbutamide [38] (**Table 2.3**). Any additional victim-perpetrator combinations (with non-index substrates) investigated in these studies where V_{ss} measurements were available were also analyzed, including alfentanil [19], antipyrine [26], and lidocaine [18] (**Table 2.4**). When only V_z values were available, these studies are summarized in **Table 2.5** and include the victim drugs antipyrine [39], desipramine [40], imipramine [40], and theophylline [39, 41-43].

Table 2.1: Enzyme Specificities of Clinical Index Substrates and Additional Victim Drugs

Substrate	BDDCS Class	Enzyme	Other Relevant Enzymes / Transporters	Reference
Antipyrine	1	CYP1A2 CYP2C9 CYP3A	Multiple CYPs (2A6, 2B6, 2C, 2E1)	[6]
Alfentanil	1	CYP3A		[4]
Caffeine	1	CYP1A2	Xanthine Oxidase N-Acetyl Transferase	[3]
Desipramine	1	CYP2D6	CYP3A	[3]
Imipramine	1	CYP2C19	CYP2D6	[4]
Lidocaine	1	CYP3A	CYP1A2	[6]
Metoprolol	1	CYP2D6	CYP3A	[3]
Midazolam	1	CYP3A	-	[3]
Theophylline	1	CYP1A2	CYP2E1 CYP3A	[3]
Tolbutamide	2	CYP2C9	OAT2	[3, 9]

Abbreviations: BDDCS, Biopharmaceutics Drug Disposition Classification System; CYP, Cytochrome P450; OAT, Organic Anion Transporter

Table 2.2: Inhibitory Specificities of Clinical Index Inhibitors and Additional Perpetrator Drugs

Index Inhibitor	BDDCS Class	Enzyme	Other Relevant Enzymes / Transporters	Reference
Cimetidine	3	OCT2 CYP2C19 CYP3A	MATE1 CYP 1A2, 2C9, 2D6	[4]
Ciprofloxacin	4	CYP1A2	CYP3A4	[3]
Clarithromycin	3	CYP3A4	CYP2C19 P-gp	[3]
Diltiazem	1	CYP3A4	CYP 1A2, 2D6 P-gp	[4]
Disulfiram	2	CYP2E1	CYP 1A2, 2C9, 2D6	[4]
Enoxacin	4	CYP1A2		[3]
Erythromycin	4	CYP3A4	P-gp	[3]
Famotidine	3	Unknown		
Fluconazole	3	CYP2C9 CYP2C19	CYP3A4	[3]
Itraconazole	2	CYP3A4	CYP2J2 P-gp	[3]
Ketoconazole	2	CYP3A4	CYP2C19 P-gp	[3]
Lidocaine	1	CYP3A4	CYP1A2	[6]
Nalidixic Acid	2	Unknown		
Nelfinavir	2	CYP3A4	CYP2D6	[7]
Norfloxacin	4	CYP1A2		[8]
Ofloxacin	3	Unknown		
Olanzapine	2	Unknown		
Ondansetron	1	Unknown		
Primaquine	1	Unknown		
Quinidine	1	CYP2D6	P-gp	[3]
Ranitidine	3	OCT2 CYP3A	CYP 2C9, 2D6	[4]
Rifampin (Single Dose)	2	OATPs	CYP3A4	[5, 10]
Rifampin (Multiple Dose)	2	(Inducer) CYP3A CYP2C9 P-gp	(Inducer) CYP 1A, 2B6, 2C8, 2C19	[5]
Ritonavir (Single Dose)	2	CYP3A4	P-gp	[3]
Ritonavir (Multiple Dose)	2	CYP Induction		[3]
Sulfaphenazole	1	CYP2C9		[7]
Terbinafine	2	CYP2D6	CYP1A2	[3]
Verapamil	1	CYP3A4	P-gp	[3]

Abbreviations: BDDCS, Biopharmaceutics Drug Disposition Classification System; CYP, Cytochrome P450; MATE, Multidrug and Toxic Extrusion; OCT, Organic Cation Transporter; P-gp, P-glycoprotein

Table 2.3: Intravenous Drug-Drug Interaction Studies of Cytochrome P450 Index Substrates

Victim	Perpetrator	Victim Enzymes or Transporters	Perpetrator Enzymes or Transporters	Population	N	$\frac{AUC^{DDI}}{AUC^{Con}}$	$\frac{CL^{DDI}}{CL^{Con}}$	$\frac{V_{ss}^{DDI}}{V_{ss}^{Con}}$	$\frac{MRT^{DDI}}{MRT^{Con}}$	$\frac{t_{1/2,z}^{DDI}}{t_{1/2,z}^{Con}}$	Percent *AUC* Extrapolation	Ref.
Caffeine	Ketoconazole (400 mg; Single Dose)	CYP1A2 NAT XO	CYP3A4 CYP2C19 P-gp	Healthy Subjects	8	1.17[b]	0.88[b]	0.97[a]	1.14[a]	1.18[b]	36%/30%[a]	[13]
Caffeine	Terbinafine (500 mg; Single Dose)	CYP1A2 NAT XO	CYP2D6 CYP1A2	Healthy Subjects	8	1.31[b]	0.81[b]	1.05[a]	1.48[a]	1.35[b]	45%/30%[a]	[13]
Metoprolol	Quinidine (50 mg; Single Dose)	CYP2D6 CYP3A4	CYP2D6 P-gp	Healthy Subjects; Male, White, CYP2D6 Extensive Metabolizers	3	2.43[d]	0.44[b]	0.87[b]	2.06[f]	1.56[a]	29%/15%[a]	[14]
Metoprolol	Quinidine (250 mg BID; 3 Days)	CYP2D6 CYP3A4	CYP2D6 P-gp	Healthy Subjects; Male, White, CYP2D6 Extensive Metabolizers	4	3.08[d]	0.36[b]	0.70[b]	1.99[f]	2.36[a]	44%/15%[a]	[14]
Metoprolol	Quinidine (50 mg; Single Dose)	CYP2D6 CYP3A4	CYP2D6 P-gp	Healthy Subjects; Male, White, CYP2D6 Poor Metabolizers	3	1.12[d]	0.98[b]	1.18[b]	1.30[f]	1.09[a]	35%/34%[a]	[14]
Metoprolol	Quinidine (250 mg BID; 3 Days)	CYP2D6 CYP3A4	CYP2D6 P-gp	Healthy Subjects; Male, White, CYP2D6 Poor Metabolizers	3	1.26[d]	0.88[b]	1.26[b]	1.39[f]	1.32[a]	43%/34%[a]	[14]
Midazolam	Clarithromycin (500 mg BID; 7 Days)	CYP3A4	CYP3A4 CYP2C19 P-gp	Healthy Subjects	16	2.66	0.37	1.05[a]	2.79[a]	2.66	38%/12%[a]	[15]
Midazolam	Clarithromycin (500 mg BID; 7 Days)	CYP3A4	CYP3A4 CYP2C19 P-gp	Healthy Subjects; Elderly	16	3.2	0.35	1.16[a]	2.24[a]	4.06	44%/20%[a]	[16]
Midazolam	Erythromycin (500 mg TID; 7 Days)	CYP3A4	CYP3A4 P-gp	Healthy Subjects	6	2.17[c]	0.46	1.40	3.03[e]	1.77	NR	[17]
Midazolam	Erythromycin (500 mg QID; 5 Days) + Lidocaine (1 mg/kg; 2 Days)	CYP3A4	CYP3A4 P-gp CYP3A4 CYP1A2	Healthy Subjects	8	1.60[d]	0.71[b]	0.93[a]	1.31[a]	1.50[b]	19%/13%[a]	[18]
Midazolam	Fluconazole (100 mg; Single Dose)	CYP3A4	CYP3A4 CYP2C9 CYP2C19	Healthy Subjects	12	1.3	0.78	1.01[a]	1.28[a]	1.16	10%/7%	[19]
Midazolam	Fluconazole (200 mg; Single Dose)	CYP3A4	CYP3A4 CYP2C9 CYP2C19	Healthy Subjects	12	1.4	0.68	1.10[a]	1.68[a]	1.20	11%/7%	[19]
Midazolam	Fluconazole (400 mg; Single Dose)	CYP3A4	CYP3A4 CYP2C9 CYP2C19	Healthy Subjects	12	2.0	0.54	0.93[a]	1.73[a]	1.56	17%/7%	[19]
Midazolam	Fluconazole (400 mg; Single Dose)	CYP3A4	CYP3A4 CYP2C9 CYP2C19	Healthy Subjects; African American CYP3A5*1/*1	6	1.62[b]	0.64[b]	0.81[a]	1.15[a]	1.35[b]	17%/14%[a]	[20]
Midazolam	Fluconazole (400 mg; Single Dose)	CYP3A4	CYP3A4 CYP2C9 CYP2C19	Healthy Subjects; African American CYP3A5*1/*X	7	1.67[b]	0.60[b]	0.99[a]	1.70[a]	1.43[b]	17%/8%[a]	[20]

Victim	Perpetrator	Victim Enzymes or Transporters	Perpetrator Enzymes or Transporters	Population	N	$\frac{AUC^{DDI}}{AUC^{Con}}$	$\frac{CL^{DDI}}{CL^{Con}}$	$\frac{V_{ss}^{DDI}}{V_{ss}^{Con}}$	$\frac{MRT^{DDI}}{MRT^{Con}}$	$\frac{t_{1/2,z}^{DDI}}{t_{1/2,z}^{Con}}$	Percent *AUC* Extrapolation	Ref.
Midazolam	Fluconazole (400 mg; Single Dose)	CYP3A4	CYP3A4 CYP2C9 CYP2C19	Healthy Subjects; African American CYP3A5*X/*X	6	1.97[b]	0.51[b]	0.79[a]	1.61[a]	1.44[b]	16%/8%[a]	[20]
Midazolam	Fluconazole (400 mg, 1 Day; 200 mg QD, 5 Days)	CYP3A4	CYP3A4 CYP2C9 CYP2C19	Healthy Subjects	12	2.02[c]	0.49	0.92	1.85[e]	1.52	1%/1%[a]	[21]
Midazolam	Itraconazole (200 mg QD; 6 Days)	CYP3A4	CYP3A4 CYP2J2 P-gp	Healthy Subjects	12	3.22[c]	0.31	1.08	3.49[e]	2.41	16%/1%[a]	[21]
Midazolam	Ketoconazole (200 mg BID; 2 Days)	CYP3A4	CYP3A4 CYP2C19 P-gp	Healthy Subjects; White	9	5.1	0.21	1.20[a]	5.97[a]	4.12	22%/6%[a]	[22]
Midazolam	Ketoconazole (400 mg QD; 4 Days)	CYP3A4	CYP3A4 CYP2C19 P-gp	Healthy Subjects; Female, Korean	12	4.61[c]	0.22	0.57[b]	4.61[b]	1.98	2%/2%[b]	[23]
Midazolam[i]	Nelfinavir (1250 mg BID; 14 Days)	CYP3A4	CYP3A4 Inhibition and Induction	Healthy Subjects	16	1.83	0.57	0.79[a]	1.22[a]	1.41	2%/3%[a]	[24]
Midazolam	Rifampin (induction) (600 mg QD; 10 Days)	CYP3A4	CYP3A4 Inhibition and Induction	Healthy Subjects; Female, Korean	12	0.48[c]	2.07	1.01[b]	0.50[b]	0.74	2%/2%[b]	[23]
Midazolam[i]	Rifampin (induction) (600 mg QD; 14 Days)	CYP3A4	CYP3A4 Inhibition and Induction	Healthy Subjects	16	0.44	2.16	1.19[a]	0.54[a]	0.61	4%/3%[a]	[24]
Midazolam[i]	Ritonavir (600 mg TID, 1 Day; 300 mg BID, 6 Days; 400 mg BID, 7 Days)	CYP3A4	CYP3A4 Inhibition and Induction	Healthy Subjects	16	3.31	0.29	1.04[a]	3.22[a]	2.85	21%/3%[a]	[24]
Theophylline	Cimetidine (400 mg BID; 7 Days)	CYP1A2 CYP3A4 CYP2E1	CYP Enzymes OCT2 MATE1	Healthy Subjects; Male, Young	8	1.31[c]	0.77	1.10	1.44[e]	1.41	NR	[25]
Theophylline	Cimetidine (400 mg BID; 7 Days)	CYP1A2 CYP3A4 CYP2E1	CYP Enzymes OCT2 MATE1	Healthy Subjects; Female, Young	8	1.42[c]	0.71	1.05	1.48[e]	1.43	NR	[25]
Theophylline	Cimetidine (400 mg BID; 7 Days)	CYP1A2 CYP3A4 CYP2E1	CYP Enzymes OCT2 MATE1	Healthy Subjects; Male, Elderly	8	1.36[c]	0.73	0.98	1.34[e]	1.31	NR	[25]
Theophylline	Cimetidine (400 mg BID; 7 Days)	CYP1A2 CYP3A4 CYP2E1	CYP Enzymes OCT2 MATE1	Healthy Subjects; Female, Elderly	8	1.33[c]	0.75	1.08	1.43[e]	1.36	NR	[25]
Theophylline	Cimetidine (1000 mg QD; 7 Days)	CYP1A2 CYP3A4 CYP2E1	CYP Enzymes OCT2 MATE1	Healthy Subjects	7	1.56[d]	0.66[b]	1.02[b]	1.58[f]	1.84[b]	NR	[26]
Theophylline	Cimetidine (1000 mg QD; 8 Days)	CYP1A2 CYP3A4 CYP2E1	CYP Enzymes OCT2 MATE1	Healthy Subjects	9	1.33[c]	0.75	1.13[g]	1.83[g]	1.24	19%/5%[g]	[27]
Theophylline	Cimetidine (1000 mg QD; 8 Days)	CYP1A2 CYP3A4 CYP2E1	CYP Enzymes OCT2 MATE1	Patients with Liver Cirrhosis	9	1.22[c]	0.82	0.97[g]	1.36[g]	1.66	15%/9%[g]	[27]

Victim	Perpetrator	Victim Enzymes or Transporters	Perpetrator Enzymes or Transporters	Population	N	$\frac{AUC^{DDI}}{AUC^{Con}}$	$\frac{CL^{DDI}}{CL^{Con}}$	$\frac{V_{ss}^{DDI}}{V_{ss}^{Con}}$	$\frac{MRT^{DDI}}{MRT^{Con}}$	$\frac{t_{1/2,z}^{DDI}}{t_{1/2,z}^{Con}}$	Percent *AUC* Extrapolation	Ref.
Theophylline	Cimetidine (300 mg QID; 2.75 Days)	CYP1A2 CYP3A4 CYP2E1	CYP Enzymes OCT2 MATE1	Healthy Subjects; Male	5	1.69[d]	0.61	1.11[h]	1.90[h]	1.73	32%/13%[h]	[28]
Theophylline	Cimetidine (300 mg QID; 6 Days)	CYP1A2 CYP3A4 CYP2E1	CYP Enzymes OCT2 MATE1	Healthy Subjects	10	1.46[d]	0.74[b]	1.12[a]	1.53[a]	1.38[b]	30%/17%[a]	[29]
Theophylline	Cimetidine (400 mg TID; 9 Days)	CYP1A2 CYP3A4 CYP2E1	CYP Enzymes OCT2 MATE1	Healthy Subjects; Male	7[j]	1.42	0.73	1.02[a]	1.30[a]	1.38	13%/8%[a]	[30]
Theophylline	Cimetidine[k] (800 mg BID; 9.5 Days)	CYP1A2 CYP3A4 CYP2E1	CYP Enzymes OCT2 MATE1	Patients with Chronic Obstructive Pulmonary Disease (COPD)	15	1.35[d]	0.77[b]	1.10[b]	1.47[b]	1.45[b]	13%/6%[a]	[31]
Theophylline	Cimetidine (600 mg QID; 6 Days)	CYP1A2 CYP3A4 CYP2E1	CYP Enzymes OCT2 MATE1	Healthy Subjects	8	1.63	0.60	1.07	2.01	1.80	NR	[32]
Theophylline	Ciprofloxacin (500 mg BID; 6 Days)	CYP1A2 CYP3A4 CYP2E1	CYP1A2 CYP3A4	Healthy Subjects	8	1.43	0.69	1.04	1.70	1.51	NR	[32]
Theophylline	Ciprofloxacin (500 mg BID; 7 Days)	CYP1A2 CYP3A4 CYP2E1	CYP1A2 CYP3A4	Healthy Subjects; Male	8	1.34[d]	0.76[b]	1.02	1.36[e]	1.43[b]	21%/12%[a]	[33]
Theophylline	Ciprofloxacin (500 mg BID; 8 Days)	CYP1A2 CYP3A4 CYP2E1	CYP1A2 CYP3A4	Healthy Subjects; Male, Young	8	1.49[c]	0.67	1.02	1.52[e]	1.51	NR	[25]
Theophylline	Ciprofloxacin (500 mg BID; 8 Days)	CYP1A2 CYP3A4 CYP2E1	CYP1A2 CYP3A4	Healthy Subjects; Female, Young	8	1.50[c]	0.67	1.02	1.53[e]	1.48	NR	[25]
Theophylline	Ciprofloxacin (500 mg BID; 8 Days)	CYP1A2 CYP3A4 CYP2E1	CYP1A2 CYP3A4	Healthy Subjects; Male, Elderly	8	1.42[c]	0.71	1.04	1.47[e]	1.40	NR	[25]
Theophylline	Ciprofloxacin (500 mg BID; 8 Days)	CYP1A2 CYP3A4 CYP2E1	CYP1A2 CYP3A4	Healthy Subjects; Female, Elderly	8	1.40[c]	0.71	1.08	1.51[e]	1.45	NR	[25]
Theophylline	Ciprofloxacin (500 mg BID; 6 Days) + Cimetidine (600 mg QID; 6 Days)	CYP1A2 CYP3A4 CYP2E1	CYP1A2 CYP3A4 / CYP Enzymes OCT2 MATE1	Healthy Subjects	8	1.80	0.55	1.11	2.26	2.03	NR	[32]
Theophylline	Ciprofloxacin (500 mg BID; 15 Days) + Cimetidine (400 mg BID; 8 Days)	CYP1A2 CYP3A4 CYP2E1	CYP1A2 CYP3A4 / CYP Enzymes OCT2 MATE1	Healthy Subjects; Male, Young	8	1.64[c]	0.61	1.08	1.78[e]	1.73	NR	[25]
Theophylline	Ciprofloxacin (500 mg BID; 15 Days) + Cimetidine (400 mg BID; 8 Days)	CYP1A2 CYP3A4 CYP2E1	CYP1A2 CYP3A4 / CYP Enzymes OCT2 MATE1	Healthy Subjects; Female, Young	8	1.79[c]	0.56	1.02	1.84[e]	1.75	NR	[25]

Victim	Perpetrator	Victim Enzymes or Transporters	Perpetrator Enzymes or Transporters	Population	N	$\frac{AUC^{DDI}}{AUC^{Con}}$	$\frac{CL^{DDI}}{CL^{Con}}$	$\frac{V_{ss}^{DDI}}{V_{ss}^{Con}}$	$\frac{MRT^{DDI}}{MRT^{Con}}$	$\frac{t_{1/2,z}^{DDI}}{t_{1/2,z}^{Con}}$	Percent *AUC* Extrapolation	Ref.
Theophylline	Ciprofloxacin (500 mg BID; 15 Days) + Cimetidine (400 mg BID; 8 Days)	CYP1A2 CYP3A4 CYP2E1	CYP1A2 CYP3A4 / CYP Enzymes OCT2 MATE1	Healthy Subjects; Male, Elderly	8	1.64[c]	0.61	1.00	1.64[e]	1.64	NR	[25]
Theophylline	Ciprofloxacin (500 mg BID; 15 Days) + Cimetidine (400 mg BID; 8 Days)	CYP1A2 CYP3A4 CYP2E1	CYP1A2 CYP3A4 / CYP Enzymes OCT2 MATE1	Healthy Subjects; Female, Elderly	8	1.60[c]	0.63	1.08	1.72[e]	1.68	NR	[25]
Theophylline	Diltiazem (120 mg TID; 6 Days)	CYP1A2 CYP3A4 CYP2E1	CYP3A4 CYP1A2 CYP2D6 P-gp	Healthy Subjects	10	1.02[c]	0.98	1.11[g]	1.01[g]	1.06	9%/9%[g]	[34]
Theophylline	Enoxacin (200 mg TID; 3 Days)	CYP1A2 CYP3A4 CYP2E1	CYP1A2	Healthy Subjects	5	2.00[c]	0.50	1.09[a]	2.35[a]	2.12	33%/7%[a]	[35]
Theophylline	Famotidine (40 mg BID; 6 Days)	CYP1A2 CYP3A4 CYP2E1	Unknown	Healthy Subjects	10	0.95[d]	1.07[b]	1.12[a]	1.06[a]	1.08[b]	17%/16%[a]	[29]
Theophylline	Famotidine[k] (40 mg BID; 9.5 Days)	CYP1A2 CYP3A4 CYP2E1	Unknown	Patients with Chronic Obstructive Pulmonary Disease (COPD)	15	0.99[d]	1.02[b]	1.03[b]	1.02[b]	1.02[b]	6%/6%[a]	[31]
Theophylline	Nalidixic Acid (500 mg QID; 7 Days)	CYP1A2 CYP3A4 CYP2E1	Unknown	Healthy Subjects; Male	8	0.99[d]	1.04[b]	1.04	1.02[e]	1.12[b]	NR	[33]
Theophylline	Norfloxacin (200 mg TID; 3 Days)	CYP1A2 CYP3A4 CYP2E1	CYP1A2	Healthy Subjects	5	1.08[c]	0.93	1.11[a]	1.29[a]	1.17	13%/7%[a]	[35]
Theophylline	Norfloxacin (400 mg BID; 7 Days)	CYP1A2 CYP3A4 CYP2E1	CYP1A2	Healthy Subjects; Male	8	1.17[d]	0.86[b]	1.02	1.19[e]	1.24[b]	18%/12%[a]	[33]
Theophylline	Ofloxacin (200 mg TID; 3 Days)	CYP1A2 CYP3A4 CYP2E1	Unknown	Healthy Subjects	5	1.00[c]	1.00	1.08[a]	1.11[a]	1.06	10%/7%[a]	[35]
Theophylline	Olanzapine (5 mg 1 Day; 7.5 mg 1 Day; 10 mg QD 7 Days)	CYP1A2 CYP3A4 CYP2E1	Unknown	Healthy Subjects; Male	12	0.94	1.04	1.08[a]	1.01[a]	1.02	7%/7%[a]	[30]
Theophylline	Ranitidine (150 mg BID; 7 Days)	CYP1A2 CYP3A4 CYP2E1	CYP3A CYP2C9 CYP2D6 OCT2	Healthy Subjects	7	1.21[d]	0.92[b]	0.97[b]	1.16[f]	1.28[b]	NR	[26]
Theophylline	Verapamil (40 mg TID; 4 Days)	CYP1A2 CYP3A4 CYP2E1	CYP3A4 P-gp	Healthy Subjects, Male, White	12	1.13	0.92	0.98	1.06[e]	1.11	15%/11%[a]	[36]
Theophylline	Verapamil (80 mg TID; 4 Days)	CYP1A2 CYP3A4 CYP2E1	CYP3A4 P-gp	Healthy Subjects, Male, White	12	1.19	0.86	0.95	1.11[e]	1.11	16%/11%[a]	[36]

Victim	Perpetrator	Victim Enzymes or Transporters	Perpetrator Enzymes or Transporters	Population	N	$\frac{AUC^{DDI}}{AUC^{Con}}$	$\frac{CL^{DDI}}{CL^{Con}}$	$\frac{V_{ss}^{DDI}}{V_{ss}^{Con}}$	$\frac{MRT^{DDI}}{MRT^{Con}}$	$\frac{t_{1/2,z}^{DDI}}{t_{1/2,z}^{Con}}$	Percent *AUC* Extrapolation	Ref.
Theophylline	Verapamil (120 mg TID; 4 Days)	CYP1A2 CYP3A4 CYP2E1	CYP3A4 P-gp	Healthy Subjects, Male, White	12	1.28	0.82	0.90	1.10[e]	1.25	18%/11%[a]	[36]
Theophylline	Verapamil (120 mg TID; 8 Days)	CYP1A2 CYP3A4 CYP2E1	CYP3A4 P-gp	Healthy Subjects	7	1.25[d]	0.81[b]	0.97[b]	1.21[f]	1.22[b]	45%/37%[g]	[37]
Theophylline	Verapamil (120 mg QID; 6 Days)	CYP1A2 CYP3A4 CYP2E1	CYP3A4 P-gp	Healthy Subjects	10	1.29[c]	0.77	0.98[g]	1.31[g]	1.33	6%/3%[g]	[34]
Tolbutamide	Cimetidine (1000 mg QD, 4 Days; 600 mg 1 Day)	CYP2C9	CYP Enzymes OCT2 MATE1	Healthy Subjects	6	1.15[c]	0.87	1.01[a]	1.19[a]	1.13	4%/2%[a]	[38]
Tolbutamide	Cimetidine (400 mg QID; 4.5 Days)	CYP2C9	CYP Enzymes OCT2 MATE1	Healthy Subjects	6	1.53[c]	0.65	0.96[a]	1.46[a]	1.46	5%/2%[a]	[38]
Tolbutamide	Primaquine (45 mg; Single Dose)	CYP2C9	Unknown	Healthy Subjects	6	1.04[c]	0.96	0.82[a]	0.89[a]	0.90	2%/4%[a]	[38]
Tolbutamide	Sulfaphenazole (500 mg BID; 3.5 Days)	CYP2C9	CYP2C9	Healthy Subjects	7	3.10[c]	0.32	0.86[a]	3.21[a]	3.07	26%/4%[a]	[38]

Pharmacokinetic values reported in the table are based on published average values, unless otherwise noted

Abbreviations: *AUC*, area under the curve; BID, twice daily; *CL*, clearance; Con, control; CYP, cytochrome P450; DDI, drug-drug interaction; MATE1, multidrug and toxic extrusion 1; *MRT*, mean residence time; NAT, N-acetyl-transferase; N, number of subjects; NR, not reported; OCT, organic cation transporter; P-gp, P-glycoprotein; QD, once daily; QID, four times a day; Refs., references; TID, three times a day; $t_{1/2,z}$, terminal half-life; V_{ss}, volume of distribution at steady state; XO, xanthine oxidase

[a]Ratios are calculated by digitization of published average plasma concentration-time profiles and performing non-compartmental analysis

[b]Ratios are calculated for each individual using published individual PK data; the reported value reflects the average of each individual ratio

[c]*AUC* was calculated with the equation *AUC = dose / CL* using known dose and reported average values of *CL*

[d]*AUC* was calculated for each individual with the equation *AUC = dose / CL* using known dose and reported individual values of *CL*; the reported value reflects the average of each individual ratio

[e]*MRT* was calculated with the equation $V_{ss} = CL \bullet MRT$ using reported average values of *CL* and V_{ss}

[f]*MRT* was calculated for each individual with the equation $V_{ss} = CL \bullet MRT$ using reported individual values of *CL* and V_{ss}; the reported value reflects the average of each individual ratio

[g]Ratios are calculated by digitization of a published plasma concentration-time profile of a single representative subject, which may not be reflective of all subjects in the study

[h]Ratios are calculated by digitization of individual published plasma concentration-time profiles and performing non-compartmental analysis; the reported value reflects the average of each individual ratio

[i]Midazolam was dosed IV at the same time as a PO probe cocktail of tolbutamide, dextromethorphan and caffeine

[j]Interaction arm included n=7 subjects, however the control arm is only n=6 due to one subject dropping out of the study

[k]A list of additional drugs being taken by these chronic obstructive pulmonary disease subjects can be found in the original article by Bachmann et al. [31]

Table 2.4: Intravenous Drug-Drug Interaction Studies with Additional Substrates (Not CYP Index Substrates)

Victim	Perpetrator	Victim Enzymes or Transporters	Perpetrator Enzymes or Transporters	Population	N	$\frac{AUC^{DDI}}{AUC^{Con}}$	$\frac{CL^{DDI}}{CL^{Con}}$	$\frac{V_{ss}^{DDI}}{V_{ss}^{Con}}$	$\frac{MRT^{DDI}}{MRT^{Con}}$	$\frac{t_{1/2,z}^{DDI}}{t_{1/2,z}^{Con}}$	Percent *AUC* Extrapolation	Ref.
Alfentanil	Fluconazole (100 mg; Single Dose)	CYP3A4	CYP3A4 CYP2C9 CYP2C19	Healthy Subjects	12	1.2	0.84	0.93[a]	1.18[a]	1.18	2%/1%	[19]
	+ Ondansetron (4 mg; Single Dose)		Unknown									
	+ Midazolam (1 mg; Single Dose)		Unknown									
Alfentanil	Fluconazole (200 mg; Single Dose)	CYP3A4	CYP3A4 CYP2C9 CYP2C19	Healthy Subjects	12	1.6	0.62	0.89[a]	1.45[a]	1.36	3%/1%	[19]
	+ Ondansetron (4 mg; Single Dose)		Unknown									
	+ Midazolam (1 mg; Single Dose)		Unknown									
Alfentanil	Fluconazole (400 mg; Single Dose)	CYP3A4	CYP3A4 CYP2C9 CYP2C19	Healthy Subjects	12	2.2	0.46	0.90[a]	1.92[a]	1.73	5%/1%	[19]
	+ Ondansetron (4 mg; Single Dose)		Unknown									
	+ Midazolam (1 mg; Single Dose)		Unknown									
Antipyrine	Cimetidine (1000 mg BD; 7 Days)	CYP Enzymes	CYP Enzymes OCT2 MATE1	Healthy Subjects	7	1.33[d]	0.76[b]	1.05[b]	1.40[f]	1.30[b]	NR	[26]
Antipyrine	Ranitidine (150 mg BID; 7 Days)	CYP Enzymes	CYP3A CYP2C9 CYP2D6 OCT2	Healthy Subjects	7	1.08[d]	0.93[b]	1.02[b]	1.09[f]	1.06[b]	NR	[26]
Lidocaine	Erythromycin (500 mg QID; 5 days)	CYP3A4 CYP1A2	CYP3A4 P-gp	Healthy Subjects	8	1.19[d]	0.96[b]	1.14[a]	1.19[a]	1.37[b]	28%/23%[a]	[18]
	+Midazolam (0.075 mg/kg; Single Dose)		Unknown									

Pharmacokinetic values reported in the table are based on published average values, unless otherwise noted

Abbreviations: *AUC*, area under the curve; BID, twice daily; *CL*, clearance; Con, control; CYP, cytochrome P450; DDI, drug-drug interaction; MATE1, multidrug and toxic extrusion 1; *MRT*, mean residence time; N, number of subjects; NR, not reported; OCT, organic cation transporter; P-gp, P-glycoprotein; QID, four times a day; Ref., references; $t_{1/2,z}$, terminal half-life; V_{ss}, volume of distribution at steady state

[a]Ratios are calculated by digitization of published average plasma concentration-time profiles and performing non-compartmental analysis

[b]Ratios are calculated for each individual using published individual PK data; the reported value reflects the average of each individual ratio

[d]*AUC* was calculated for each individual with the equation *AUC = dose / CL* using known dose and reported individual values of *CL*; the reported value reflects the average of each individual ratio

[f]*MRT* was calculated for each individual with the equation $V_{ss} = CL \bullet MRT$ using reported individual values of *CL* and V_{ss}; the reported value reflects the average of each individual ratio

Table 2.5: Intravenous Drug-Drug Interaction Studies that Only Report Terminal Volume of Distribution (V_z)

Victim	Perpetrator	Victim Enzymes or Transporters	Perpetrator Enzymes or Transporters	Population	N	$\frac{AUC^{DDI}}{AUC^{Con}}$	$\frac{CL^{DDI}}{CL^{Con}}$	$\frac{V_z^{DDI}}{V_z^{Con}}$	$\frac{MRT^{DDI}}{MRT^{Con}}$	$\frac{t_{1/2,z}^{DDI}}{t_{1/2,z}^{Con}}$	Percent *AUC* Extrapolation	Ref.
Antipyrine	Cimetidine (1000 QD; 10 Days)	CYP1A2 CYP2C9 CYP3A4	CYP Enzymes OCT2 MATE1	Healthy Subjects	7	1.41	0.79	1.24	NR	1.59	NR	[39]
Desipramine	Disulfiram (500 mg QD; 31 Days)	CYP2D6 CYP3A4	CYP2E1 CYP1A2 CYP2C9 CYP2D6	Healthy Subject; Male	1	1.32	0.76	0.93	NR	1.20	NR	[40]
Imipramine	Disulfiram (500 mg QD; 14 Days)	CYP2C19 CYP2D6	CYP2E1 CYP1A2 CYP2C9 CYP2D6	Healthy Subjects; Male	2	1.30[b]	0.77[b]	0.89[b]	NR	1.16[b]	NR	[40]
Theophylline	Cimetidine (300 mg PO QID; 1.5 Days)	CYP1A2 CYP3A4 CYP2E1	CYP Enzymes OCT2 MATE1	Healthy Subjects; Male	10	1.27[c]	0.79	1.00	NR	1.24	NR	[41]
Theophylline	Cimetidine (300 mg IV Infusion QID; 1.5 Days)	CYP1A2 CYP3A4 CYP2E1	CYP Enzymes OCT MATE1	Healthy Subjects; Male	10	1.21[c]	0.83	1.02	NR	1.20	NR	[41]
Theophylline	Cimetidine (400 mg BID; 7 Days)	CYP1A2 CYP3A4 CYP2E1	CYP Enzymes OCT MATE1	Healthy Subjects; Male	6	1.34[c]	0.74	1.04	NR	1.42	NR	[42]
Theophylline	Cimetidine (1000 QD; 10 Days)	CYP1A2 CYP3A4 CYP2E1	CYP Enzymes OCT MATE1	Healthy Subjects	7	1.10	0.90	1.04	NR	1.15	NR	[39]
Theophylline	Ciprofloxacin (500 mg BID; 7 Days)	CYP1A2 CYP3A4 CYP2E1	CYP1A2 CYP3A4	Healthy Subjects; Male	6	1.48[c]	0.68	1.00	NR	1.47	NR	[42]
Theophylline	Ciprofloxacin (400 mg BID; 7 Days) + Cimetidine (500 mg BID; 7 Days)	CYP1A2 CYP3A4 CYP2E1	CYP1A2 CYP3A4 CYP Enzymes OCT2 MATE1	Healthy Subjects; Male	6	1.70[c]	0.59	1.00	NR	1.78	NR	[42]
Theophylline	Erythromycin (250 mg QID; 7 Days)	CYP1A2 CYP3A4 CYP2E1	CYP3A4 P-gp	Healthy Subjects; Male	8	1.38[c]	0.74[b]	0.92[b]	NR	1.27[b]	NR	[43]

Pharmacokinetic values reported in the table are based on published average values, unless otherwise noted

Abbreviations: *AUC*, area under the curve; BID, twice daily; *CL*, clearance; Con, control; CYP, cytochrome P450; DDI, drug-drug interaction; MATE1, multidrug and toxic extrusion 1; *MRT*, mean residence time; N, number of subjects; NR, not reported, OCT, organic cation transporter; QD, once daily; QID, four times a day; Ref., references; $t_{1/2,z}$, terminal half-life; V_z, terminal volume of distribution

[b]Ratios are calculated for each individual using published individual PK data; the reported value reflects the average of each individual ratio

[c]*AUC* was calculated with the equation *AUC = dose / CL* using known dose and reported average values of *CL*

Table 2.6: Intravenous Pharmacogenomic Interaction Studies and Disease State Drug-Drug Interaction Studies

Drug	Enzyme	Population	N	$\frac{AUC^{Int}}{AUC^{Con}}$	$\frac{CL^{Int}}{CL^{Con}}$	$\frac{V_{ss}^{Int}}{V_{ss}^{Con}}$	$\frac{MRT^{Int}}{MRT^{Con}}$	$\frac{t_{1/2,z}^{Int}}{t_{1/2,z}^{Con}}$	Percent *AUC* Extrapolation	Ref.
Metoprolol	**CYP2D6**	**Control**: Healthy Subjects, White, Male, CYP2D6 Extensive Metabolizers; 58-80 kg	3	2.56[c]	0.40	0.51	1.29[e]	1.81[a]	34%/15%[a]	[14]
		Phenotype: Healthy Subjects, White, Male, CYP2D6 Poor Metabolizers; 65-86 kg	4							
Midazolam	**CYP3A**	**Control:** Healthy Subjects, African American, CYP3A5*1/*1; 57-97 kg for all subjects	6	0.98	1.04	0.79[a]	0.70[a]	0.93	8%/14%[a]	[20]
		Phenotype: Healthy Subjects, African-American, CYP3A5*1/*X; 57-97 kg for all subjects	7							
Midazolam	**CYP3A**	**Control:** Healthy Subjects, African American, CYP3A5*1/*1; 57-97 kg for all subjects	6	1.05	0.99	0.72[a]	0.70[a]	0.96	8%/14%[a]	[20]
		Phenotype: Healthy Subjects, African-American, CYP3A5*1/*X; 57-97 kg for all subjects	6							
Theophylline	**CYP1A2 CYP3A4 CYP2E1**	**Control:** Healthy Subjects; average weight 80.7 kg	9	1.54[c]	0.65	0.70[g]	1.2[g]	1.76	8%/14%[a]	[27]
		Disease State: Liver Cirrhosis Patients; average weight 68.6 kg	9							

Pharmacokinetic values reported in the table are based on published average values, unless otherwise noted
Abbreviations: *AUC*, area under the curve; *CL*, clearance; Con, control (indicating the wild-type pharmacogenomic phenotype or healthy subject group); CYP, cytochrome P450; Int, interaction (indicating the reduced function pharmacogenomic phenotype or disease state group); *MRT*, mean residence time; N, number; Ref., references; $t_{1/2,z}$, terminal half-life; V_{ss}, volume of distribution at steady state
[a]Ratios are calculated by digitization of published average plasma concentration-time profiles and performing non-compartmental analysis
[c]*AUC* was calculated with the equation *AUC = dose / CL* using known dose and reported average values of *CL*
[e]*MRT* was calculated with the equation $V_{ss} = CL \bullet MRT$ using reported average values of *CL* and V_{ss}
[g]Ratios are calculated by digitization of a published plasma concentration-time profile of a single representative subject (one healthy subject and one liver cirrhosis patient), which may not be reflective of all subjects in the study

The changes in pharmacokinetic parameters (*AUC*, *CL*, V_{ss}, *MRT* and $t_{1/2,z}$) of clinically recommended index substrates are listed in **Table 2.3** and additional victim drugs in **Table 2.4**, totaling 72 DDI studies. For these primarily metabolized drugs, *AUC* ratios ranged from 0.44 - 5.1 while V_{ss} ranged from 0.57 - 1.40. The average absolute difference in *AUC* ratios for these 72 DDI studies averaged 1.69 ± 0.78, while the average absolute difference in V_{ss} averaged 1.10 ± 0.12. For the 49 interactions with at least a 30% change, i.e., those interactions that could potentially be clinically significant, the absolute *AUC* changes averaged 1.95 ± 0.83, while V_{ss} averaged 1.11 ± 0.13. **Figure 2.1** depicts box plot representations of these values. Of the 72 DDI studies examined, only three (4.2%) resulted in greater than a 30% change in V_{ss} (i.e. ratios outside of the range of 0.77 to 1.30) with ratios of 0.70 [14], 1.40 [17] and 0.57 [23].

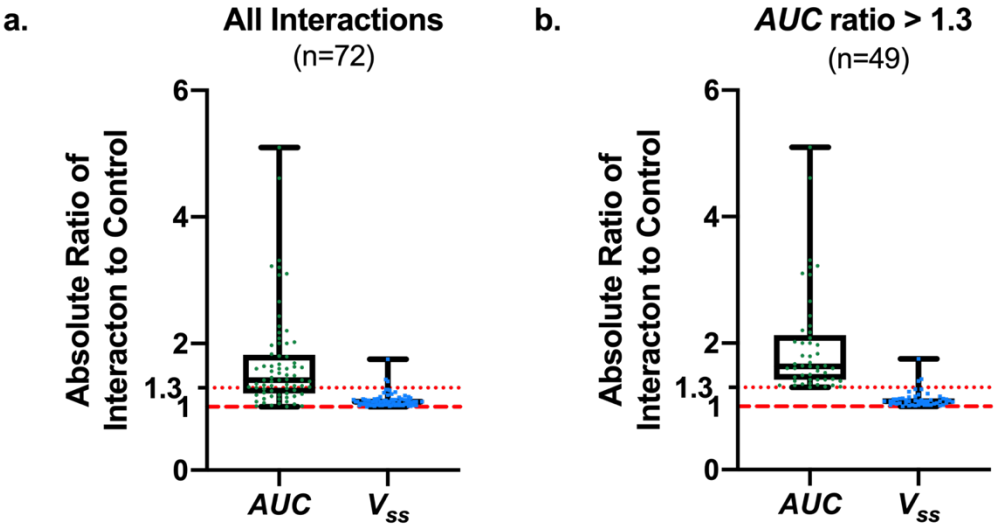

Figure 2.1: Box plot depictions of the absolute magnitude of change in victim drug exposure (*AUC*) and volume of distribution at steady state (V_{ss}). Ratios are expressed as ratios of interaction to control for (a) all drug-drug interactions (n=72) and (b) the subset of these interactions that are potentially clinically significant (with absolute *AUC* ratios > 1.3; n=49). The box indicates the median, 25th and 75th percentiles, the whiskers range from minimum to maximum values, and each individual data point is also depicted.

An additional ten DDI studies were identified from five studies for which only V_z was reported and V_{ss} could not be determined (due to lack of published pharmacokinetic profiles) (**Table 2.5**). Changes in *AUC* ranged from 1.10 – 1.70, but V_z only ranged from 0.89 – 1.24.

While the inclusion criteria of this analysis focused on studies that include the same patients in the control and interaction phases, three DDI studies investigated here performed the same drug interaction study in multiple groups, either with respect to pharmacogenomic variance of metabolizing enzyme [14, 20] or disease state [27]. To investigate the impact of inter-individual variability on V_{ss}, the control phase (victim drug only) between each group were compared to one another (**Table 2.6**). When comparing the PK of the index substrate alone between groups, V_{ss} for victim drug was observed to change with ratios of 0.51 (metoprolol with CYP2D6 pharmacogenomics), 0.72 and 0.79 (midazolam with CYP3A5 pharmacogenomics), and 0.70 (healthy versus liver cirrhosis patients), while *AUC* was observed to change 0.98- to 2.56-fold in these studies. In the same studies, however, minimal change in V_{ss} was observed in the same individual between the drug interaction versus control phases, with ratios ranging from 0.70 – 1.13 (**Table 2.3**).

Discussion

For primarily metabolized drugs, IV drug interaction studies resulted in minimal changes to V_{ss}. Changes in drug exposure (*AUC*) up to 5.1-fold were observed, however ratios of V_{ss} changes only had a range of 0.70 – 1.40, with one outlier displaying a 43% decrease in V_{ss} (ratio of 0.57) (**Table 2.3**) for a midazolam-ketoconazole interaction in healthy female Koreans where the *AUC* ratio was 4.61 [23]. In contrast, a second midazolam-ketoconazole interaction study in

healthy White subjects with a similar *AUC* ratio of 5.1 only exhibited a V_{ss} ratio of 1.20 [22]. The trend of unchanged V_{ss} was observed for all index substrates and CYP isoforms investigated (caffeine and theophylline, CYP1A2; metoprolol, CYP2D6; tolbutamide, CYP2C9; midazolam, CYP3A4) [data not shown].

It should be noted that a listed high percent *AUC* extrapolation value does not necessarily indicate that *AUC* (or pharmacokinetic parameters derived from *AUC*) are unreliable if the slope of the elimination phase is adequately captured. Additionally, the pharmacokinetic parameters reported by the original authors were used in priority to calculate the ratios presented in this analysis, such as the frequently reported parameters *AUC*, *CL* and $t_{1/2,z}$. Estimation of less-frequently reported parameters, such as V_{ss} and *MRT*, proceeded via digitization of the average concentration-time profiles reported by the original authors, and it should be noted that these average profiles may not accurately represent changes within any one particular individual in the DDI study.

When V_{ss} was not reported (and could not be calculated due to the lack of published pharmacokinetic curves), changes in V_z were examined (**Table 2.5**). Changes in V_z were minimal (0.89 – 1.24). Examination of theophylline PK curves from the other studies in this analysis indicate that the distribution phase of theophylline is very short, and therefore V_z changes would likely be similar to V_{ss} changes. No such conclusions related to the potential similarity between V_z and V_{ss} could be made for the antipyrine, desipramine or imipramine data due to the lack of published IV pharmacokinetic curves in the other studies examined here.

Of note, the clinical studies included in this analysis were all conducted with the same individuals in the control versus interaction arms, to minimize the confounding effects of inter-

individual variability. Three of the studies examined here also conducted DDIs in multiple subject groups with respect to disease state [27] or pharmacogenomic variance of drug metabolizing enzyme [14, 20]. To examine the potential impact of inter-individual differences in V_{ss}, the pharmacokinetic parameters associated with the control arms (victim drug only) of each group were compared to one another, resulting in V_{ss} ratios of 0.51 – 0.79 associated with *AUC* changes of 0.98 – 2.56 (**Table 2.6**). In comparison to the earlier part of this analysis where changes in V_{ss} within the same individual (with and without addition of a perpetrator drug) were examined, these same studies displayed V_{ss} ratios of 0.70 – 1.26 associated with *AUC* increases of 1.12 – 3.08. Reported data related to the body weights of individuals in each arm are also noted in **Table 2.6**. However, accounting for average differences in body weight between the two groups does not necessarily result in V_{ss} ratios that are closer to unity. For instance, the reported differences in metoprolol V_{ss} between CYP2D6 poor metabolizers (PM) and extensive metabolizers (EM) resulted in a ratio of 0.51, and the reported values used to calculate this ratio were normalized by body weight of each individual by the original investigators. This indicates that volume of distribution differences in different individuals can be significant and do not only depend on total body weight differences. Further, the variability associated with V_{ss} values was much greater in EM than PM, with CV values of 44% and 22%, respectively. The issue of variability between individuals is further compounded in pharmacogenomic studies where often only a very small number of individuals can be recruited for the less frequently occurring genotypes.

This highlights that for the same drug, V_{ss} may change significantly between subjects. These findings are in contradiction to the belief that all pharmacokinetic parameters are expected to be similar in homogenous populations, such as in healthy subjects, since the

pharmacogenomic interactions studied here included healthy subjects in each arm. As a result, we suggest that it may not appropriate to assume that V_{ss} is unchanged across different subject populations and therefore, it is crucial to consider clinical study design (parallel versus crossover). Further, based on this observation, we emphasize that examination of differences in pharmacokinetics in different pharmacogenomic variance or disease state populations should be considered as a qualitative outcome. Although changes in *AUC* and *CL* can reasonably be compared between groups, however, since V_{ss} may inherently be different between individuals in each group, changes in terminal half-life should not be considered significant nor be utilized to suggest changes in dosing regimen between the two populations studied. Further investigation into this finding is warranted, and is an area of high interest to our laboratory.

It should be noted that perpetrator drugs have the potential to displace victim drug from plasma or tissue-binding sites, which may result in V_{ss} changes. Changes in protein binding should result in comparable changes for *CL* and V_{ss}, resulting in no change in *MRT* or half-life. However, we find no examples of such an interaction in the same subjects within our dataset. Thus, the data presented here for IV metabolic drug interaction studies very strongly support our contention that V_{ss} does not change to any significant degree for metabolic DDIs.

The DDI studies evaluated here follow the classic pharmacokinetic trend of changes in *CL* resulting in an equal but opposite change in *MRT*, due to the fact that V_{ss} remains unchanged for metabolic interactions [44]. These relationships are depicted in **Figure 2.2**, where the inverse of ratios of *CL* changes are plotted against both *MRT* and $t_{1,2,z}$ ratios. The results for each comparison fall very close to the line of unity, highlighting the intuitive trend that decreases in *CL* result in increases in MRT and $t_{1/2,z}$ of approximately equal magnitude. In comparing the *AUC*-

MRT relationship to the *AUC*-$t_{1/2,z}$ relationship, as expected the *MRT* relationship falls closer to the line of unity than a few of the $t_{1/2,z}$ points associated with larger 1/*CL*, as $t_{1/2,z}$ may change differently than *MRT* for drugs that display multi-compartment kinetics, and this difference is likely amplified in DDI studies of a larger magnitude. In general, **Figure 2.2** highlights that changes in clearance are opposite in direction but similar in magnitude to *MRT* and $t_{1/2,z}$ and this is in sharp contrast to significant transporter-drug interactions, where decreases in clearance can often be associated with decreases in half-life and *MRT*, due to changes in V_{ss} [2].

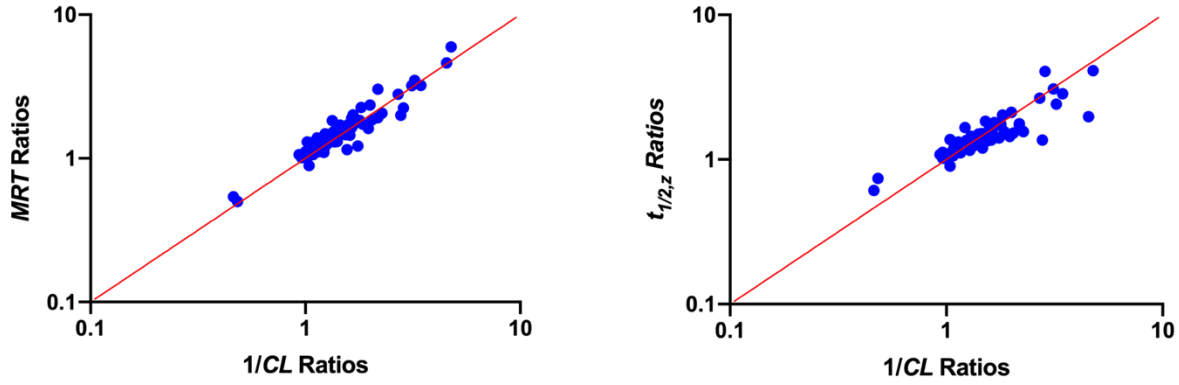

Figure 2.2: Ratios of change in mean residence time (*MRT*) and terminal half-life ($t_{1/2,z}$) compared with the inverse of change in clearance (*CL*). Red lines indicate the line of unity.

Knowledge that V_{ss} largely remains unchanged for IV metabolic DDIs (based on the analysis presented here) indicates that following an orally dosed DDI, changes in apparent volume of distribution at steady state (V_{ss}/F) will reflect changes in *F* alone. Such estimates of changes in *F* can subsequently be utilized to estimate changes in systemic *CL* from measured changes in apparent clearance (*CL*/*F*). Although this clearance versus bioavailability

differentiation methodology will be discussed in further detail in Chapter 3, here the methodology is introduced.

In the Quinney et al. [16] investigation of the interaction of midazolam and clarithromycin in elderly subjects, the interaction was conducted following both oral and IV dosed midazolam. Thus, estimates of changes in *CL* versus *F* based on the oral interaction study can be confirmed by examining the observed changes resulting from the IV midazolam interaction study. Following oral dosing, an 8.2-fold increase in midazolam exposure was observed (compared to only a 3.2-fold increase in midazolam *AUC* in the IV drug interaction study) when clarithromycin was dosed 500 mg BID for 7 days (**Table 2.7**). Examination of changes in V_{ss}/F following oral dosing provided a predicted increase in *F* of 2.84-fold, and thus clearance was predicted to decrease by 60% (ratio of 0.40). The observed change in bioavailability was a 2.12-fold increase and a 65% reduction of *CL* (ratio of 0.35) (**Table 2.7**). Thus, recognition that Vss remains unchanged in metabolic interactions allows the discrimination of two pharmacokinetic parameters thought to be indistinguishable from one another following oral dosing. This methodology will be evaluated in detail in Chapter 3.

Conclusions

Based on an extensive evaluation of 72 clinical DDI studies, V_{ss} remains unchanged for IV metabolic drug interactions as expected, with a small minority of outliers (only three) with ratios indicating a change, where for the largest V_{ss} change, a second study of the same interacting drugs in a different population did not show this marked V_{ss} change. These results uphold the widely-held founding tenant of pharmacokinetics that *CL* and V_{ss} are independent parameters.

Differences in victim drug V_{ss} can significantly vary throughout the population due to inter-individual variability that may not necessarily be accounted for by body weight. This highlights that differences in pharmacokinetic parameters observed between groups in pharmacogenomic and disease state studies (or any clinical trial with a parallel study design) should be accompanied with the understanding that V_{ss} could differ significantly between groups. Therefore, although changes in *AUC* and *CL* between groups indicate meaningful differences, terminal half-life differences should be considered qualitative due to their dependence on the inherently variable V_{ss} value between individuals. Further, following oral dosing the changes in V_{ss}/F will reflect only changes in *F* for metabolic interactions. Therefore, this estimation of *F* change can subsequently be utilized to assess changes in *CL* alone from calculations of *CL*/*F*, two parameters that are considered indistinguishable from one another following oral dosing.

Table 2.7: Discrimination of Clearance (*CL*) from Bioavailability (*F*) Changes for Orally Dosed Midazolam (Victim) and Clarithromycin (Perpetrator) from the Study of Quinney et al. [16]

Victim	Perpetrator	$\frac{AUC^{DDI}}{AUC^{Control}}$	Percent *AUC* Extrapolation (DDI/Control)	$\frac{V_{ss}/F^{DDI}}{V_{ss}/F^{Control}}$	$\frac{V_{ss}^{DDI}}{V_{ss}^{Control}}$	$\frac{F^{DDI}}{F^{Control}}$	$\frac{CL/F^{DDI}}{CL/F^{Control}}$	$\frac{CL^{DDI}}{CL^{Control}}$	Ref.
Midazolam (IV)	Clarithromycin (500 mg BID; 7 Days)	Observed: 3.2	Observed: 44% / 19%[a]	–	Observed: 1.16[a]	Observed: 2.12	–	Observed: 0.35	[16]
$^{15}N_3$-Midazolam (Oral)	Clarithromycin (500 mg BID; 7 Days)	Observed: 8.2	Observed: 33% / 12%[a]	Observed: 0.35[a]	Assumed: 1	Estimated: 2.84[b]	Observed: 0.14	Estimated: 0.40[b]	[16]

Pharmacokinetic values reported in the table are based on published average values, unless otherwise noted
Abbreviations: *AUC*, area under the curve; BID, twice daily; *CL*, clearance; DDI, drug-drug interaction; *F*, bioavailability; Ref., reference; V_{ss}, volume of distribution at steady state
[a]Ratios are calculated by digitization of published average plasma concentration-time profiles and performing non-compartmental analysis
[b]Ratios are calculated for each individual using published individual PK data; the reported value reflects the average of each individual ratio

References

1. Grover A, Benet LZ. Effects of drug transporters on volume of distribution. *AAPS J*. 2009;11(2):250-261.
2. Benet LZ, Bowman CM, Sodhi JK. How transporters have changed basic pharmacokinetic understanding. *AAPS J*. 2019;21(6):103.
3. Tornio A, Filppula AM, Niemi M, Backman JT. Clinical studies on drug-drug interactions involving metabolism and transport: methodology, pitfalls and interpretation. *Clin Pharmacol Ther*. 2019;105(6):1345-1361.
4. Isoherranen N, Lutz JD, Chung SP, Hachad H, Levy RH, Ragueneau-Majlessi I. Importance of multi-P450 inhibition in drug-drug interactions: evidence of incidence, inhibition magnitude, and prediction from in vitro data. *Chem Res Toxicol*. 2012;25(11):2285-2300.
5. Niemi M, Backman JT, Fromm MF, Neuvonen PJ, Kivistö KT. Pharmacokinetic interactions with rifampicin. *Clin Pharmacokinet*. 2003*;*42(9):819-850.
6. Pelkonen O, Mäeenpäeä J, Taavitsainen P, Rautio A, Paunio H. Inhibition and induction of human cytochrome P450 (CYP) enzymes. Xenobiotica. 1998;28:1203-1253.
7. Pelkonen O, Turpeinen M, Hakkola J, Honkakoski P, Hukkanen J, Raunio H. Inhibition and induction of human cytochrome P450 enzymes: current status. *Arch Toxicol*. 2008;82(10):667-715.
8. Polasek TM, Lin FPY, Miners JO, Doogue MP. Perpetrators of pharmacokinetic drug-drug interactions arising from altered cytochrome P450 activity: a criteria-based assessment. *Br J Clin Pharmacol*. 2011;71(5):727-736.

9. Bi Y, Mathialagan S, Tylaska L, Fu M, Keefer J, Vildhede A, Costales C, Rodrigues AD, Varma MVS. Organic anion transporter 2 mediates hepatic uptake of tolbutamide, a CYP2C9 probe drug. J Pharmacol Exp Ther. 2018;364(3):390-398.
10. Kajosaari LI, Laitila J, Neuvonen PJ, Backman JT. Metabolism of repaglinide by CYP2C8 and CYP3A4 in vitro: effect of fibrates and rifampicin. *Basic Clin Pharmacol Toxicol.* 2005;97:249-256.
11. Wu C-Y, Benet LZ. Predicting drug disposition via application of BCS: transport / absorption / elimination interplay and development of a biopharmaceutics drug disposition classification system. *Pharm Res*. 2005;22(1):11-23.
12. Benet LZ, Galeazzi RL. Noncompartmental determination of the steady-state volume of distribution. *J Pharm Sci*. 1979;68(8):1071-1074.
13. Wahlländer A, Paumgartner G. Effect of ketoconazole and terbinafine on the pharmacokinetics of caffeine in healthy volunteers. *Eur J Clin Pharmacol*. 1989;37(3):279-283.
14. Leemann TD, Devi KP, Dayer P. Similar effect of oxidation deficiency (debrisoquine polymorphism) and quinidine on the apparent volume of distribution of (±)-metoprolol. *Eur J Clin Pharmacol*. 1993;45(1):65-71.
15. Gorski JC, Jones DR, Haehner-Daniels BD, Hamman MA, O'Mara EM, Hall SD. The contribution of intestinal and hepatic CYP3A4 to the interaction between midazolam and clarithromycin. *Clin Pharmacol Ther*. 1998;64(2):133-143.
16. Quinney SK, Haehner BD, Rhoades MB, Lin Z, Gorski JC, Hall SD. Interaction between midazolam and clarithromycin in the elderly. *Br J Clin Pharmacol*. 2008;65(1):98-109.

17. Olkkola KT, Aranko K, Luurila H, Hiller A, Saarnivarra L, Himberg JJ, Neuvonen PJ. A potentially hazardous interaction between erythromycin and midazolam. *Clin Pharmacol Ther*. 1993;53(3):298-305.
18. Swart EL, van der Hoven B, Groeneveld ABJ, Touw DJ, Danhof M. Correlation between midazolam and lignocaine pharmacokinetics and MEGX formation in healthy volunteers. *Br J Clin Pharmacol*. 2002;53(2):133-139.
19. Kharasch ED, Walker A, Hoffer C, Sheffels P. Sensitivity of intravenous and oral alfentanil and pupillary miosis as minimally invasive and noninvasive probes for hepatic and first-pass CYP3A activity. *J Clin Pharmacol.* 2005;45(1):1187-1197.
20. Isoherranen N, Ludington SR, Givens RC, Lamba JK, Pusek SN, Dees EC, Blough DK, Iwanaga K, Hawke RL, Schuetz EG, Watkins PB, Thummel KE, Paine MF. The influence of CYP3A5 expression on the extent of hepatic CYP3A inhibition is substrate-dependent: an in vitro-in vivo evaluation. *Drug Metab Dispos*. 2008;36(1):146-154 (2008).
21. Olkkola KT, Ahonen J, Neuvonen PJ. The effect of systemic antimycotics, itraconazole and fluconazole, on the pharmacokinetics and pharmacodynamics of intravenous and oral midazolam. *Anesth Analg*. 1996;82(3):511-516.
22. Tsunoda SM, Velez RL, von Moltke LL, Greenblatt DJ. Differentiation of intestinal and hepatic cytochrome P450 3A activity with use of midazolam as an in vivo probe: effect of ketoconazole. *Clin Pharmacol Ther.* 1999;66(5):461-471.
23. Shin K-H, Ahn LY, Choi MH, Moon J-Y, Lee J, Jang I-J, Yu K-S, Cho J-Y. Urinary 6β-hydroxycortisol/cortisol ratio most highly correlates with midazolam clearance under

hepatic CYP3A inhibition and induction in females: a pharmacometabolomics approach. *AAPS J*. 2016;18(5):1254-1261.

24. Kirby BJ, Collier AC, Kharasch ED, Whittington D, Thummel KE, Unadkat JD. Complex drug interactions of HIV protease inhibitors 1: inactivation, induction, and inhibition of cytochrome P450 3A by ritonavir or nelfinavir. *Drug Metab Dispos*. 2011;39(6):1070-1078.
25. Loi C-M, Parker BM, Cusak BJ, Vestal RE. Aging and drug interactions. III. Individual and combined effects of cimetidine and ciprofloxacin on theophylline metabolism in healthy male and female nonsmokers. *J Pharmacol Exp Ther*. 1997;280(2):627-637.
26. Breen KJ, Bury R, Desmond MB, Mashford MB, Morphett B, Westwood B, Shaw RG. Effects of cimetidine and ranitidine on hepatic drug metabolism. *Clin Pharmacol Ther*. 1982;31(3):297-300.
27. Gugler R, Wolf M, Hansen H-H, Jensen JC. The inhibition of drug metabolism by cimetidine in patients with liver cirrhosis. Klin Wochenschr. 1984;62(23):1126-1131.
28. Jackson JE, Powell JR, Wandell M, Bentley J, Dorr R. Cimetidine decreases theophylline clearance. *Am Rev Respir Dis*. 1981;123(6):615-617.
29. Lin JH, Chremos AN, Chiou R, Yeh KC, Williams R. Comparative effect of famotidine and cimetidine on the pharmacokinetics of theophylline in normal volunteers. *Br J Clin Pharmacol*. 1987;24(5):669-672.
30. Macias WL, Bergstrom RF, Cerimele BJ, Kassahun K, Tatum DE, Callagan JT. Lack of effect of olanzapine on the pharmacokinetics of a single aminophylline dose in healthy men. *Pharmacotherapy*. 1998;18(6):1237-1248.

31. Bachmann K, Sullivan TJ, Reese JH, Jauregui L, Miller K, Scott M, Yeh KC, Stepanavage M, King JD, Schwartz J. Controlled study of the putative interaction between famotidine and theophylline in patients with chronic obstructive pulmonary disease. *J Clin Pharmacol*. 1995;35(5):529-535.
32. Davis RL, Quenzer RW, Kelly HW, Powell JR. Effect of the addition of ciprofloxacin on theophylline pharmacokinetics in subjects inhibited by cimetidine. *Ann Pharmacother*. 1992;26(1):11-13.
33. Prince RA, Casabar E, Adair CG, Wexler DB, Lettieri J, Kasik JE. Effect of quinolone antimicrobials on theophylline pharmacokinetics. *J Clin Pharmacol*. 1989;29(7):650-654.
34. Abernethy DR, Egan JM, Dickinson TH, Carrum G. Substrate-selective inhibition by verapamil and diltiazem: differential disposition of antipyrine and theophylline in humans. *J Pharmacol Exp Ther*. 1988;224(3):994-999.
35. Sano M, Kawakatsu K, Ohkita C, Yamamoto I, Takeyama M, Yamashina H, Goto M. Effects of enoxacin, ofloxacin and norfloxacin on theophylline disposition in humans. *Eur J Clin Pharmacol*. 1988;35(2):161-165.
36. Stringer KA, Mallet J, Clarke M, Lindenfeld JA. The effect of three different oral doses of verapamil on the disposition of theophylline. *Eur J Clin Pharmacol*. 1992;43(1):35-38.
37. Nielsen-Kudsk JE, Buhl JS, Johannessen AC. Verapamil-induced inhibition of theophylline elimination in healthy humans. *Pharmacol Toxicol*. 1990;66(2):101-103.

38. Back DJ, Tjia J, Mönig H, Ohnhaus EE, Park BK. Selective inhibition of drug oxidation after simultaneous administration of two probe drugs, antipyrine and tolbutamide. *Eur J Clin Pharmacol*. 1988;34(2):157-163.

39. Roberts RK, Grice J, Wood L, Petroff V, McGuffie C. Cimetidine impairs the elimination of theophylline and antipyrine. *Gastroenterology*. 1981;81(1):19-21.

40. Ciraulo DA, Barnhill J, Boxenbaum H. Pharmacokinetic interaction of disulfiram and antidepressants. *Am J Psychiatry*. 1985;142(11):1373-1374.

41. Cremer KF, Secor J, Speeg KV Jr. The effect of route of administration on the cimetidine-theophylline drug interaction. *J Clin Pharmacol*. 1989;29(5):451-456.

42. Loi C-M, Parker BM, Cusack BJ, Vestal RE. Individual and combined effects of cimetidine and ciprofloxacin on theophylline metabolism in male nonsmokers. *Br J Clin Pharmacol*. 1993;36(3):195-200.

43. Prince RA, Wing DS, Weinberger MM, Hendeles LS, Riegelman S. Effects of erythromycin on theophylline kinetics. *J Allergy Clin Immunol*. 1981;68(6):427-431.

44. Benet LZ, Bowman CM, Koleske ML, Rinaldi CL, Sodhi JK. Understanding drug-drug interaction and pharmacogenomic changes in pharmacokinetics for metabolized drugs. *J Pharmacokinet Pharmacodyn*. 2019;46(2):155-163.

CHAPTER 3: A SIMPLE METHODOLOGY TO DIFFERENTIATE CHANGES IN BIOAVAILABILITY FROM CHANGES IN CLEARANCE FOLLOWING ORAL DOSING OF METABOLIZED DRUGS[*]

Abstract

Accurately discriminating changes in clearance (*CL*) from changes in bioavailability (*F*) following an oral drug-drug interaction is difficult without carrying out an intravenous interaction study. This may be true for drugs that are clinically-significant transporter substrates, however, for interactions that are strictly metabolic it has been recognized that volume of distribution remains unchanged between both phases of the interaction study. With the understanding that changes in volume of distribution will be minimal for metabolized drugs, the inverse of the change in apparent volume of distribution at steady-state (V_{ss}/F) can provide adequate estimates of the change in bioavailability alone. Utilization of this estimate of *F* change in tandem with the observed apparent clearance (*CL*/*F*) change in an oral drug-drug interaction can provide an estimate of the change in clearance alone. Here, we examine drug-drug interactions involving five known inhibitors and inducers of cytochrome P450 (CYP) 3A4 on victim drugs midazolam and apixaban for which the interaction was carried out both orally and intravenously, allowing for evaluation of this methodology. Predictions of *CL* and *F* changes based on oral data were reasonably close to observed changes based on intravenous studies, demonstrating that this simple yet powerful methodology can reasonably differentiate changes in *F* from changes in *CL* for oral metabolic drug interactions when only oral data are available. Utilization of this relatively

[*] Modified from the publication: Sodhi JK, Benet LZ. A simple methodology to differentiate changes in bioavailability from changes in clearance following oral dosing of metabolized drugs. *Clin Pharmacol Ther.* 2020;108(2):306-315.

simple methodology to evaluate DDIs for orally dosed drugs will have a significant impact on how DDIs are interpreted from a drug development and regulatory perspective.

Introduction

Anticipation of extent of change in (*CL*) of victim drugs in drug-drug interaction (DDI) studies is critical in recognizing potential drug combinations that may result in loss of efficacy or a safety finding due to alterations in drug exposure (area under the curve; *AUC*), as changes in clearance are inversely related to exposure changes (referred to subsequently as Equation 1):

$$AUC = \frac{F \cdot Dose}{CL}$$

Following oral dosing, however, changes in bioavailability (*F*) must also be considered since changes in extent of absorption or first pass extraction due to a DDI may also result in *AUC* changes. As evident in the above relationship, knowledge of dose and the readily measurable *AUC* results in a ratio of *CL* to *F*, two parameters that are difficult to distinguish from one another after oral dosing. Oral bioavailability can be estimated if the drug is also dosed intravenously (IV) via examination of the dose-normalized *AUC* ratio from oral to IV administration. However, most orally approved drugs have not been studied under IV dosing conditions and therefore these clearance determinations are confounded by bioavailability.

Changes in half-life and mean residence time (*MRT*) are not related to *F*. Therefore, for primarily metabolized drugs, one may attempt to differentiate changes in *CL* versus *F* in a DDI by examining the magnitude of change in half-life and *MRT* compared to *AUC* and C_{max}, as we have recently reviewed [1]. If a drug were to follow simple one compartment disposition kinetics, the change in half-life would reflect the change in *CL*, and knowing the change in *AUC* for an orally dosed drug with a metabolic DDI, the change in *F* could be determined using the above

relationship. However, for drugs only dosed orally this would not be known. Alternatively, low extraction ratio drugs will have minimal first pass elimination, therefore changes in *CL*/*F* can be primarily attributed to a change in *CL* rather than *F*. However, extraction ratio cannot be determined if only oral data are available.

It is important to recognize that *MRT* and half-life are a function of both clearance and volume of distribution as given in the following relationship [2]:

$$MRT = \frac{V_{SS} \,/\, F}{CL \,/\, F}$$

where V_{ss} is the volume of distribution at steady-state. And, it has been recognized that when transporters are involved in drug disposition, significant transporter drug interactions may result in volume of distribution changes in addition to potential changes in clearance [3]. Due to the dependence of *MRT* and terminal half-life on both clearance and volume of distribution, attempts to predict changes in drug concentration-time curves following DDI or pharmacogenomic variance studies may prove challenging if changes in volume of distribution are not considered. It is possible that interactions can alter V_{ss} differently than *CL*, even resulting in half-life changes that are counterintuitive to the direction of change in clearance (i.e. an interaction with a decrease in clearance can also display a decrease in half-life due to large decreases in volume of distribution). Recently, our laboratory has critically analyzed [4] and summarized [5] such changes in apparent clearance (*CL*/*F*), apparent volume of distribution at steady state (V_{ss}/*F*), *MRT* and terminal half-life for orally dosed transporter substrates (atorvastatin [6], glyburide [7] and rosuvastatin [8]) in clinical DDI studies with concomitant IV rifampin (an OATP1B1 and BCRP

inhibitor). In all of these DDIs, a decrease in *CL*/*F* was associated with a decrease in terminal half-life (rather than a prolonged half-life) due to a significant decrease in V_{ss}/F.

However, for a metabolic drug interaction (no transporter involvement) it is expected that volume of distribution would remain unchanged. In **Table 3.1** V_{ss} changes are summarized for exemplary clinical DDI studies involving IV administration of the primarily metabolized drugs caffeine [9], midazolam [10, 11] and theophylline [12]. The magnitude of change in exposure ranged from 1.3 – 3.2 in these DDI studies, however V_{ss} remains unchanged (0.92 – 1.1). A comprehensive analysis of changes in V_{ss} for CYP index substrates in clinical IV DDI studies was presented in Chapter 2, concluding that V_{ss} is unaffected in strictly metabolic DDI studies. Here we demonstrate how this understanding can be further applied to distinguish *CL* and *F* for DDIs that only involve metabolism.

Utilization of the Clearance and Bioavailability Discrimination Methodology

With knowledge that V_{ss} does not change for metabolic drug interactions, the inverse of the change in V_{ss}/F in the interaction versus control phase for oral metabolic interactions can provide an estimate of change in *F*, as depicted in **Figure 3.1**. In other words, the change in V_{ss}/F is approximately equal to the inverse of the change in bioavailability in the interaction versus control phase for metabolic interactions.

By accounting for the estimated change in bioavailability (from **Figure 3.1**) in the observed ratio of change in apparent clearance (*CL*/*F*), it is possible to estimate the change in systemic clearance alone, as depicted in **Figure 3.2**.

This methodology is quite simple yet powerful, as it can provide reasonable estimates of how changes in *F* can be differentiated from changes in *CL* for oral metabolic drug interactions when only oral data are available.

Table 3.1: Changes in Exposure (*AUC*), Clearance (*CL*) and Volume of Distribution at Steady State (V_{ss}) in Intravenous Metabolic Drug-Drug Interactions

Victim Drug	Primary Enzyme	Perpetrator Drug	Inhibition Target	$\frac{AUC^{DDI}}{AUC^{Con}}$	$\frac{CL^{DDI}}{CL^{Con}}$	$\frac{V_{ss}^{DDI}}{V_{ss}^{Con}}$	Reference
Caffeine	CYP1A2	Terbinafine	CYP2D6 CYP1A2	1.3	0.79	1.1	[9]
Midazolam	CYP3A4	Erythromycin	CYP3A4 P-gp	1.5	0.66	0.93	[10]
Midazolam	CYP3A4	Fluconazole	CYP3A4 CYP2C9 CYP2C19	2.0	0.49	0.92	[11]
Midazolam	CYP3A4	Itraconazole	CYP3A4 CYP2J2 P-gp	3.2	0.31	1.1	[11]
Theophylline	CYP1A2	Cimetidine	CYP1A2 OCT2	1.6	0.60	1.1	[12]
Theophylline	CYP1A2	Ciprofloxacin	CYP1A2 CYP3A4	1.4	0.69	1.0	[12]
Theophylline	CYP1A2	Cimetidine + Ciprofloxacin	CYP1A2 CYP3A4 OCT2	1.8	0.55	1.1	[12]

Ratios are expressed as interaction / control

Abbreviations: AUC, area under the curve; *CL*, clearance; *Con*, control; CYP, cytochrome P450; OCT, organic cation transporter; P-gp, P-glycoprotein; V_{ss}, volume of distribution at steady-state

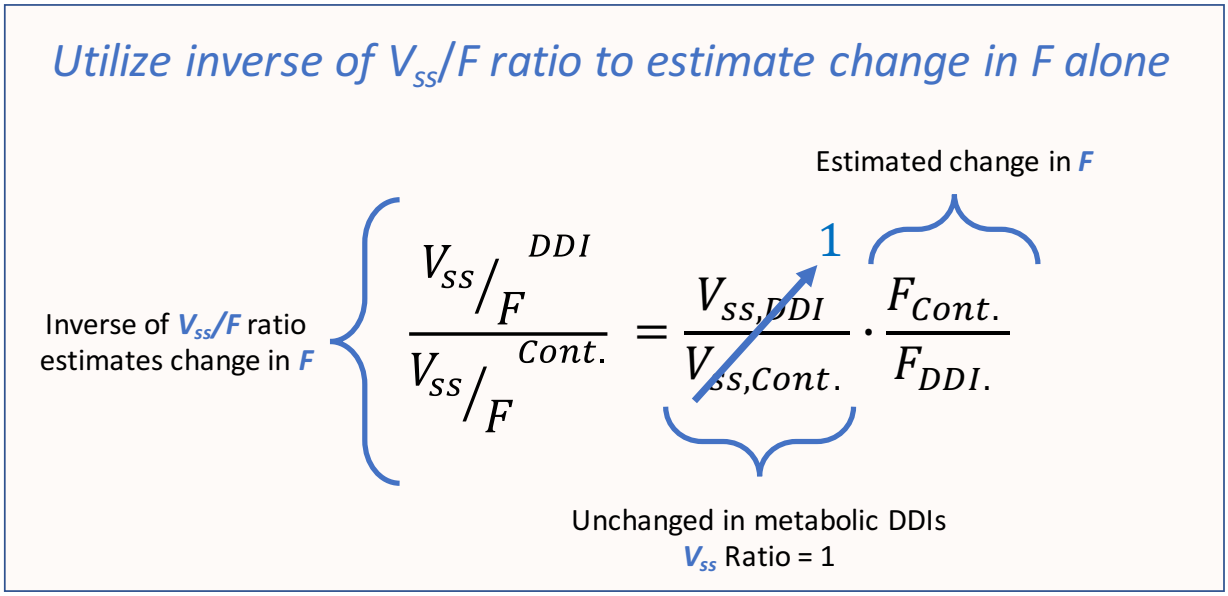

Figure 3.1: The inverse of change in the apparent volume of distribution at steady state (V_{ss}/F) can provide estimates of change in bioavailability (F) in oral metabolic drug-drug interactions.

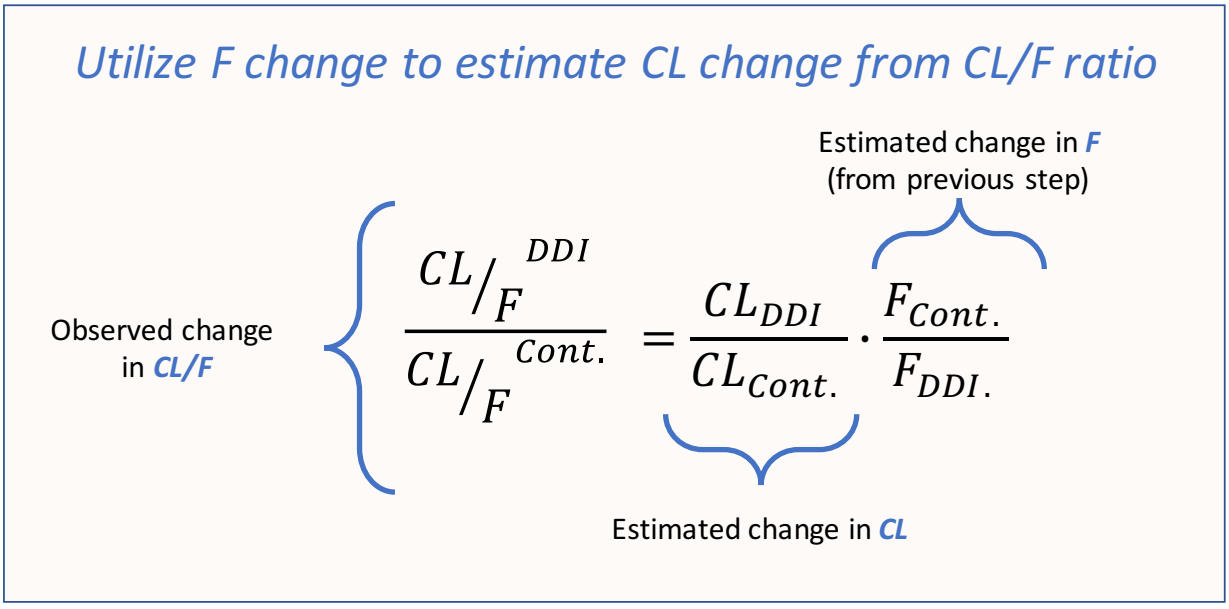

Figure 3.2: Utilization of estimated change in bioavailability (F) can discriminate the change in clearance (CL) from apparent clearance (CL/F) ratios.

Methods

The CYP3A4 *in vivo* index substrate midazolam was selected as a model metabolized drug for evaluation of the proposed methodology. Drug interaction studies were identified for which midazolam was dosed both orally and IV as the victim drug, and the perpetrator was a clinically recommended CYP3A4 inhibitor or inducer based on a recent compilation of clinical index substrates and inhibitors [13]. Apixaban was also selected as an additional drug to further evaluate this methodology.

Changes in exposure (*AUC*), clearance (*CL*), apparent clearance (*CL*/*F*), volume of distribution at steady state (V_{ss}), apparent volume of distribution at steady state (V_{ss}/F), bioavailability (*F*), and percent extrapolation of *AUC* were examined and reported as ratios of interaction/control. The published pharmacokinetic values reported by the original investigators were utilized in priority, however all clinical studies investigated here did not report V_{ss}/F, therefore it was necessary to utilize the published pharmacokinetic profiles to estimate this ratio and supplement any other parameters not reported. This was achieved by digitization of victim drug mean plasma-concentration time profiles that were subsequently analyzed by noncompartmental analysis using WinNonlin Professional Edition Version 2.1 (Pharsight, Mountain View, CA, USA). All pharmacokinetic ratios calculated from digitization of published pharmacokinetic profiles are specifically indicated as a footnote for clarity. Digitized *AUC* values were compared to reported *AUC* values and differences were found to be less than 20%, indicating that the reported average concentration-time profiles investigated here reasonably represented the study population. The percent of *AUC* extrapolations are listed following both

IV and oral drug administration as an indication of the potential confidence in the derived pharmacokinetic parameters.

Mean absorption time (*MAT*) was estimated, as we previously described [6], as the reciprocal of the first-order absorption rate constant after the oral concentration-time data were fit to a 2-compartment model with absorption from the gut compartment using WinNonlin. Mean residence time (*MRT*) was calculated as the ratio of the area under the first moment curve ($AUMC_{0-\infty}$) divided by $AUC_{0-\infty}$ for intravenous interactions. However, for oral interactions calculation of *MRT* requires that *MAT* must be subtracted from the ratio of *AUMC / AUC*. The second equation presented in this chapter was utilized to calculate V_{ss} or V_{ss}/F.

Prediction of extent of change of *F* and *CL* following oral dosing was calculated using the methodology presented in **Figure 3.1** and **Figure 3.2**, respectively. In each DDI presented, the comparison of the change in terminal half-life following IV and oral dosing is also reported as footnotes in **Tables 2.2 – 2.5**. Assuming the change in half-life following oral dosing accurately reflected the change in *CL*, it is possible to then predict the change in *F* using the first equation presented in this chapter.

Results

We identified clinical DDIs in the literature where the effects of widely-used metabolic inhibitors or inducers were examined following both IV and oral dosing of the primarily metabolized victim drug midazolam, as well as for an additional drug apixaban to further evaluate this methodology. Sufficient data and concentration-time curves were available in the publications for us to demonstrate the utility and potential reliability of this methodology.

Midazolam was dosed orally and IV with and without the inhibitors clarithromycin [14], fluconazole [15], itraconazole [11], and ritonavir [16], and both midazolam and apixaban were dosed orally and IV with and without multiple dosing of the inducer rifampin [16, 17]. In each of these six metabolic interactions, no significant change in V_{ss} was observed following IV dosing of the victim drug, with V_{ss} ratios ranging from 0.87 to 1.19.

Table 3.2 displays the ratios of change in IV and oral midazolam pharmacokinetic parameters in the perpetrator versus control phase for the clarithromycin [14], fluconazole [15], and ritonavir [16] interaction studies. In the clarithromycin study, clarithromycin (500 mg BID; 7 days) caused a 63% decrease in midazolam IV clearance [14]. Assuming that this decrease in clearance would also occur following oral dosing, the investigators estimated clarithromycin increased oral bioavailability by 2.42-fold. Using the methodology proposed here to predict changes in *CL* and *F* for the oral data only, with the assumption that V_{ss} is unchanged for this metabolic interaction, the predicted change in *F* was a 2.94-fold increase and that *CL* had decreased 59%. In the fluconazole study, concomitant fluconazole administration (200 mg; single dose) resulted in a 32% decrease in midazolam IV clearance (predicted 40% decrease from oral study), and a 2.33-fold increase in oral bioavailability (predicted 2.38 increase from oral study) [15]. In the ritonavir interaction, multiple dosing of ritonavir (800 mg; 14 days) resulted in a 71% decrease in midazolam IV clearance (predicted 72% decrease from oral only study) and a 2.55-fold increase in bioavailability (predicted 2.78 increase from oral only study) [16].

Changes in midazolam pharmacokinetic parameters in the interaction with itraconazole (200 mg; 4 days (IV); 6 days (oral)) are listed in **Table 3.3** [11]. Administration of itraconazole for 4 days resulted in a 69% decrease in IV midazolam clearance. The oral interaction between

itraconazole and midazolam was studied on day 6, and with the assumption that alteration in midazolam clearance is similar between day 4 (IV DDI) and day 6 (oral DDI), the resulting increase in bioavailability is 2.46-fold. The methodology predicted a 2.00-fold increase in bioavailability and a 70% reduction in clearance.

Table 3.4 shows the changes in oral and IV midazolam pharmacokinetic parameters due to multiple doses of rifampin (600 mg QD; 14 days), which resulted in a 2.16-fold increase in midazolam IV clearance and 81% decrease in bioavailability [16]. The oral midazolam interaction data results in an 11.7-fold increase in *CL*/*F*, but by utilizing the methodology presented here, it is possible to predict that the large change in *CL*/*F* is a result of an approximate 2.93-fold increase in clearance and a 75% reduction in oral bioavailability.

Table 3.5 shows that multiple doses of rifampin caused a 1.64-fold increase in apixaban IV clearance and a 24% decrease in oral bioavailability [17]. Using the methodology proposed here for the oral data-only predicts that *CL* had increased 1.50-fold and that *F* decreased by 30%.

Discussion

Utilization of this relatively simple methodology to evaluate DDIs for orally dosed drugs will have a significant impact on how DDIs are interpreted from a drug development and regulatory perspective. For metabolic interactions, this methodology can reasonably differentiate the extent of change in *F* from changes in *CL* when IV dosing data are unavailable. Here we demonstrate the utility of this methodology for the primarily metabolized drug midazolam, a commonly-used *in vivo* index substrate of CYP3A4, and for one study with apixaban, for which both oral and IV interaction data were available in the same subjects.

Table 3.2: Utilization of the Proposed Methodology to Discriminate Clearance from Bioavailability Changes for Orally Dosed Midazolam (Victim) and the Perpetrators: Clarithromycin, Fluconazole, Ritonavir

Victim	Perpetrator	$\frac{AUC^{DDI}}{AUC^{Control}}$	Percent *AUC* Extrapolation (DDI/Control)	$\frac{V_{ss}/F^{DDI}}{V_{ss}/F^{Control}}$	$\frac{V_{ss}^{DDI}}{V_{ss}^{Control}}$	$\frac{F^{DDI}}{F^{Control}}$	$\frac{CL/F^{DDI}}{CL/F^{Control}}$	$\frac{CL^{DDI}}{CL^{Control}}$
Gorski et al., 1998 [14]								
Midazolam (IV)	Clarithromycin (500 mg BID; 7 Days)	Observed: 2.66	Observed: 38% / 12%[a]	–	Observed: 1.05[a]	Observed: 2.42	–	Observed: 0.37
Midazolam (Oral)	Clarithromycin (500 mg BID; 7 Days)	Observed: 7.00	Observed: 34% / 22%[a]	Observed: 0.34[a]	Assumed: 1	Estimated: 2.94[b]	Observed: 0.14	Estimated: 0.41[b]
Kharasch et al., 2005 [15]								
Midazolam (IV)	Fluconazole (200 mg; single dose)	Observed: 1.4	Observed: 17% / 7%	–	Observed: 1.10[a]	Observed: 2.33	–	Observed: 0.68
Midazolam (Oral)	Fluconazole (200 mg; single dose)	Observed: 3.9	Observed: 19% / 8%	Observed: 0.42[a]	Assumed: 1	Estimated: 2.28[b]	Observed: 0.25	Estimated: 0.60[c]
Kirby et al., 2011 [16]								
Midazolam (IV)	Ritonavir (800 mg QD; 8 Days)	Observed: 3.31	Observed: 21% / 3%[a]	–	Observed: 1.04[a]	Observed: 2.55	–	Observed: 0.29
Midazolam (Oral)	Ritonavir (800 mg QD; 8 Days)	Observed: 8.28	Observed: 25% / 5%[a]	Observed: 0.36[a]	Assumed: 1	Estimated: 2.78[b]	Observed: 0.10	Estimated: 0.28[d]

Pharmacokinetic values reported in the table are based on published average values, unless otherwise noted
Abbreviations: *AUC*, area under the curve; *CL*, clearance; DDI, drug-drug interaction; *F*, bioavailability; IV, intravenous; V_{ss}, volume of distribution at steady state
[a]Ratios are calculated by digitization of published average plasma concentration-time profiles and performing non-compartmental analysis
[b]Terminal half-life increased 2.7-fold following IV dosing and 2.6-fold following oral dosing. Therefore, similar estimates of the change in *F* and *CL* could have been made by using the change in oral terminal half-life and Eq. 1
[c]Terminal half-life increased 1.2-fold following IV dosing and 1.5-fold following oral dosing. Therefore, similar estimates of the change in *F* and *CL* could have been made by using the change in oral terminal half-life and Eq. 1
[d]Terminal half-life increased 3.0-fold following IV dosing and 2.9-fold following oral dosing. Therefore, similar estimates of the change in *F* and *CL* could have been made by using the change in oral terminal half-life and Eq. 1

Table 3.3: Utilization of the Proposed Methodology to Discriminate Clearance from Bioavailability Changes for Orally Dosed Midazolam (Victim) and Itraconazole (Perpetrator) from the Study of Olkkola et al. [11]

Victim	Perpetrator	$\frac{AUC^{DDI}}{AUC^{Control}}$	Percent *AUC* Extrapolation (DDI/Control)	$\frac{V_{ss}/F^{DDI}}{V_{ss}/F^{Control}}$	$\frac{V_{ss}^{DDI}}{V_{ss}^{Control}}$	$\frac{F^{DDI}}{F^{Control}}$	$\frac{CL/F^{DDI}}{CL/F^{Control}}$	$\frac{CL^{DDI}}{CL^{Control}}$	Ref.
Midazolam (IV; Day 4)	Itraconazole (200 mg QD; Day 4)	Observed: 3.22[a]	Observed: 16% / 1%[b]	–	Observed: 1.08	Observed: 2.46	–	Observed: 0.31	[11]
Midazolam (Oral; Day 6)	Itraconazole (200 mg QD; Day 6)	Observed: 6.64	Observed: 22% / 0%[b]	Observed: 0.50[b]	Assumed: 1	Estimated: 2.00[c]	Observed: 0.15[a]	Estimated: 0.30[c]	[11]

Pharmacokinetic values reported in the table are based on published average values, unless otherwise noted
Abbreviations: *AUC*, area under the curve; *CL*, clearance; DDI, drug-drug interaction; *F*, bioavailability; Ref, reference; V_{ss}, volume of distribution at steady state
[a]*AUC* or *CL* was calculated with the equation *AUC* = *dose / CL* using known dose and reported values of *CL* or *AUC*
[b]Ratios are calculated by digitization of published average plasma concentration-time profiles and performing non-compartmental analysis
[c]Terminal half-life increased 2.4-fold following IV dosing and 3.6-fold following oral dosing. Estimates of the changes in *F* and *CL* would not have been accurate by using the change in oral terminal half-life and Eq. 1

Table 3.4: Utilization of the Proposed Methodology to Discriminate Clearance from Bioavailability Changes for Orally Dosed Midazolam (Victim) and Multiple Dosed Rifampin (Perpetrator) from the Study of Kirby et al. [16]

Victim	Perpetrator	$\frac{AUC^{DDI}}{AUC^{Control}}$	Percent *AUC* Extrapolation (DDI/Control)	$\frac{V_{ss}/F^{DDI}}{V_{ss}/F^{Control}}$	$\frac{V_{ss}^{DDI}}{V_{ss}^{Control}}$	$\frac{F^{DDI}}{F^{Control}}$	$\frac{CL/F^{DDI}}{CL/F^{Control}}$	$\frac{CL^{DDI}}{CL^{Control}}$	Ref.
Midazolam (IV)	Rifampin (600 mg QD; 14 Days)	Observed: 0.44	Observed: 4% / 3%[a]	–	Observed: 1.19[a]	Observed: 0.19	–	Observed: 2.16	[16]
Midazolam (Oral)	Rifampin (600 mg QD; 14 Days)	Observed: 0.081	Observed: 6% / 5%[a]	Observed: 3.93[a]	Assumed: 1	Estimated: 0.25[b]	Observed: 11.7	Estimated: 2.93[b]	[16]

Pharmacokinetic values reported in the table are based on published average values, unless otherwise noted
Abbreviations: *AUC*, area under the curve; *CL*, clearance; DDI, drug-drug interaction; *F*, bioavailability; V_{ss}, volume of distribution at steady state
[a]Ratios are calculated by digitization of published average plasma concentration-time profiles and performing non-compartmental analysis
[b]Terminal half-life decreased by 39% following IV dosing and by 74% following oral dosing. Estimates of the changes in *F* and *CL* would be significantly poorer and inaccurate using Eq. 1

Table 3.5: Utilization of the Proposed Methodology to Discriminate Clearance from Bioavailability Changes for Orally Dosed Apixaban (Victim) and Multiple Dosed Rifampin (Perpetrator) from the Study of Vakkalagadda et al. [17]

Victim	Perpetrator	$\frac{AUC^{DDI}}{AUC^{Control}}$	Percent *AUC* Extrapolation (DDI/Control)	$\frac{V_{ss}/F^{DDI}}{V_{ss}/F^{Control}}$	$\frac{V_{ss}^{DDI}}{V_{ss}^{Control}}$	$\frac{F^{DDI}}{F^{Control}}$	$\frac{CL/F^{DDI}}{CL/F^{Control}}$	$\frac{CL^{DDI}}{CL^{Control}}$	Ref.
Apixaban (IV)	Rifampin (Multiple Dose)	Observed: 0.61	Observed: 1% / 2%	–	Observed: 0.87	Observed: 0.76	–	Observed: 1.64	[17]
Apixaban (Oral)	Rifampin (Multiple Dose)	Observed: 0.48	Observed: 10% / 9%	Observed: 1.42[a]	Assumed: 1	Estimated: 0.70[b]	Observed: 2.14	Estimated: 1.50[b]	[17]

[a]Ratios are calculated by digitization of published average plasma concentration-time profiles and performing non-compartmental analysis

[b]Terminal half-life decreased by 49% following IV dosing but slightly increased 1.03-fold following oral dosing. Estimates of the changes in *F* and *CL* would be significantly poorer and inaccurate using Eq. 1

Table 3.2 outlines the results of the clarithromycin [14], fluconazole [15], and ritonavir [16] drug interaction studies. In the clarithromycin-midazolam interaction study [14] significant differences in exposure change (*AUC* ratios) were observed when comparing the IV and oral DDI studies (2.66- and 7.0-fold, respectively), indicating that a significant change in both oral bioavailability and clearance occurred as a result of the interaction. The methodology presented here adequately distinguished the contribution of change in clearance from bioavailability in the oral DDI; the estimated change in *F* differed by 21% from the observed change (2.94 estimated vs. 2.42 observed), while the estimated change in *CL* only differed by 11% from the observed change with IV dosing (0.41 estimated vs. 0.37 observed). In the midazolam-fluconazole interaction study [15], the predicted changes in *F* and *CL* were quite close to observed changes calculated with IV dosing data, with only a 2% difference in *F* (2.38 estimated vs. 2.33 observed) and a 12% difference in *CL* (0.60 estimated versus 0.68 observed). In the ritonavir-midazolam DDI [16], a 9% difference in *F* and only a 3% difference in *CL* was observed between predicted and actual values. For all three of these interactions, assuming that changes in oral terminal half-life accurately reflected the change in *CL* and using Eq. 1 would also have given reasonable estimates of *CL* and *F* (as noted in footnotes b-d of **Table 3.2**).

In **Table 3.3** for the itraconazole-midazolam DDI [11], the observed changes in *CL* were remarkably close to predictions based on oral data only (3% difference in *CL*) accompanied by a 19% difference in *F*. Utilizing changes in oral terminal half-life to predict *CL* changes, then subsequently using the first relationship presented in this chapter to estimate the changes in *F*, would not have been as accurate, with prediction errors of 25% for both parameters.

The induction effect of multiple dosing of rifampin on midazolam was examined [16] (**Table 3.4**); the estimated change in *F* differed by 32% and the estimated change in *CL* differed by 35% from observed values. Although a prediction error of 30% may be considered to be quite high, it should be noted that the 12.3-fold decrease in exposure as a result of the rifampin-midazolam oral DDI was significantly larger in magnitude than other midazolam DDIs investigated, which ranged from 3.9 [15] to 8.3 [16]. Of note, the estimated change in *F* and *CL* based on oral terminal half-life changes and Eq. 1 resulted in much less accurate predictions, with errors in *F* and *CL* of 63% and 78%, respectively.

In contrast to the midazolam-rifampin DDI, estimates for the apixaban-rifampin interaction study [17] were much closer to observed values with both *F* and *CL* differing by only 9% (although *AUC* only changed approximately 2-fold). As noted in footnote b of Table 5, the estimated change in *F* and *CL* when using oral terminal half-life to predict *CL* changes resulted in markedly poorer predictions, with errors in *F* and *CL* of 40% and 41%, respectively. Of note, apixaban V_{ss} following IV dosing indicates minimal change with a ratio of 0.87, suggesting that transporters inhibited by rifampin are not involved in apixaban disposition, as was initially discussed in Chapter 2. The success of the methodology in discriminating *F* and *CL* further supports this observation since it relies on the assumption that V_{ss} is unchanged. These findings are contrary to the apixaban FDA label, which proposes that the efflux transporters BCRP and P-gp may play a clinically significant role, and further demonstrates the utility of this simple methodology in recognizing transporter versus metabolism drug interactions. A critical examination of all available apixaban clinical interaction data will be discussed in Chapter 5.

Methodology Scheme

Step-by-Step Guide to Appropriate Use of the Clearance and Bioavailability Discrimination Methodology

STEP 1: DETERMINE IF A DRUG INTERACTION AFFECTS ONLY METABOLIC ENZYMES

A. Does a Metabolic Interaction Exist?

- Victim Drug: Perform *in vitro* metabolic stability in human liver microsomes and/or human hepatocytes
- Perpetrator Drug: Perform *in vitro* reversible and/or time-dependent CYP inhibition assays

***in vitro* ADME assays**

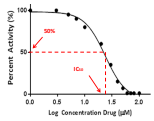

B. Is there Basis for a Transporter Interaction?

- Victim Drug: Perform *in vitro* uptake experiments in human hepatocytes and/or transporter-overexpressing cell lines; utilization of transporter inhibitors can bolster conclusions
- Perpetrator Drug: Perform *in vitro* transporter inhibition studies with probe substrates of major xenobiotic transporters

***in vitro* uptake assays**

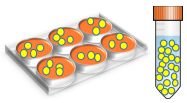

C. Will an *in vitro* Transporter Interaction be Clinically Significant?

- BDDCS Class 1: Methodology is appropriate for use; *in vitro* transporter involvement is not clinically significant
- BDDCS Class 2: Use methodology with caution; transporters may or may not be involved in clinical disposition
- BDDCS Class 3 and 4: Methodology not recommended; transporter involvement is clinically significant

BDDCS theory

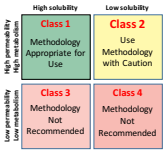

D. Does *in vivo* Pharmacokinetic Data Suggest a Transporter Interaction?

- Compare ratios of changes in *CL*/*F* to V_{ss}/F of victim drug in the interaction versus control
- If the magnitude of change is greater in V_{ss}/F than *CL*/*F* a transporter interaction is likely

Examine *in vivo* data

$$\frac{CL/F^{treated}}{CL/F^{control}} < \frac{V_{ss}/F^{treated}}{V_{ss}/F^{control}}$$

Signifies a significant transporter interaction

E. Is there Potential for Protein Binding Changes to Alter Volume of Distribution?

- Perform *in vitro* studies to determine if the perpetrator affects protein binding of the victim drug

***in vitro* binding assays**

STEP 2: ASSUME V_{SS} IS UNCHANGED FOR STRICTLY METABOLIC INTERACTIONS

Utilize the inverse of the V_{ss}/F ratio to estimate change in bioavailability (*F*)

$$\frac{V_{ss}/F^{treated}}{V_{ss}/F^{control}} = \frac{V_{ss}^{treated}}{V_{ss}^{control}} \cdot \frac{F^{control}}{F^{treated}}$$

($V_{ss}^{treated}/V_{ss}^{control} \rightarrow 1$)

$$\frac{V_{ss}/F^{treated}}{V_{ss}/F^{control}} \cong \frac{F^{control}}{F^{treated}}$$

STEP 3: UTILIZE BIOAVAILABILITY CHANGE TO ESTIMATE CHANGE IN CLEARANCE

Utilize the estimated change in F to discriminate change in clearance (*CL*)

$$\frac{CL^{treated}}{CL^{control}} = \frac{CL/F^{treated}}{CL/F^{control}} \cdot \frac{F^{control}}{F^{treated}}$$

Figure 3.3: Methodology scheme to guide appropriate use of the clearance (*CL*) and bioavailability (*F*) discrimination methodology for strictly metabolic interactions. ADME, Absorption, Distribution, Metabolism, Excretion; BDDCS, Biopharmaceutics Drug Disposition Classification System; CYP, cytochrome P450; IC_{50}, concentration of drug producing half-maximal inhibition; V_{ss}, volume of distribution at steady state

Considerations to Guide the Appropriate Use of the Discrimination Methodology

It is important to recognize the assumptions and limitations of this methodology to appropriately guide its use and prevent misinterpretations of interaction data. Calculation of V_{ss}/F relies on measurements of *CL*/*F* and *MRT*, two parameters that are derived from *AUC*, which highlights the importance of accurate determination of *AUC* for the success of this methodology. Adequate plasma sampling describing the terminal slope of the concentration-time profiles is crucial since *AUC* must be extrapolated from the final time-point to infinity. Therefore, it is imperative to inspect the percentage of *AUC* that has been extrapolated after the final sampling time point to ensure that data estimates can be reliably interpreted. In our analysis, we point out the percentage of total *AUC* that was extrapolated in each phase of the DDIs to highlight the degree of *AUC* estimation; low extrapolation percentages indicate lower probability of error in *AUC* determination, however, the converse is not necessarily true. Higher percent extrapolations may or may not indicate inaccuracies in *AUC* determination; if the terminal phase of the concentration-time profile is accurate, then the degree of extrapolation does not introduce error. The degree of extrapolation in *AUC* determinations is magnified in calculations of the area under the moment-time curve (*AUMC*), further affecting calculations of *MRT* following IV dosing (which is calculated by the ratio of *AUMC* /*AUC*). Following oral dosing, the ratio of *AUMC* /*AUC* results in the sum of *MRT* and mean absorption time (*MAT*). We proposed that *MAT* may be reasonably approximated by estimating the oral absorption rate constant (k_a) from pharmacokinetic profiles ($MAT = 1/k_a$) by fitting the data to a compartmental model that assumes first order absorption from a single compartment absorption site [6]. Certainly, all drug absorption will not follow first order kinetics from a one compartment absorption site, but the objective here is not to calculate

MAT in each phase, but rather how *MAT* changes under conditions where a perpetrator is present versus in its absence. The high relative accuracy of our predictions in **Tables 3.2 – 3.5** suggests that this assumption is reasonable. In three of the six interactions presented in **Tables 3.2 – 3.5**, attempts to use changes in terminal half-life and Eq. 1 to predict the changes of *CL* and *F* would not have been as accurate as the methodology proposed here. Since, when only oral DDI data are available, it is not possible to know if estimates using Eq. 1 may be accurate, we recommend that the procedure here always be preferred.

The methodology is only applicable to interactions where V_{ss} is unchanged, hence its appropriate application to strictly metabolic drug-drug interactions. Another scenario where it is possible that V_{ss} may change (even for purely metabolic interactions) is if a perpetrator drug alters protein binding of the victim drug by displacing it from plasma or tissue proteins, resulting in increased fraction unbound of victim drug. We believe that a protein binding interaction can be adequately predicted based on *in vitro* analysis as detailed in **Figure 3.3**. Perpetrator drugs could potentially alter blood flow that may result in increased or decreased clearance of victim drugs, however changes in V_{ss} are not anticipated with changes in blood flow. Therefore, the impact of such perpetrators is not expected to affect the utility of this methodology.

Finally, although the pharmacokinetic values reported by the original authors were utilized in priority, the data analyzed here are partially based on average reported concentration-time profiles since digitization was required to estimate the unreported V_{ss}/F for all oral interactions. When available, it may be more appropriate to utilize individual PK profiles to make predictions of changes in *CL* and *F* for each subject based on this methodology. The limitation of utilizing average pharmacokinetic concentration-time profiles is that in many cases average

profiles do not accurately represent changes within a particular individual in the drug interaction study. Utilizing the average drug concentrations of each subject at each time point results in pharmacokinetic profiles that do not necessarily represent a single subject within the study. Individual patient pharmacokinetic data are very rarely published, and further, drug interaction studies for which a victim drug is administered both orally and IV in the same patients are quite uncommon (we do not have such drug interaction data in our clinical archive), therefore it was impossible to identify such data in the literature for utilization here. Thus, we propose that utilization of this methodology be carried out for each subject in the DDI study. Efforts are underway towards establishing collaborations with laboratories that may have access to such data for further evaluation of the methodology.

For well-studied marketed drugs such as midazolam, it is often known whether or not transporters are significantly involved in drug disposition due to the availability of well-designed IV or oral interaction studies utilizing clinically-demonstrated transporter inhibitors. And for most investigational drugs, there is good evidence of the pathways governing drug disposition before drug-drug interaction studies are undertaken. However, if such data are not available for a particular drug-of-interest, we suggest the use of the Biopharmaceutics Drug Disposition Classification System (BDDCS) to anticipate which drugs may be susceptible to transporters *in vivo* [18]. The unfavorable membrane permeability of BDDCS Class 3 and 4 compounds implies their reliance on xenobiotic transporters to cross biological membranes *in vivo*, and this theory is supported by the observation that Class 3 and 4 drugs are primarily eliminated by transporter-dependent processes (i.e. renal or biliary excretion of unchanged drug). BDDCS Class 1 and 2 drugs have favorable permeability characteristics that allow passage across biological

membranes via passive processes, which is supported by the observation that these drugs are primarily metabolized. It is theorized that the rapid membrane permeability combined with the high solubility of BDDCS Class 1 drugs allows these drugs to rapidly cross membranes at concentrations high enough to saturate active transport, or alternatively the active transport amounts are small compared to the passive permeability amounts, overcoming any potential transporter effects *in vivo*, even if shown to be a transporter substrate *in vitro* [18]. BDDCS Class 2 drugs also display high permeability, but due to their low solubility it is thought that the resulting lower soluble concentrations available for passive diffusion may be incapable of saturating transporters, or passive transport may not be much greater than the contribution of active transport. Therefore, involvement of uptake or efflux transporters cannot be ruled out in the absorption and disposition of BDDCS Class 2 drugs despite their status as being primarily metabolized. However, the *in vitro* transporter interaction studies proposed in our guide to appropriate use of the methodology (**Figure 3.3**) will assist in making this decision. In summary, the proposed methodology is appropriate for BDDCS class 1 drugs, not recommended for BDDCS class 3 and 4, and should be used with caution for BDDCS class 2 drugs with recognition that transporter involvement may or may not be clinically relevant. Evaluation of the association of BDDCS class with the extent of change in V_{ss} in IV interactions is an ongoing effort in our laboratory to validate this hypothesis.

In addition to utilization of BDDCS to inform the appropriate use of our methodology, we have outlined additional *in vitro* studies that may be helpful in identifying strictly metabolic interactions (**Figure 3.3**). The recommendations outlined in **Figure 3.3** will be helpful for investigational compounds that inherently are less well-characterized than marketed drugs, as

there is increased likelihood of clinical evidence regarding the potential involvement of transporters versus enzymes with known index inhibitors.

Although our methodology relies on the assumption that V_{ss} changes in transporter drug-drug interactions, our laboratory has previously summarized how volume of distribution was observed to change based on localization of the transporter (in the liver versus kidney) and if the transporter affected is an uptake versus efflux transporter [3]. In general, large decreases in volume of distribution are observed for hepatic uptake transporters, whereas renal uptake transporter interactions do not result in volume of distribution changes, although there were exceptions observed. Inhibition of hepatic efflux transporters generally leads to a decrease in volume of distribution while renal tubule efflux transporter inhibition results in increased volume of distribution. In analysis of transporter interactions, further consideration of the inhibitory specificity of perpetrator drugs is necessary, as currently there are a limited number of well-characterized and specific clinical transporter inhibitors [13]. Therefore, there may be specific transporter interactions where V_{ss} does not change significantly and this methodology may appropriately discriminate *CL* from *F* changes. However, further validation is warranted prior to applying this methodology to transporter interactions and is an ongoing effort of our laboratory, and therefore we do not recommend its use for transporter interactions at this time.

Conclusions

For decades, the field has believed that changes in clearance could not be accurately discriminated from changes in bioavailability for oral drug interaction studies without performing an IV interaction study to confirm the extent of clearance changes. This has led to challenges in

understanding the contribution of bioavailability change in oral DDI studies, often resulting in an overprediction of clearance change and an underestimation of the impact bioavailability changes can have on observed exposure. The ingenuity of this relatively simple methodology leverages the understanding that volume of distribution appears to remain unchanged where disposition is limited to metabolism, therefore calculation of changes in oral volume of distribution can reliably provide estimation of bioavailability versus clearance changes. We recommend that this methodology be routinely utilized in the evaluation of clinical drug-drug interaction studies. Utilization of this relatively simple methodology to evaluate DDIs for orally dosed drugs will have a significant impact on how DDIs are interpreted from a drug development and regulatory perspective.

References

1. Benet LZ, Bowman CM, Koleske ML, Rinaldi CL, Sodhi JK. Understanding drug-drug interaction and pharmacogenomic changes in pharmacokinetics for metabolized drugs. *J Pharmacokinet Pharmacodyn*. 2019;46(2):155-163.
2. Benet LZ, Galeazzi RL. Noncompartmental determination of the steady-state volume of distribution. *J Pharm Sci*. 1979;68(8):1071-1074.
3. Grover A, Benet LZ. Effects of drug transporters on volume of distribution. *AAPS J*. 2009;11(2):250-261.
4. Benet LZ, Bowman CM, Liu S, Sodhi JK. The extended clearance concept following oral and intravenous dosing: theory and critical analyses. *Pharm Res*. 2018;35(12):242.
5. Benet LZ, Bowman CM, Sodhi JK. How transporters have changed basic pharmacokinetic understanding. *AAPS J*. 2019;21(6):103.
6. Lau YY, Huang Y, Frassetto L, Benet LZ. Effect of OATP1B transporter inhibition on the pharmacokinetics of atorvastatin in healthy volunteers. *Clin Pharmacol Ther.* 2007;81(2):194-204.
7. Zheng HX, Huang Y, Frassetto LA, Benet LZ. Elucidating rifampin's inducing and inhibiting effects on glyburide pharmacokinetics and blood glucose in healthy volunteers: unmasking the differential effects of enzyme induction and transporter inhibition for a drug and its primary metabolite. *Clin Pharmacol Ther*. 2009;85(1):78-85.

8. Wu H-F, Hristeva N, Chang J, Liang X, Li R, Frassetto L, Benet LZ. Rosuvastatin pharmacokinetics in Asian and White subjects wild type for both OATP1B1 and BCRP under control and inhibited conditions. *J Pharm Sci.* 2017;106(9):2751-2757.
9. Wahlländer A, Paumgartner G. Effect of ketoconazole and terbinafine on the pharmacokinetics of caffeine in healthy volunteers. *Eur J Clin Pharmacol*. 1989;37(3):279-283.
10. Swart EL, van der Hoven B, Groeneveld ABJ, Touw DJ, Danhof M. Correlation between midazolam and lignocaine pharmacokinetics and MEGX formation in healthy volunteers. *Br J Clin Pharmacol*. 2002;53(2):133-139.
11. Olkkola KT, Ahonen J, Neuvonen PJ. The effect of systemic antimycotics, itraconazole and fluconazole, on the pharmacokinetics and pharmacodynamics of intravenous and oral midazolam. *Anesth Analg*. 1996;82(3):511-516.
12. Davis RL, Quenzer RW, Kelly HW, Powell JR. Effect of the addition of ciprofloxacin on theophylline pharmacokinetics in subjects inhibited by cimetidine. *Ann Pharmacother*. 1992;26(1):11-13.
13. Tornio A, Filppula AM, Niemi M, Backman JT. Clinical studies on drug-drug interactions involving metabolism and transport: methodology, pitfalls and interpretation. *Clin Pharmacol Ther*. 2019;105(6):1345-1361.
14. Gorski JC, Jones DR, Haehner-Daniels BD, Hamman MA, O'Mara EM, Hall SD. The contribution of intestinal and hepatic CYP3A4 to the interaction between midazolam and clarithromycin. *Clin Pharmacol Ther*. 1998;64(2):133-143.

15. Kharasch ED, Walker A, Hoffer C, Sheffels P. Sensitivity of intravenous and oral alfentanil and pupillary miosis as minimally invasive and noninvasive probes for hepatic and first-pass CYP3A activity. *J Clin Pharmacol.* 2005;45(1):1187-1197.
16. Kirby BJ, Collier AC, Kharasch ED, Whittington D, Thummel KE, Unadkat JD. Complex drug interactions of HIV protease inhibitors 1: inactivation, induction, and inhibition of cytochrome P450 3A by ritonavir or nelfinavir. *Drug Metab Dispos*. 2011;39(6):1070-1078.
17. Vakkalagadda B, Frost C, Byon W, Boyd RA, Wang J, Zhang D, Yu Z, Dias C, Shenker A, LaCreta F. Effect of rifampin on the pharmacokinetics of apixaban, an oral direct inhibitor of factor Xa. Am J Cardiovasc Drugs. 2016;16(2):119-127.
18. Wu C-Y, Benet LZ. Predicting drug disposition via application of BCS: transport / absorption / elimination interplay and development of a biopharmaceutics drug disposition classification system. *Pharm Res*. 2005;22(1):11-23.

CHAPTER 4: THE NECESSITY OF USING CHANGES IN ABSORPTION TIME TO IMPLICATE INTESTINAL TRANSPORTER INVOLVEMENT IN ORAL DRUG-DRUG INTERACTIONS[*]

Abstract

In drug discovery and development, it is of high interest to characterize the potential for intestinal drug-drug interactions to alter bioavailability of a victim drug. For drugs that are substrates of both intestinal transporters and enzymes, estimating the relative contribution of each process has proved challenging, especially since the susceptibility of drug to uptake or efflux transporters *in vitro* does not always translate to clinically significant *in vivo* involvement. Here we introduce a powerful methodology to implicate intestinal transporters in drug-drug interactions based on the theory that clinically relevant intestinal transporter interactions will result in altered rate of absorption of victim drugs. We present exemplary clinical drug-drug interaction studies that utilize well-characterized clinical substrates and perpetrators to demonstrate how mean absorption time (*MAT*) and time to maximum concentration (t_{max}) are expected to change (or remain unchanged) when either intestinal transporters or metabolic enzymes were/are altered. Acute inhibition of gut efflux transporters resulted in decreased *MAT* and t_{max} values, induction increased these values, while inhibition of intestinal metabolic enzymes did not result in altered *MAT* or t_{max}. Apixaban was selected to demonstrate the utility of the methodology, as the purported involvement of both intestinal enzymes and transporters has been suggested in its FDA package insert. Involvement of intestinal efflux transporters in

[*] Modified from the publication: Sodhi JK, Benet LZ. The necessity of using changes in absorption time to implicate intestinal transporter involvement in oral drug-drug interactions. *AAPS J*. 2020;22(5):111.

apixaban disposition is unlikely. Utilization of this simple but powerful methodology to implicate intestinal transporter involvement will have significant impact on how drug-drug interactions are interpreted.

Introduction

Bioavailability is one of the most important factors in determining the dosing regimens of orally dosed drugs. Oral bioavailability (*F*) is defined as the fraction of an oral dose that reaches systemic circulation intact and therefore *F* is influenced by the extent of absorption of drug from the intestinal gut lumen into the enterocyte (which may vary depending on both gut uptake and efflux transporters), the degree of intestinal metabolism within the enterocyte, as well as the extent of first-pass hepatic elimination, as defined by the following relationship:

$$F = F_A \cdot F_G \cdot F_H$$

where F_A is the cumulative fraction of dosed drug arriving intact into the enterocytes, F_G is the fraction of dose that escapes intestinal metabolism within the enterocyte and enters the portal vein, and F_H is the fraction that is not metabolized on first pass through the liver. Bioavailability is directly proportional to drug exposure (*AUC*, area under the concentration-time curve):

$$AUC = \frac{F \cdot Dose}{CL}$$

where *CL* is clearance. Therefore, the extent to which an orally dosed drug can reach the systemic circulation, defined by its degree of intestinal absorption and ability to avoid intestinal and hepatic first pass metabolism, directly defines the dose required to achieve therapeutically effective drug concentrations.

Consequently, in the discovery and development of new chemical entities, it is of high interest to not only predict intestinal bioavailability, but also to characterize the potential for intestinal drug-drug interactions to alter bioavailability of a victim drug [1-4]. Since *CL* measurements are inherently confounded by *F* following oral dosing, measurement of *F* can be achieved by comparing dose-normalized *AUC* values following oral and intravenous dosing of drug (assuming *CL* has not changed between studies). As discussed in Chapter 3, we have recently developed a methodology that allows discrimination of changes in *CL* from changes in *F* in metabolic DDIs [5]. This is possible due to the recognition that volume of distribution at steady state (V_{ss}) remains unchanged in metabolic DDIs [6, 7] and therefore changes in apparent V_{ss} (V_{ss}/F) will reflect the change in *F* alone, allowing one to differentiate changes in *F* from *CL* in oral metabolic DDIs. This methodology may not be appropriate for use in clinically significant systemic transporter DDIs, since V_{ss} is expected to change in such interactions [8, 9].

Metabolic drug-drug interactions (DDIs) will have the potential to alter total bioavailability via increasing or decreasing drug metabolism in the intestine and/or liver, thereby altering the extent of F_G and/or F_H. Interactions involving xenobiotic transporters, however, will have the potential to not only alter the extent of absorption (F_A) by allowing or disallowing entry of drug from the gut lumen into the enterocyte, but also can result in alterations of the rate of absorption (k_a). Efflux transporters expressed on the apical side of the enterocytes, such as P-glycoprotein (P-gp) and Breast Cancer Resistance Protein (BCRP), are able to pump drug from inside the enterocyte back into the gut lumen, where drug may then re-enter the enterocytes. Thus, for clinically significant transporter substrates, inhibition of intestinal efflux transporters would prevent drug cycling between the enterocytes and gut lumen, thereby decreasing

absorption time, while induction would increase absorption time. For apically expressed intestinal uptake transporters, such as organic anion transporting polypeptide (OATP) 2B1, inhibition would result in prolonged absorption, while induction would decrease absorption time for clinically significant substrates. Therefore, it is expected that clinically significant intestinal transporter DDIs will result in noteworthy changes in mean absorption time (*MAT*), the inverse of the first order absorption rate constant (k_a) and time of maximal concentration (t_{max}).

Often in complex DDIs, those in which both metabolic enzymes and transporters may be implicated, it is difficult to discern the contribution of each process to overall disposition [10, 11]. This is true not only for understanding the contribution of metabolism versus transporter-mediated elimination to systemic clearance, but also their individual impact on bioavailability, and both sets of parameters contribute directly to changes in observed drug exposure. Understanding of both of these complimentary aspects will allow investigators to anticipate the magnitude of a potential DDI when either transporters or enzymes (or both) are affected. We are concerned that a number of papers, and even approved drug labeling, have proposed that drug interactions leading to changes in *AUC* are the result of intestinal transporter interactions based primarily on *in vitro* measures of the interaction potential when, in fact, no changes in *MAT* and t_{max} are observed. In this investigation, we further explore how to interpret changes in *MAT* and t_{max} to implicate intestinal absorptive transporter involvement in oral DDIs.

Methods

To determine if intestinal absorptive transporters are involved in an oral DDI, changes in *MAT* and t_{max} were examined for the interaction versus control phases of published clinical DDI

studies. In addition, *AUC*, apparent clearance (*CL*/*F*), mean residence time (*MRT*), terminal half-life ($t_{1/2,z}$), and V_{ss}/F were also examined and all parameters were reported as ratios of interaction/control. Percent *AUC* extrapolation was also examined as a potential indication of accuracy of parameters derived from *AUC*, with understanding that a high percent extrapolation does not necessarily indicate inaccuracies if the elimination phase is accurately represented. All reported ratios of *AUC* are dose-normalized. For studies in which victim drug was dosed to steady-state, the *AUC* within the dosing interval (from 0 to τ) was utilized since this value is mathematically equivalent to *AUC* extrapolated to infinity for a single dose [12], and in these cases percent *AUC* extrapolation was not reported.

Clinical studies routinely publish t_{max} values, however, *MAT* or k_a are less frequently reported. Therefore, in cases where *MAT* values were not available, these values were calculated by one of two means: (A) estimation from published concentration-time profiles via compartmental fitting of the data, or (B) calculation using reported $t_{1/2,z}$ and t_{max} values and the following relationships:

$$t_{max} = \frac{\ln(k_a/k_e)}{k_a - k_e}$$

$$t_{max} = \frac{\ln\left(\frac{k_a \cdot (1-e^{-k_e \cdot \tau})}{k_e \cdot (1-e^{-k_a \cdot \tau})}\right)}{k_a - k_e}$$

where k_e is the elimination rate constant (that reflects the slope of the terminal half-life) and τ is the dosing interval. The first relationship describes t_{max} for a one-compartment model with first order absorption following a single dose, while the second reflects the multiple-dose relationship at steady state [13], where here k_e is the elimination rate constant determined during a dosing interval, not necessarily the terminal elimination rate constant after dosing has stopped [14].

Both relationships ignore the drug distribution that almost all drugs will experience following a single dose, therefore less faith can be attributed to calculations of k_a using the first single dose relationship. In contrast, at steady state, peripheral compartments will contain accumulated drug and there will be far less distribution following oral dosing so that utilization of the second t_{max} relationship is reasonably appropriate for any dug that has been dosed to steady state, since all drugs approximate a one-compartment model at steady state regardless of how many compartments are required to describe its kinetics following a single dose [14]. Therefore, more credence can be attributed to k_a estimation based on the steady state t_{max} relationship. Of note, there are no explicit solutions of either relationship, however, they can be solved iteratively for k_a with known k_e and t_{max} values.

The alternative methodology relies on digitization of published concentration-time profiles of victim drug to estimate the *MAT* ratio, and this methodology was also used to supplement any unreported pharmacokinetic ratios. In such cases, the mean plasma-concentration time profiles of victim drug were digitized with WebPlotDigitizer Version 4.2 (San Francisco, CA, USA) and subsequently analyzed using WinNonlin Professional Edition Version 2.1 (Pharsight, Mountain View, CA, USA). Mean absorption time (*MAT*) was calculated as the

reciprocal of the first-order absorption rate constant (k_a) from fitting of the victim drug oral concentration-time data to a 2-compartment model with absorption from the gut as we have previously described [15]. If mean residence time (*MRT*) was not reported, *MRT* was calculated by the following relationship:

$$MRT_{single\ dose} = \frac{AUMC_{0\rightarrow\infty}}{AUC_{0\rightarrow\infty}} - MAT$$

where *AUMC* is the area under the moment curve, and both *AUC* and *AUMC* are extrapolated to infinity for single dose studies. For steady state studies, the *AUC* within the dosing interval from 0 to τ ($AUC_{0\rightarrow\tau}$) without extrapolation to infinity is mathematically equivalent to *AUC* extrapolated to infinity for a single dose ($AUC_{0\rightarrow\infty}$) [12]. However, the *AUMC* within a dosing interval at steady-state ($AUMC_{0\rightarrow\tau}$) is less than $AUMC_{0\rightarrow\infty}$ for a single dose [16, 17], therefore the following relationship for orally dosed drugs was utilized to calculate *MRT* for steady-state studies [18]:

$$MRT_{steady\ state} = \frac{AUMC_{0\rightarrow\tau} + \tau \cdot AUC_{\tau\rightarrow\infty}}{AUC_{0\rightarrow\tau}} - MAT$$

where $AUC_{\tau\rightarrow\infty}$ refers to the extrapolation of steady-state *AUC* from the end of the dosing interval to infinity, which is calculated as the quotient of the concentration at the end of the dosing interval divided by the terminal phase rate constant. Calculation of V_{ss}/F was achieved using the following relationship [19]:

$$\frac{V_{ss}}{F} = \frac{CL}{F} \cdot MRT$$

where *CL/F* was calculated by dividing dose by $AUC_{0\to\infty}$ for single dose studies, and by dividing dose by $AUC_{0\to\tau}$ for steady-state studies.

All pharmacokinetic ratios were calculated using published data in priority, and supplemented with data derived from digitized values only when necessary. The source of all data used in calculated pharmacokinetic ratios is noted as footnotes.

A number of substrates of metabolic enzymes and transporters were selected for evaluation of the proposed methodology, with clinically recommended *in vivo* index substrates used in priority [20]. The studies investigated here were selected to include an example of (A) inhibition of intestinal transporters (BCRP; rosuvastatin with single-dose rifampin) [21], (B) induction of intestinal transporters (P-gp; talinolol with multiple-dosed rifampin) [22], (C) inhibition of intestinal / hepatic metabolic enzymes (CYP3A4; triazolam with fluconazole) [23], and (D) inhibition of primarily hepatic metabolic enzymes only (CYP2C19; omeprazole with clarithromycin) [24]. In addition, the proposed methodology was used to evaluate the purported involvement of intestinal efflux transporters in apixaban disposition [25], a drug for which involvement of both metabolic enzymes and efflux transporters has been suggested throughout the literature.

All selected clinical studies had a crossover design, in order to minimize the impact of any potential inter-individual variability between treatment and control groups, which was

highlighted in Chapter 2, and with the assumption that within the same individual, the dissolution and distribution of drug within the intestinal lumen are similar for both arms of the clinical study.

Analysis of involvement of intestinal transporters proceeded via examination of ratios of change in *MAT* and t_{max}. Ratios that indicated greater than 30% change (i.e. ratios outside of the range of 0.77 and 1.30) were considered to be a potentially clinically significant intestinal transporter interaction.

Simulations were conducted based on the t_{max} relationships presented above to examine the relationship between *MAT* and t_{max} for a rapidly versus more slowly absorbed drug with *MAT* values of 0.5 hr and 2 hr, respectively. The impact of 15 min changes in *MAT* on single-dose and steady-state t_{max} were examined.

Results

We identified and analyzed orally dosed clinical DDI studies from the literature in which intestinal transporters or metabolic enzymes were affected, as well as for an additional drug apixaban to further evaluate the utility of this methodology to implicate intestinal transporter involvement in oral DDIs. Intestinal transporter DDI studies were selected to include examples of both inhibition [21] and induction [22] by rifampin. Metabolic DDI studies were selected to highlight a significant intestinal metabolic interaction of the victim drug triazolam [23] versus a metabolic interaction that primarily occurs in the liver for omeprazole [24]. Details of these drug interaction studies, including the substrate and inhibitory specificities of victim and perpetrator drugs, respectively, are outlined in **Table 4.1**.

Table 4.1: Substrate Specificities of Victim Drugs and Inhibitory Potential of Perpetrator Drugs for Metabolic Enzymes and Xenobiotic Transporters from Investigated Oral Drug-Drug Interactions

Victim Drug	Dose	BDDCS Class	Substrate Specificity	Perpetrator Drug	Dose	BDDCS Class	Inhibitory Specificity	Reference
Rosuvastatin (Single Dose)	20 mg PO	3	**BCRP** OATP1B1 OATP1B3	Rifampin (Single Dose)	600 mg IV infusion	2	**BCRP** OATP1B1 OATP1B3 CYP3A	[20, 21]
Talinolol (Multiple Dose)	100 mg PO 7 Days	3	**P-gp**	Rifampin (Multiple Dose)	600 mg PO QD 9 Days	2	(Inducer) **CYP3A** CYP2C9 **P-gp**	[22, 54]
Triazolam (Single Dose)	0.25 mg PO	1	**CYP3A**	Fluconazole (Multiple Dose)	100 mg PO QD 4 Days	3	**CYP3A** CYP2C19 CYP2C9	[20, 23]
Omeprazole (Multiple Dose)	40 mg PO 6 Days	1	CYP2C19 **CYP3A** (minor)	Clarithromycin (Multiple Dose)	500 mg PO TID 5.33 Days	3	**CYP3A** CYP2C19 **P-gp**	[20, 24]
Apixaban (Single Dose)	10 mg PO	1	**CYP3A** **P-gp**	Rifampin (Multiple Dose)	600 mg PO QD 11 Days	2	(Inducer) **CYP3A** **P-gp**	[25, 54]

Intestinally expressed enzymes and transporters are highlighted in bold

Abbreviations: BCRP, Breast Cancer Resistance Protein; BDDCS, Biopharmaceutics Drug Disposition Classification System; BID, twice daily; CYP, Cytochrome P450; IV, Intravenous; OATP, Organic Anion-Transporting Polypeptide; P-gp, P-glycoprotein; QD, once daily

Table 4.2 displays the ratios of change in oral pharmacokinetics in the DDI studies that affect intestinal transporters, namely, acute inhibition of intestinal transporters (BCRP) with single dose rifampin (victim drug rosuvastatin) [21] and the induction of intestinal transporters (P-gp) with multiple dose rifampin (victim drug talinolol) [22]. In the single dose rifampin study, 600 mg IV rifampin caused a 3.37-fold and 3.21-fold increase in *AUC* in White and Asian subjects, respectively. Additionally, a significant decrease in *MAT* and t_{max} was observed in both groups; Whites showed a 53% decrease in *MAT* and 50% decrease in t_{max} and Asians displayed a 66% decrease in *MAT* and 45% decrease in t_{max}. In the multiple-dose rifampin study, 600 mg PO rifampin for 9 days resulted in a 35% reduction in talinolol *AUC*, accompanied by marked increases in *MAT* (1.70-fold) and t_{max} (1.35-fold).

Table 4.3 displays the ratios of change in oral pharmacokinetics in the DDI studies that affect metabolic enzymes, outlining (1) a triazolam–fluconazole interaction in which CYP3A4 (both intestinally and hepatically expressed) is inhibited [23] and (2) an omeprazole-clarithromycin DDI in which the primary interaction is due to CYP2C19 (primarily expressed in the liver with minor intestinal expression) [24]. In the CYP3A4 inhibition study, multiple doses of PO fluconazole resulted in a 2.46-fold increase in oral exposure of single-dosed triazolam. This was accompanied by minimal changes in *MAT* (ratio of 0.87) and t_{max} (ratio of 1.11). In the CYP2C19 inhibition study, multiple doses of clarithromycin resulted in a 1.91-fold increase in steady-state omeprazole *AUC*, while *MAT* only decreased by 8% and t_{max} increased 11%.

Table 4.4 displays the ratios of change in oral pharmacokinetics of apixaban dosed with multiple doses of rifampin, and shows a 52% decrease in apixaban exposure [25]. This change is accompanied with minimal change in *MAT* (8% decrease) and an unchanged t_{max} ratio.

Table 4.2: Changes in Pharmacokinetic Parameters in Oral Drug-Drug Interaction Studies that Affect Intestinal Xenobiotic Transporters

Victim Drug	Perpetrator Drug	Major Enzyme or Transporter	Population	$\frac{MAT^{DDI}}{MAT^{Con}}$	$\frac{t_{max}^{DDI}}{t_{max}^{Con}}$	$\frac{AUC^{DDI}}{AUC^{Con}}$	$\frac{CL/F^{DDI}}{CL/F^{Con}}$	$\frac{V_{ss}/F^{DDI}}{V_{ss}/F^{Con}}$	$\frac{MRT^{DDI}}{MRT^{Con}}$	$\frac{t_{1/2,z}^{DDI}}{t_{1/2,z}^{Con}}$	Percent *AUC* Extrapolation (DDI/Con)	Ref.
Rosuvastatin (Single Dose)	Rifampin (Single Dose)	BCRP (Inhibition)	Whites (n=7)	0.47	0.50	3.37	0.28	0.082	0.30[a]	0.64	1%/8%	[21]
Rosuvastatin (Single Dose)	Rifampin (Single Dose)	BCRP (Inhibition)	Asians (n=8)	0.34	0.55	3.21	0.31	0.11	0.34[a]	0.59	1%/7%	[21]
Talinolol (Multiple Dose)	Rifampin (Multiple Dose)	P-gp (Induction)	Healthy Men (n=8)	1.70[b]	1.35	0.65	1.54	1.24[c]	0.79[c]	0.85	n/a (steady-state)	[22]

Pharmacokinetic values reported in the table are based on published average values, unless otherwise noted. All ratios are expressed as ratios of interaction / control.

Abbreviations: *AUC*, area under the curve; BCRP, breast cancer resistance protein; Con, control; *CL/F*, apparent clearance; DDI, drug-drug interaction; *MAT*, mean absorption time; *MRT*, mean residence time; n/a, not applicable; P-gp, P-glycoprotein; Ref, reference; t_{max}, time to maximal concentration; $t_{1/2,z}$, terminal half-life; V_{ss}/F, apparent volume of distribution at steady state

[a]*MRT* was calculated using average reported values of *CL/F* and V_{ss}/F

[b]*MAT* was calculated by utilization of the steady-state relationship between reported t_{max} and $t_{1/2,z}$

[c]Ratios are calculated by digitization of published average plasma concentration-time profiles and performing compartmental analysis, where *MRT* was calculated using the steady-state relationship

Table 4.3: Changes in Pharmacokinetic Parameters in Oral Drug-Drug Interaction Studies that Affect Metabolic Enzymes

Victim Drug	Perpetrator Drug	Major Enzyme or Transporter	Population	$\frac{MAT^{DDI}}{MAT^{Con}}$	$\frac{t_{max}^{DDI}}{t_{max}^{Con}}$	$\frac{AUC^{DDI}}{AUC^{Con}}$	$\frac{CL/F^{DDI}}{CL/F^{Con}}$	$\frac{V_{ss}/F^{DDI}}{V_{ss}/F^{Con}}$	$\frac{MRT^{DDI}}{MRT^{Con}}$	$\frac{t_{1/2,z}^{DDI}}{t_{1/2,z}^{Con}}$	Percent *AUC* Extrapolation (DDI/Con)	Ref.
Triazolam (Single Dose)	Fluconazole (Multiple Dose)	CYP3A4	Healthy Subjects (n=12)	0.87[c]	1.11	2.46	0.41[b]	0.79[a]	1.91[a]	1.84	20%/6%	[23]
Omeprazole (Multiple Dose)	Clarithromycin (Multiple Dose)	CYP2C19 CYP3A4 (minor)	Healthy Men (n=23)	0.92[d]	1.11	1.91	0.52[b]	1.11[a]	2.08[a]	1.33	n/a steady-state	[24]

Pharmacokinetic values reported in the table are based on published average values, unless otherwise noted. All ratios are expressed as ratios of interaction / control.

Abbreviations: *AUC*, area under the curve; Con, control; *CL/F*, apparent clearance; CYP, cytochrome P450; DDI, drug-drug interaction; *MAT*, mean absorption time; *MRT*, mean residence time; n/a, not applicable; t_{max}, time to maximal concentration; $t_{1/2,z}$, terminal half-life; V_{ss}/F, apparent volume of distribution at steady state

[a]Ratios are calculated by digitization of published average plasma concentration-time profiles and performing non-compartmental and/or compartmental analysis, where single dose *MRT* and steady-state *MRT* was calculated using the appropriate relationships

[b]*CL/F* was calculated using known dose and reported *AUC*

[c]*MAT* was calculated by utilization of the single-dose relationship between reported t_{max} and $t_{1/2,z}$

[d]*MAT* was calculated by utilization of the steady-state relationship between reported t_{max} and $t_{1/2,z}$

Table 4.4: Changes in Pharmacokinetic Parameters for Orally Dosed Apixaban (Victim) and Rifampin (Perpetrator)

Victim Drug	Perpetrator Drug	Major Enzyme or Transporter	Population	$\frac{MAT^{DDI}}{MAT^{Con}}$	$\frac{t_{max}^{DDI}}{t_{max}^{Con}}$	$\frac{AUC^{DDI}}{AUC^{Con}}$	$\frac{CL/F^{DDI}}{CL/F^{Con}}$	$\frac{V_{ss}/F^{DDI}}{V_{ss}/F^{Con}}$	$\frac{MRT^{DDI}}{MRT^{Con}}$	$\frac{t_{1/2,z}^{DDI}}{t_{1/2,z}^{Con}}$	Percent *AUC* Extrapolation (DDI/Con)	Ref.
Apixaban (Single Dose)	Rifampin (Multiple Dose)	CYP3A4 P-gp (Induction)	Healthy Subjects (n=20)[a]	0.92[b]	1.00	0.48	2.14	1.42[b]	0.65[b]	1.03	10%/9%	[25]

Pharmacokinetic values reported in the table are based on published average values, unless otherwise noted. All ratios are expressed as ratios of interaction / control.

Abbreviations: *AUC*, area under the curve; Con, control; *CL/F*, apparent clearance; CYP, cytochrome P450; DDI, drug-drug interaction; *MAT*, mean absorption time; *MRT*, mean residence time; P-gp, P-glycoprotein; t_{max}, time to maximal concentration; $t_{1/2,z}$, terminal half-life; V_{ss}/F, apparent volume of distribution at steady state

[a]Interaction phase was n=18

[b]Ratios are calculated by digitization of published average plasma concentration-time profiles and performing non-compartmental and/or compartmental analysis where *MRT* was calculated using the single dose relationship

Table 4.5: Regional Expression of Clinically Significant Efflux and Uptake Transporters in the Intestine, Liver, Kidney and Brain

Transporter Type	Transporter	Intestinal Localization	Hepatic Localization	Renal Localization	Brain Localization
Efflux	BCRP	Apical	Bile Canaliculi		Apical (Blood)
	MDR1 (P-gp)	Apical	Bile Canaliculi	Apical (Urine)	Apical (Blood)
	MRP2	Apical	Bile Canaliculi	Apical (Urine)	
	MRP3	Basolateral	Sinusoidal (Basolateral)		
	THTR1	Basolateral		Basolateral	
	BSEP		Bile Canaliculi		
	MDR3		Bile Canaliculi		
	MATE1		Bile Canaliculi	Apical (Urine)	
	MATE2-K			Apical (Urine)	
	MRP4		Sinusoidal (Basolateral)	Apical (Urine)	Apical (Blood)
	MRP6		Sinusoidal (Basolateral)		
Uptake	OATP2B1	Apical	Sinusoidal (Basolateral)		
	ASBT	Apical			
	MCT1	Apical			
	PEPT1/PEPT2	Apical		Apical (Urine)	
	THTR2	Apical		Apical (Urine)	
	OCT1		Sinusoidal (Basolateral)		
	OAT2		Sinusoidal (Basolateral)	Basolateral	
	OAT7		Sinusoidal (Basolateral)		
	OATP1A2				Apical (Blood)
	OATP1B1		Sinusoidal (Basolateral)		
	OATP1B3		Sinusoidal (Basolateral)		
	NTCP		Sinusoidal (Basolateral)		
	OAT1/3			Basolateral	
	OATP4C1			Basolateral	
	OCT2			Basolateral	
	URAT1			Apical (Urine)	
Bidirectional	OSTα/ß	Basolateral	Sinusoidal (Basolateral)		
	ENT1	Basolateral	Bile Canaliculi Sinusoidal (Basolateral)	Apical (Urine)	Basolateral (Brain)
	ENT2	Basolateral	Sinusoidal (Basolateral)	Basolateral	Basolateral (Brain) Apical (Blood)
	OAT4			Apical	
	OCTN1/2			Apical (Urine)	

Discussion

The methodology proposed here is a simple but powerful tool to evaluate the clinically significant involvement of intestinal transporters for orally dosed drugs. Utilization of this simple methodology will allow pharmaceutical scientists to better predict when an intestinal DDIs is expected to occur, as well as anticipate the degree to which exposure may change based on an improved understanding of potential determinants of *F* for a drug-of interest. In this chapter, we present exemplary clinical DDI studies that utilize well-characterized clinical substrates and perpetrators to understand how *MAT* and t_{max} are expected to change (or remain unchanged) when either intestinal transporters or metabolic enzymes were/are altered.

Table 4.2 outlines two clinical studies in which the major apical efflux transporters BCRP or P-gp were either inhibited [21] or induced [22] by rifampin. In the single-dose rifampin study, intestinal inhibition of BCRP resulted in a greater than 3-fold increase in exposure of the BCRP substrate rosuvastatin in both Whites and Asians that were wild-type carriers for both BCRP and OATP1B1 [21]. This significant interaction was accompanied by decreases in MAT and t_{max} (ranging from approximately 2- to 3-fold reduction) as would be expected for inhibition of an intestinal efflux transporter. In the multiple-dose rifampin study, induction of P-gp resulted in a 35% decrease in talinolol exposure and both MAT and t_{max} markedly increased (1.70- and 1.35-fold, respectively) [22].

In summary, inhibition of efflux transporters results in decreased MAT and induction of efflux increases MAT values. Changes in t_{max} trend in the same direction, although not always to the same degree since changes in elimination half-life will also have an impact on t_{max}, as evidenced by the single dose and steady state t_{max} relationships presented above.

Table 4.3 displays two metabolic DDIs in which the interaction either occurs due to CYP3A4 in both the intestine and liver [23], or due to CYP2C19 (with minor CYP3A4 contribution) that is primarily expressed in the liver with minimal intestinal involvement [24]. No changes in MAT values were observed in either study, as would be expected when transporters are not involved in absorption processes. These observations further demonstrate the utility of the proposed MAT methodology to implicate intestinal transporter involvement.

In order to identify clinically significant transporter involvement in DDIs, we have recently published guides to understanding DDIs involving transporters [8] and metabolic enzymes [6]. As discussed in the Introduction to this chapter, in clinically significant transporter interactions the magnitude of change in V_{ss} can often be larger than the change in *CL*, resulting in counterintuitive changes in $t_{1/2,z}$ and *MRT* (i.e., decreases in *CL* can be associated with a shorter elimination half-life). This trend can be observed in the rosuvastatin – rifampin DDI, where an approximate 70% reduction in *CL* is associated with shorter $t_{1/2,z}$ and *MRT* values due to an approximate 90% reduction in V_{ss}/F as a result of the inhibition of the hepatic uptake transporters OATP1B1/1B3 (**Table 4.2)**. This is in contrast to the classic pharmacokinetic trend where changes in *CL* are associated with an equal but opposite change in $t_{1/2,z}$ and *MRT* (due to unchanged V_{ss} in metabolic DDIs), which was extensively reviewed for a large number of strictly metabolic DDIs in Chapter 2. These guiding concepts, in addition to the *MAT* methodology proposed here, can help discern transporter involvement in purported complex DDIs and were applied to the drug apixaban.

Apixaban is an anticoagulant factor Xa inhibitor that is primarily metabolized by CYP3A4. The involvement of the efflux transporters P-gp and BCRP has also been suggested throughout the literature as well as in the apixaban FDA label [26-28]. Multiple dosing of rifampin resulted

in an approximate 2-fold reduction in apixaban exposure, however, there was no change in MAT (ratio of 0.92) and t_{max} (ratio of 1.00) (**Table 4.4**), suggesting that the *in vitro* susceptibility of apixaban to P-gp is not clinically significant. Additionally, the increase in clearance is associated with a decrease in MRT of similar magnitude, as would be expected for a metabolic interaction as outlined in Chapter 2.

These results are consistent with the Biopharmaceutics Drug Disposition Classification System (BDDCS), a simple drug classification system based on permeability rate and solubility that can anticipate which drugs may be susceptible to transporters *in vivo* [29]. Apixaban is a BDDCS Class 1 drug with favorable membrane permeability characteristics and high solubility, allowing free passage across biological membranes via passive processes (rather than reliance on xenobiotic transporters to cross membranes). It is theorized that due to the rapid membrane permeability and high solubility of BDDCS Class 1 drugs, these drugs can rapidly cross biological membranes at concentrations high enough to either saturate active transport or render the active uptake to only be a minimal part of total uptake. Thus, the clinically relevant involvement of transporters *in vivo* may be negligible even if the drug is demonstrated to be a substrate in *in vitro* studies [29]. BDDCS Class 2 drugs are also highly permeable, but due to their low solubility it is thought that the lower soluble concentrations available for passive diffusion may (in some cases) either be incapable of saturating transporters or passive uptake due to the low solubility does not outweigh the active process, and therefore transporters may or may not be involved for these primarily metabolized BDDCS Class 2 drugs. BDDCS Class 3 and 4 have unfavorable membrane permeability characteristics and thus rely on transporters to cross membranes, and this theory is supported by the fact that Class 3 and 4 drugs are primarily eliminated in the urine

or bile (i.e. transporter-dependent processes) rather than being metabolized. The BDDCS classes of the victim drugs investigated here are displayed in **Table 4.1** and nicely highlights that the transporter interactions are associated with BDDCS class 3 victim drugs, while the metabolic interactions are associated with BDDCS class 1 drugs. We propose that BDDCS can be utilized for development compounds (that are inherently less well-studied than the index substrates highlighted here) to help anticipate contributing factors in prediction of intestinal DDIs.

Utilization of the Clearance and Bioavailability Discrimination Methodology to Predict Major Site of Drug-Drug Interaction

As presented in Chapter 3, knowledge that V_{ss} is unchanged in strictly metabolic interactions can help differentiate changes in *CL* from changes in *F* in metabolic DDIs, a very useful finding to allow investigators to understand the contribution of each parameter in overall observed exposure changes [5]. For the two metabolic DDIs investigated here, the *CL* and *F* differentiation methodology estimated that in the CYP3A4 triazolam-fluconazole DDI, the observed 2.46-fold increase in exposure was due to a 48% reduction in *CL* and a 1.27-fold increase in *F*, while in the omeprazole-clarithromycin CYP2C19 DDI, the observed 1.91-fold increase in exposure was due almost entirely to a 53% decrease *CL* (with a minor 10% reduction in *F*). Although confirming IV data were not available, these estimates are consistent with the fact that CYP3A4 is expressed extensively in the intestine and liver, whereas CYP2C19 expression is minor in the intestine, therefore it is expected that the interaction would primarily occur hepatically.

In the apixaban-rifampin DDI investigated above, the DDI study was conducted after both PO and IV dosing of apixaban, allowing for confirmation (from the IV interaction study) of the

estimated change in *CL* versus *F* based on the oral interaction data. These results were presented in Chapter 3, and showed that the observed 52% reduction in apixaban oral exposure following multiple dosing of rifampin was estimated to be a result of a 30% reduction in *F* and a 1.5-fold increase in *CL* based on oral interaction data. This result is consistent with the susceptibility of apixaban to CYP3A4, as this isoform is expressed both intestinally and systemically. The IV interaction data confirmed that these estimates were remarkably close to the observed changes in *F* (24% reduction) and *CL* (1.64-fold observed), with estimated and observed values only differing by 9% for each parameter.

Considerations to Guide the Appropriate Use of the Mean Absorption Time Methodology

To appropriately guide use of the *MAT* methodology, it is important to highlight its assumptions and limitations to prevent any misinterpretations of interaction data. First, following oral dosing, changes in *MAT* can only implicate modulation of those transporters that are expressed in the intestine, but will not necessarily provide information on involvement of transporters that are only expressed in the liver and/or kidney (but not the intestine). **Table 4.5** outlines the regional expression of major xenobiotic transporters in the intestine, liver, kidney and brain adapted from the International Transporter Consortium's recommendations on clinically significant xenobiotic transporters [30].

Second, in this investigation we examined commonly used index substrates and inhibitors with known specificities for transporters and enzymes, however this may not be the case for compounds in development. For victim drugs, *in vitro* metabolic stability and transporter assays can be conducted to characterize potential determinants of drug disposition, and in tandem with

BDDCS theory, conclusions can be made on the clinical relevance of such results. For perpetrator drugs, the intestinal inhibitory potential can be calculated by comparing the maximum perpetrator concentration in the gut [I_{gut}] to its inhibitory potential (IC_{50}) for the major enzymes or transporters involved in intestinal disposition, where ratios of [I_{gut}]/IC_{50} greater than 10 indicate potential for clinically significant inhibition [31]. This aspect is quite important as currently there are a limited number of well-characterized (and specific) clinical inhibitors of transporters [20] and commonly-used metabolic inhibitors may have the potential to inhibit xenobiotic transporters [32]. Further, consideration towards the rate of absorption of potential inhibitors relative to that of substrate drugs should be accounted for, as intestinal inhibition will only occur if inhibitor is still present in the intestine. It has been demonstrated that predictions of changes in overall exposure as a result of a DDI have been improved by incorporating the k_a of perpetrator drug [33, 34]. Here, we extend this concept towards understanding the potential for an intestinal DDI to occur if perpetrator drug is more rapidly absorbed, and suggest that further investigation is warranted.

The third crucial aspect in utilization of the *MAT* methodology is ensuring that for analysis of rapidly absorbed drugs, there is sufficient clinical sampling in the absorption phase to adequately estimate *MAT*. For instance, the absorption rate of the CYP3A4 index substrate midazolam is extremely rapid, with reported k_a values of 9.6 hr^{-1} [35] and greater than 5 hr^{-1} [36], which correspond to *MAT* values of 6.25 min and less than 12 min, respectively. The study by Smith and coworkers (1981) included intensive sampling up to 1 hour (8 points) and reported t_{max} was approximately 20 min [35], while the study by Heizmann et al. (1983) only included 4 time points up to 1 hour and t_{max}ranged from 15 – 30 min between individuals [36]. However,

in the large majority of DDI studies, average *MAT* or k_a values are rarely reported, and in the absence of access to individual patient data, digitization of average concentration-time profiles introduces additional error for drugs with short *MAT* values. The reported pharmacokinetic profiles are generated from the average drug concentrations of all subjects at each time point, and therefore results in profiles that do not necessarily represent any single subject within the study. As a result, these profiles may not be able to adequately account for potential inter-individual variability in aspects such as lag-time, absorption rate, secondary peaks, and thus we recommend that in practice, this methodology be carried out for each individual in a DDI study. Of the numerous midazolam DDI studies available in the literature, we were only able to identify one ketoconazole interaction study that not only had extensive absorption phase sampling (with time points at 10, 20, 30, 45, 60 and 90 min), but of equal importance, absorption rate was calculated for each subject and average values were reported [37], resulting in an *MAT* ratio of 1.19 but a 1.50-fold increase in t_{max} (due to a 15 min increase from 30 min to 45 min).

Simulations have been previously conducted investigating the impact of a reduced sampling schedule on estimations of *MAT*, confirming that minimal error was associated for a theoretical drug with an *MAT* of 1 hr, however, the resulting error in *MAT* estimation becomes increasingly larger for drugs that are more rapidly absorbed (for theoretical drugs for which the *MAT* was decreased to 0.33 hr and 0.2 hr) [38]. The issue of estimating *MAT* when sampling is not adequate could potentially be overcome by using the two t_{max} relationships presented above for (A) a victim drug that follows one-compartment kinetics after a single dose or (B) any victim drug that is dosed to steady state in tandem with reported t_{max} and $t_{1/2,z}$ values to calculate *MAT*. However, this still depends on adequate capture of $t_{1/2,z}$, which is quite

reasonable in most DDI studies, and t_{max}, which may pose a challenge for rapidly absorbed drugs. Rapidly absorbed drugs will inherently have less time points describing the absorption phase as compared to drugs with larger t_{max} values.

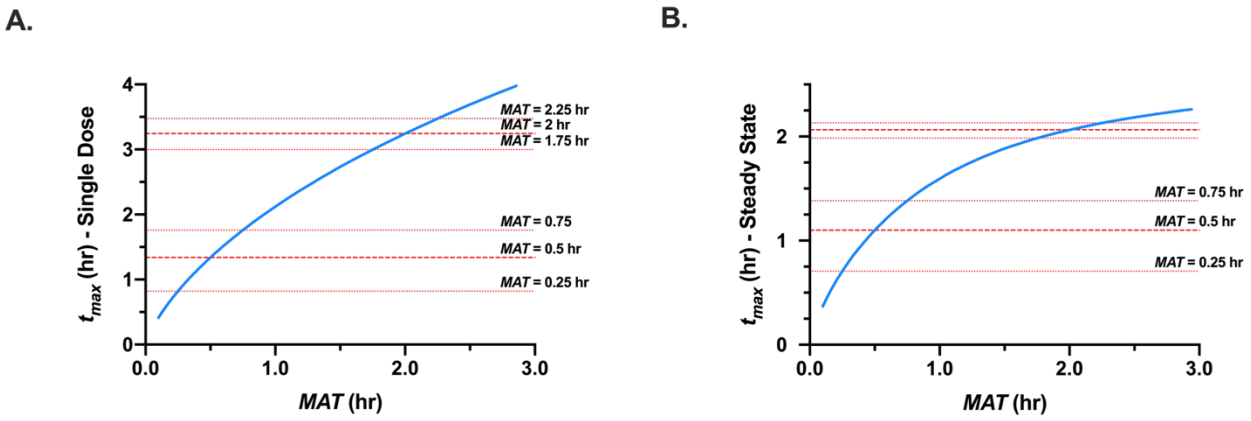

Figure 4.1: Simulated changes in time to maximal concentration (t_{max}) based on changes in mean absorption time (*MAT*). Simulated t_{max} is indicated as a blue line. Values of *MAT* range from 0.1 to 3 hr. Panel A depicts a one-compartment drug, with an elimination half-life of 4 hr, following a single dose. Panel B depicts a drug dosed to steady state, with an elimination half-life of 4 hr, and a dosing interval of 6 hr. Horizontal red lines in each panel indicate the impact of 15 min changes in *MAT* on t_{max} for a rapidly absorbed drug (*MAT* = 0.5 hr; *MAT* ranges from 0.25 to 0.75 hr) versus a less-rapidly absorbed drug (*MAT* = 2 hr; *MAT* ranges from 1.75 to 2.25 hr)

Figure 4.1 depicts the impact that 15 min changes in *MAT* will have on t_{max} for both a rapidly absorbed drug (*MAT* = 0.5 hr) and a drug that that is less-rapidly absorbed (*MAT* = 2 hr), for both a single-dose of a drug that follows one-compartment kinetics and for the steady-state t_{max} relationship. Clearly, a small change in *MAT* has a greater impact on t_{max} for rapidly absorbed drugs, compared to a drug with larger *MAT* values. This also highlights that if t_{max} is not adequately captured due to minimal absorption phase sampling, calculated *MAT* values can display large differences for rapidly absorbed drugs, that may not reflect real changes in

absorption. Examination of the midazolam-ketoconazole pharmacokinetic profiles reported by Lee and coworkers (1996) clearly demonstrates a significantly larger degree of variability with the absorption-phase time points as compared to the elimination phase [37], indicating the possibility that at inter-individual differences in drug absorption are more pronounced for rapidly absorbed drugs.

Because absorption rate may be inherently different for different people, it is crucial that an analysis using this methodology proceeds only when the DDI was conducted within the same subjects using a crossover study design. In Chapter 2, V_{ss} differences for victim drugs in DDI studies conducted in multiple populations were investigated, revealing significant differences that could not be accounted for by body weight [7]. It is expected that the same may be true for *MAT* values in different people, for instance, depending on the differences in degree of transporter expression throughout the population. Indeed, there is evidence in the literature of the association of *MAT* with age [39] and disease state potentially as a result of changes in blood flow, gut motility, pH or edema [40-42]. Thus, it is recommended that this *MAT* methodology should only be used qualitatively for parallel design studies to implicate transporter involvement; that is, for disease state and pharmacogenomic studies that are conducted with different subjects in each arm.

In situations where absorptive processes have the potential to be saturated, or in situations of dose-limited solubility of victim drug, the relationship between *MAT* and dose should be taken into account. This point is particularly relevant when different doses of victim drug are administered in the control versus interaction arms, as this practice is common for clinical DDI studies for which a significant systemic interaction is expected, and therefore a lower

dose is given in the interaction arm. Such differences in victim drug dosage levels will result in significant differences in drug concentrations within the intestinal lumen, which can be particularly relevant to saturation of absorptive processes because drug concentrations in the intestinal lumen can approach concentrations in the mM range. For example, cefatrizine has been observed to display dose-dependent absorption characteristics [43] and incorporation by Reigner et al. [44] of saturable absorption by Michaelis-Menten type kinetics into compartmental models resulted in improved data fitting. These authors concluded that involvement of a carrier-mediated transporter system was the most likely explanation, and involvement of the intestinal uptake polypeptide transporter (PEPT) has more recently been implicated in cefatrizine absorption [45].

A relevant point to mention here is that even if rate of absorption has the potential to be saturated, overall extent of absorption (reflected in bioavailability measurements) will only be decreased if absorption changes are such that there is insufficient time for absorption to occur. In other words, the overall rate of absorption may decrease, however, extent of absorption as reflected in total bioavailability measurements may or may not change. Indeed, in the cefatrizine bioavailability investigation mentioned above, a dose-dependent *MAT* increase was observed when dose was increased from 250 mg to 500 mg and 1000 mg, however, total bioavailability (approximately 75%) was unchanged between the two lower doses, whereas the 1000 mg dose was associated with a marked decrease in *F* to 46.8% [43].

It is important to note that there are situations in which *MAT* (and t_{max}) may change outside of transporter modulation, as was briefly mentioned above. Such scenarios primarily include modulation of gastric emptying [46] and food effects [47], but might also be due to

viscosity [48], osmolality that can have an effect on luminal fluid volume [49], intestinal pH and solubility [50], which could potentially result in changes in absorption rate of victim drug. However, it would be expected that for the great majority of DDI studies these factors would be kept constant in both phases of the study when conducted within the same individual. It is possible that perpetrator drug may influence victim drug absorption, for instance, by altering intestinal pH or solubility of victim drug, resulting in changes in victim drug absorption rate that are not transporter-related. It is proposed that that such false-positive results can be rationalized based on *in vitro* transporter studies or further understood if dose-dependent DDIs are conducted. Further, this approach relies on the reasonable assumption that within the same individual, dissolution and distribution of drug within the intestinal lumen remain relatively constant between both arms of the clinical study. As discussed in detail above, investigations into validating this assumption should rely heavily on utilization of individual subject data and intensive absorptive phase sampling, particularly for rapidly absorbed drugs.

Improvements to Current Clinical Pharmacology and Translational Science Approaches

Very recently, the efforts of many groups have been directed towards better predicting drug disposition related to complex DDIs and identifying clinical evidence of transporter-mediated DDIs [10, 11, 51, 52]. Rodrigues et al. presented a review to identify clinical evidence of induction of hepatic and intestinal OATPs [51], while Yu et al. focused on intestinal OATP2B1 interactions for known substrates [52]. In general, the basis of these investigations focuses only on changes in *AUC* and/or C_{max}. However, it is proposed here that the potential for intestinal

OATP-mediated DDIs would be strengthened by incorporation of the presently discussed *MAT* methodology, that significant intestinal transporter interactions will alter rate of absorption.

The localization of OATP2B1 (the primary intestinal OATP) in the apical versus basolateral membrane has been debated in recent years, as recently highlighted by the International Transporter Consortium [30]. Even amongst those scientists who agree on basolateral expression of OATP2B1, the direction of transport has been further questioned (enterocyte to blood versus blood to enterocyte), and the evidence for both sides has been nicely summarized by McFeely et al. [53]. In addition to the development of specific probe substrates and inhibitors of OATP2B1, it is proposed here that the *MAT* methodology will provide our field with an additional tool to confirm the apical versus basolateral localization of OATP2B1, and such evaluations are currently of high interest to our laboratory.

Alluri et al. [10] in their recent article "Transporter-enzyme interplay and the hepatic drug clearance: what have we learned so far?" outline approaches to predict potential complex DDIs, however, discussion of intestinal interactions is notably lacking. For orally dosed drugs, the contribution of intestinal interactions to overall exposure changes can be significant and is often overlooked. This highlights that improved methodologies to predict or characterize intestinal DDIs is an area that warrants further efforts by the field, and it is recommended that such efforts be founded on the *MAT* and t_{max} theory presented here.

Conclusions

Here a powerful methodology is introduced to implicate intestinal transporters in DDIs, based on the theory that clinically relevant intestinal transporter interactions will result in altered

rate of absorption of victim drugs. Interactions involving the two major intestinal drug transporters, BCRP and P-gp, are highlighted and demonstrate that the expected directional changes in *MAT* and t_{max} are observed for both inhibition and induction of intestinally expressed transporters. If *MAT* and t_{max} remain unchanged in a DDI, it can be inferred that (A) intestinal absorptive transporters are not significantly involved clinically in the DDI and (B) any changes in *F* as a result of the interaction are not due to alteration in intestinal transporters activity or expression. It is also possible that equivalent effects on uptake and efflux transporters may be observed resulting in unchanged *MAT*, and this possibility is currently being investigated by our laboratory. Based on the t_{max} relationships presented above, it is recognized that changes in $t_{1/2,z}$ can impact t_{max} values. Therefore, in such situations focus should be on *MAT* changes, although both of these parameters should trend in the same direction if *MAT* has been adequately captured. This simple but powerful methodology will allow investigators to implicate transporters in complex DDIs, allow clinical validation of additional transporter inhibitors due to the current lack of specific inhibitors, further investigate the potential for transporter induction, characterize emerging intestinal transporters, and help the field solve transporter-related debates, such as the localization and/or direction of OATP2B1 within the enterocyte.

References

1. Benet LZ, Cummins CL, Wu CY. Transporter-enzyme interactions: implications for predicting drug-drug interactions from in vitro data. *Curr Drug Metab*. 2003;4(5):393-398.
2. Shugarts S, Benet LZ. The role of transporters in the pharmacokinetics of orally administered drugs. *Pharm Res*. 2009;26:2039-2054.
3. van de Waterbeemd H, Jones BC. Predicting oral absorption and bioavailability. *Prog Med Chem*. 2003;41:1-59.
4. Yoshida K, Maeda K, Sugiyama Y. Hepatic and intestinal transporters: prediction of pharmacokinetic effects caused by drug-drug interactions and genetic polymorphisms. *Annu Rev Pharmacol Toxicol*. 2013;53:581-612.
5. Sodhi JK, Benet LZ. A simple methodology to discriminate changes in bioavailability from changes in clearance following oral dosing of metabolized drugs. *Clin Pharmacol Ther*. 2020;108(2):306-315.
6. Benet LZ, Bowman CM, Koleske ML, Rinaldi CL, Sodhi JK. Understanding drug-drug interaction and pharmacogenomic changes in pharmacokinetics for metabolized drugs. *J Pharmacokinet Pharmacodyn*. 2019;46(2):155-163.
7. Sodhi JK, Huang CH, Benet LZ. Volume of distribution is unaffected by metabolic drug-drug interactions. *Clin Pharmacokinet*. 2020; [E-pub ahead of print, July 28, 2020].
8. Benet LZ, Bowman CM, Sodhi JK. How transporters have changed basic pharmacokinetic understanding. *AAPS J*. 2019;21(6):103.

9. Grover A, Benet LZ. Effects of drug transporters on volume of distribution. *AAPS J*. 2009;11(2):250-261.
10. Alluri RV, Li R, Varma MVS. Transporter-enzyme interplay and the hepatic drug clearance: what have we learned so far? *Expert Opin Drug Metab Toxicol*. 2020;16(5):387-401.
11. Varma MV, Pang KS, Isoherranen N, Zhao P. Dealing with complex drug-drug interactions: towards mechanistic models. *Biopharm Drug Dispos*. 2015;36(2):71-92.
12. Wagner JG, Northam JI, Alway CD, Carpenter OS. Blood levels of drug at the equilibrium state after multiple dosing. *Nature*. 1965;207(5003):1301-1302.
13. Greenberg HE, England MJ, Hellriegel ET, Bjornsson TD. Time of peak drug concentration after a single dose and a dose at steady state. *J Clin Pharmacol*. 1997;37(6):480-485.
14. Sahin S, Benet LZ. The operational multiple dosing half-life: a key to defining drug accumulation in patients and to designing extended release dosage forms. *Pharm Res*. 2008;25(12):2869-2877.
15. Lau YY, Huang Y, Frassetto L, Benet LZ. Effect of OATP1B transporter inhibition on the pharmacokinetics of atorvastatin in healthy volunteers. *Clin Pharmacol Ther.* 2007;81(2):194-204.
16. Cheng H, Jusko WJ. Noncompartmental determination of the mean residence time and steady-state volume of distribution during multiple dosing. *J Pharm Sci*. 1991;80(2):202-204.

17. Pfeffer M. Estimation of mean residence time from data obtained when multiple-dosing steady state has been reached. *J Pharm Sci*. 1984;73(6):854-856.
18. Rohatagi S, Kan S, Derendorf H. Non-compartmental analysis of pharmacokinetic data after multiple intravenous and oral administration. *Pharmazie*. 1997;52(7):529-532.
19. Benet LZ, Galeazzi RL. Noncompartmental determination of the steady-state volume of distribution. *J Pharm Sci*. 1979;68(8):1071-1074.
20. Tornio A, Filppula AM, Niemi M, Backman JT. Clinical studies on drug-drug interactions involving metabolism and transport: methodology, pitfalls and interpretation. *Clin Pharmacol Ther*. 2019;105(6):1345-1361.
21. Wu H-F, Hristeva N, Chang J, Liang X, Li R, Frassetto L, Benet LZ. Rosuvastatin pharmacokinetics in Asian and White subjects wild type for both OATP1B1 and BCRP under control and inhibited conditions. *J Pharm Sci.* 2017;106(9):2751-2757.
22. Westphal K, Weinbrenner A, Zschiesche M, Franke G, Knoke M, Oertel R, Fritz P, von Richter O, Warzok R, Hachenberg T, Kauffmann HM, Schrenk D, Terhaag B, Kroemer HK, Siegmund W. Induction of P-glycoprotein by rifampin increases intestinal secretion of talinolol in human beings: a new type of drug/drug interaction. *Clin Pharmacol Ther*. 2000;68(4):345-355.
23. Varhe A, Olkkola KT, Neuvonen PJ. Fluconazole, but not terbinafine, enhances the effects of triazolam by inhibiting its metabolism. *Br J Clin Pharmacol*. 1996;41(4):319-323.

24. Gustavson LE, Kaiser JF, Edmonds AL, Locke CS, DeBartolo ML, Schneck DW. Effect of omeprazole on concentrations of clarithromycin in plasma and gastric tissue at steady state. *Antimicrob Agents Chemother*. 1995;39(9):2078-2083.
25. Vakkalagadda B, Frost C, Byon W, Boyd RA, Wang J, Zhang D, Yu Z, Dias C, Shenker A, LaCreta F. Effect of rifampin on the pharmacokinetics of apixaban, an oral direct inhibitor of factor Xa. Am J Cardiovasc Drugs. 2016;16(2):119-127.
26. ELIQUIS (apixaban) [package insert]. Princeton, NJ: Bristol-Myers Squibb Company; 2012.
27. Jacqueroux E, Mercier C, Margelidon-Cozzolino V, Hodin S, Bertoletti L, Delavenne X. In vitro assessment of P-gp and BCRP transporter-mediated drug-drug interactions of riociguat with direct oral anticoagulants. Fundam Clin Pharmacol. 2020;34(1):109-119.
28. Zhang D, He K, Herbst JJ, Kolb J, Shou W, Wang L, Balimane PV, Han Y-H, Gan J, Frost CE, Humphreys WG. Characterization of efflux transporters involved in distribution and disposition of apixaban. Drug Metab Dispos. 2013;41(4):827-835.
29. Wu C-Y, Benet LZ. Predicting drug disposition via application of BCS: transport / absorption / elimination interplay and development of a biopharmaceutics drug disposition classification system. *Pharm Res*. 2005;22(1):11-23.
30. Zamek-Gliszczynski MJ, Taub ME, Chothe PP, Chu X, Giacomini KM, Kim RB, Ray AS, Stocker SL, Unadkat JD, Wittwer MB, Xia C, Yee S-W, Zhang L, Zhang Y, International Transporter Consortium. Transporters in drug development: 2018 ITC

recommendations for transporters of emerging clinical importance. *Clin Pharmacol Ther*. 2018;104(5):890-899.

31. U.S. Food and Drug Administration, Center for Drug Evaluation and Research. In vitro drug interaction studies – cytochrome P450 enzyme- and transporter- mediated drug interactions guidance for industry. Silver Spring, MD; 2020.
32. Cheong J, Halladay JS, Plise E, Sodhi JK, Salphati L. The effects of drug metabolizing enzymes inhibitors on hepatic efflux and uptake transporters. *Drug Metab Lett*. 2017;11(2):111-118.
33. Brown HS, Ito K, Galetin A, Houston JB. Prediction of in vivo drug-drug interactions from in vitro data: impact of incorporating parallel pathways of drug elimination and inhibitor absorption rate constant. *Br J Clin Pharmacol*. 2005;60(5):508-518.
34. Ito K, Iwatsubo T, Kanamitsu S, Ueda K, Suzuki H, Sugiyama Y. Prediction of pharmacokinetic alterations caused by drug-drug interactions: metabolic interaction in the liver. *Pharmacol Rev*. 1998;50(3):387-412.
35. Smith MT, Eadie MJ, Brophy TO. The pharmacokinetics of midazolam in man. *Eur J Clin Pharmacol*. 1981;19(4):271-278.
36. Heizmann P, Eckert M, Ziegler WH. Pharmacokinetics and bioavailability of midazolam in man. *Br J Clin Pharmacol*. 1983;16(S1):43S-49S.
37. Lee JI, Chaves-Gnecco D, Amico JA, Kroboth PD, Wilson JW, Frye RF. Application of semisimultaneous midazolam administration for hepatic and intestinal cytochrome P450 3A phenotyping. *Clin Pharmacol Ther*. 2002;72(6):718-728.

38. Brazzell RK, Kaplan SA. Factors affecting the accuracy of estimated mean absorption times and mean dissolution times. *J Pharm Sci*. 1983;72(6):713-715.

39. Veering BT, Burm AGL, Vletter AA, van den Hoeven RAM, Spierdijk J. The effect of age on systemic absorption and systemic disposition of bupivacaine after subarachnoid administration. *Anesthesiology*. 1991;74(2):250-257.

40. Fredrick MJ, Pound DC, Hall SD, Brater DC. Furosemide absorption in patients with cirrhosis. *Clin Pharmacol Ther*. 1991;49(3):241-247.

41. Holt S, Heading RC, Clements JA, Tothill P, Prescott LF. Acetaminophen absorption and metabolism in celiac disease and Crohn's disease. *Clin Pharmacol Ther*. 1981;30(2):232-238.

42. Kitis G, Lucas ML, Bishop H, Sargent A, Schneider RE, Blair JA, Allan RN. Altered jejunal surface pH in coeliac disease: its effect on propranolol and folic acid absorption. *Clin Sci*. 1982;63(4):373-380.

43. Pfeffer M, Gaver RC, Ximenez J. Human intravenous pharmacokinetics and absolute oral bioavailability of cefatrizine. *Antimicrob Agents Chemother*. 1983;24(6):915-920.

44. Reigner BG, Couet W, Guedes JP, Fourtillan JB, Tozer TN. Saturable rate of cefatrizine absorption after oral administration to humans. *J Pharmacokinet Biopharm*. 1990;18(1):17-24.

45. Estudante M, Morais JG, Soveral G, Benet LZ. Intestinal drug transporters: an overview. *Adv Drug Deliv Rev*. 2013;65(10):1340-1356.

46. Morse BL, Alberts JJ, Posada MM, Rehmel J, Kolur A, Tham LS, Loghin C, Hillgren KM, Hall SD, Dickinson GL. Physiologically-based pharmacokinetic modeling of atorvastatin

incorporating delayed gastric emptying and acid-to-lactone conversion. *CPT Pharmacometrics Syst Pharmacol*. 2019;8(9):664-675.

47. Custodio JM, Wu CY, Benet LZ. Predicting drug disposition, absorption / elimination / transporter interplay and the role of food on drug absorption. *Adv Drug Deliv Rev*. 2008;60(6):717-733.
48. Levy G, Jusko WJ. Effect of viscosity on drug absorption. *J Pharm Sci*. 1965;54:219-225.
49. Tanaka Y, Goto T, Kataoka M, Sakuma S, Yamashita S. Impact of luminal fluid volume on the drug absorption after oral administration: analysis based on in vivo drug concentration-time profile in the gastrointestinal tract. *J Pharm Sci*. 2015;104(9):3120-3127.
50. Martinez MN, Amidon GL. A mechanistic approach to understanding factors affecting drug absorption: a review of fundamentals. *J Clin Pharmacol*. 2002;42(6):620-643.
51. Rodrigues AD, Lai Y, Shen H, Varma MVS, Rowland A, Oswald S. Induction of human intestinal and hepatic organic anion transporting polypeptides: where is the evidence for its relevance in drug-drug interactions? *Drug Metab Dispos*. 2020;48(3):205-216.
52. Yu J, Zhou Z, Tay-Sontheimer J, Levy RH, Ragueneau-Majlessi I. Intestinal drug interactions mediated by OATPs: a systemic review of preclinical and clinical findings. *J Pharm Sci*. 2017;106(9):2312-2325.
53. McFeely SJ, Wu L, Ritchie TK, Unadkat J. Organic anion transporting polypeptide 2B1 – more than a glass-full of drug interactions. *Pharmacol Ther*. 2019;196:204-215.
54. Niemi M, Backman JT, Fromm MF, Neuvonen PJ, Kivistö KT. Pharmacokinetic interactions with rifampicin. *Clin Pharmacokinet*. 2003;42(9):819-850.

CHAPTER 5: INTESTINAL EFFLUX TRANSPORTERS P-GP AND BCRP ARE NOT CLINICALLY RELEVANT IN APIXABAN DISPOSITION[*]

Abstract

The involvement of the intestinally expressed xenobiotic transporters P-glycoprotein (P-gp) and Breast Cancer Resistance Protein (BCRP) have been implicated in apixaban disposition based on *in vitro* studies. Recommendations against co-administration of apixaban with inhibitors of these efflux transporters can be found throughout the literature as well as in the apixaban FDA label. However, the clinical relevance of such findings is questionable due to the high permeability and high solubility characteristics of apixaban. Using recently developed methodologies to discern metabolic- from transporter- mediated drug-drug interactions described in detail in previous chapters, a critical evaluation of all published apixaban drug-drug interaction studies was conducted to investigate the purported clinical significance of efflux transporters in apixaban disposition. Examination of mean absorption time changes in these clinical studies does not support the clinical significance of intestinal efflux transporters in apixaban disposition. Further, there is little evidence that efflux transporters are clinically significant determinants of systemic clearance based on changes in apparent clearance being equal in magnitude to changes in mean residence time and terminal half-life. Inhibition or induction of intestinal CYP3A4 can account for exposure changes of apixaban in all clinically significant drug-drug interactions, and lack of intestinal CYP3A4 inhibition can explain all studies

[*] Modified from the publication: Sodhi JK, Liu S, Benet LZ. Intestinal efflux transporters P-gp and BCRP are not clinically relevant in apixaban disposition. *Pharm Res*. 2020; 37(10):208.

with no exposure changes, regardless of the potential for these perpetrators to inhibit intestinal or systemic efflux transporters.

Introduction

Apixaban is an anticoagulant factor Xa inhibitor approved for a number of indications including stroke or blood clot prevention and treatment of deep vein thrombosis or pulmonary embolism [1]. Apixaban is primarily metabolized by cytochrome P450 (CYP) 3A4 (with minor contributions of other isoforms such as CYP 1A2, 2C8, 2C9, 2C19, and 2J2) [1]. The involvement of the intestinally-expressed efflux transporters P-glycoprotein (P-gp) and Breast Cancer Resistance Protein (BCRP) has also been suggested throughout the literature [2, 3], as well as in the apixaban Food and Drug Administration (FDA) label [1]. However, *in vitro* susceptibility to transporters does not always translate to clinically significant outcomes, and this is particularly true for high-solubility drugs that display high membrane permeability characteristics (i.e. Biopharmaceutics Drug Disposition Classification System (BDDCS) Class 1 drugs) [4] for which a significant degree of passive passage across biological membranes is achieved, potentially rendering any transporter-assisted passage clinically insignificant. Thus, the purported clinically significant involvement of efflux transporters in the disposition of apixaban (BDDCS Class 1) is questionable. Understanding major contributors to drug disposition is critical in the clinical setting to allow for appropriate dosing and in particular, how to adjust dose based on disease state, due to pharmacogenomic variance, or in anticipation of a drug-drug interaction (DDI).

Clearance (*CL*) is a critical determinant of drug dosing regimens, as it is inversely related to drug exposure (*AUC;* area under the concentration-time curve) that ultimately is believed to drive the therapeutic efficacy and potential toxicity of a drug:

$$AUC = \frac{F \cdot Dose}{CL}$$

where *F* denotes fractional bioavailability following an oral dose, and is assumed to be 1 for an intravenous (IV) dose. Characterization of the contributors to clearance pathways, i.e., metabolic enzymes and/or xenobiotic transporters, is crucial in anticipating potential changes in clearance due to DDIs or pharmacogenomic variance of metabolic enzymes or transporters.

Our laboratory has thoroughly detailed and documented the expected changes in pharmacokinetic parameters for interactions involving purely metabolic enzymes [5, 6] versus xenobiotic transporters [7, 8]. As thoroughly discussed in Chapter 2, inhibition or induction of metabolic enzymes results in changes in *CL* and *AUC* that are directionally intuitive and translate to rational changes in mean residence time (*MRT*) and terminal half-life ($t_{1/2,z}$), as volume of distribution at steady state (V_{ss}) remains unchanged for metabolic interactions [5, 6], as depicted in the following relationship [9]:

$$MRT = \frac{V_{ss} \,/\, F}{CL \,/\, F}$$

It is considered reasonable to predict strictly metabolic interactions based on *in vitro* studies [10] due to a strong understanding by the field of the metabolizing enzymes commonly implicated in drug metabolism, which is further bolstered by well-characterized clinical specificities of routinely used metabolic inhibitors and inducers [11].

The FDA has provided guidance on predicting clinically significant transporter interactions [10], however, such predictions are not as straightforward and are even more challenging when both enzymes and transporters are involved in drug disposition, i.e., in so-called “complex DDIs”.

We have recently thoroughly discussed how to appropriately predict changes in exposure when transporters are involved using the Extended Clearance Model, which not only requires understanding of how transporter-mediated active influx and efflux intrinsic clearances will potentially change, but also requires estimation of passive diffusion and changes in metabolic and biliary elimination [12]. The methodologies employed to estimate each of these elimination processes are not trivial, and each requires a different set of experimental conditions. Further, the susceptibility of a drug to uptake or efflux transporters *in vitro* does not always translate to clinically significant *in vivo* involvement [4]. Additionally, validated clinical transporter probe substrates and inhibitors are lacking [11]; routinely-used inhibitors are often not specific and may have inhibitory potential towards both enzymes and transporters [13], and additional xenobiotic transporters are continuously emerging and suggested to be clinical relevant by the field [14-16]. Furthermore, clinically significant transporter interactions can affect V_{ss} for victim drugs [8] in addition to potential *CL* changes, resulting in counterintuitive changes in changes in *MRT* and $t_{1/2,z}$ that are not necessarily opposite in magnitude to *CL* changes [7], further complicating pharmacokinetic predictions. Thus, the challenge in predicting exposure changes for complex DDIs is beyond simply accurately estimating the contribution of metabolism versus transporters, is further complicated by the potential for enzyme-transporter interplay, and is currently an area of significant efforts by the field [17, 18].

Oral dosing changes in *F* (due to altered absorption or first pass extraction) are often underemphasized as an important contributor in DDI-related exposure changes as compared to *CL* changes, as depicted in the *AUC* relationship presented earlier in this chapter. Discriminating changes in *CL* from changes in *F* has been believed not possible without also performing an IV

DDI study to estimate changes in *CL* alone; however, most orally approved drugs have only been studied when orally administered. We have recently discussed that for low extraction ratio drugs, the minimal first pass elimination can indicate that changes in apparent clearance (*CL/F*) are primarily due to changes in *CL* alone [5]. Further, as discussed in Chapter 3 for purely metabolic interactions, knowledge that V_{ss} is unchanged can allow for estimation of *F* changes by examining the change in apparent volume of distribution at steady state (V_{ss}/F), which can further be utilized to predict changes in *CL* alone [19]. As presented in Chapter 4 for clinically significant intestinal transporter substrates, alteration of transporter activity or expression will result in significant changes in absorption rate and we maintain that such changes should always be used to implicate transporter involvement *in vivo* [20]. However, changes in absorption rate may not necessarily translate to changes in extent of absorption if there is still sufficient time for absorption to occur, an additional consideration that complicates pharmacokinetic predictions of intestinal transporter substrates.

Utilization of these guiding principles in analyzing clinical data of purported complex DDIs, such as examining changes in absorption rate or V_{ss}, can allow validation of the clinical significance of transporter involvement based on *in vitro* predictions. In Chapters 3 and 4, we have applied these concepts in the evaluation of an apixaban-rifampin interaction, however, additional apixaban interaction studies are available in the literature. Here, we critically evaluate all published apixaban clinical DDI studies using the guiding principles mentioned above to investigate the purported clinical significance of P-gp and BCRP in apixaban disposition.

Methods

As presented in Chapter 4, to determine if intestinal transporter involvement is clinically significant in oral DDIs, changes in mean absorption time (*MAT*) or time to maximum concentration (t_{max}) can be compared between the interaction versus control phase of clinical DDI studies [20]. For clinically significant intestinal transporter DDIs, inhibition would result in decreased *MAT* and t_{max}, and induction would result in increases in these values. Values of t_{max} are routinely reported, however, *MAT* values are less frequently reported and therefore were estimated by digitizing published pharmacokinetic concentration-time profiles using WebPlotDigitizer Version 4.2 (San Francisco, CA, USA) and fitting resulting data to a 2-compartmental model with first-order absorption from the gut using WinNonlin Professional Edition Version 2.1 (Pharsight, Mountain View, CA, USA) to estimate absorption rate (k_a; *MAT* = 1 / k_a), as previously described by our laboratory [21]. If pharmacokinetic curves were not published, *MAT* was calculated using published t_{max} and $t_{1/2,z}$ values using the single-dose relationship between the three parameters, as presented in Chapter 4. It should be noted that t_{max} values are observed values and these values depend heavily on the sampling scheme employed by the clinical investigators. However, any such errors have much less impact on drugs with large t_{max} values such as apixaban (3-4 hr) [1]. Simulations presented in Chapter 4 in **Figure 4.1** illistrate the impact of 15 min errors in *MAT* (which could occur due to minimal absorption phase sampling) for both a rapidly absorbed drug (*MAT* = 0.5 hr; t_{max} = 1.33 hr) and a less-rapidly absorbed drug (*MAT* = 2 hr; t_{max} = 3.2 hr) highlight that such errors have markedly less impact on drugs with larger t_{max} values [20].

Changes in *AUC*, *CL/F*, V_{ss}/F, *MRT*, $t_{1/2,z}$ are reported as ratios of interaction to control, where ratios of *AUC* were dose-normalized. Percent *AUC* extrapolation is also examined as a potential indication of the accuracy of any parameters derived from *AUC*, with the understanding that high percent extrapolations are only indicative of inaccuracies if terminal half-life is not adequately captured. *MRT* was calculated using the following relationship:

$$MRT = \frac{AUMC}{AUC} - MAT$$

where *AUMC* is area under the moment curve, and both *AUC* and *AUMC* are extrapolated to infinity since all clinical investigations were conducted for a single-dose of apixaban. V_{ss}/F is calculated using the second equation above. Published clinical values are utilized in calculation of ratios in priority, with digitization utilized only to supplement any unreported parameters-of-interest.

Ratios of change in *MAT* or t_{max} that indicated greater than 30% change (i.e. ratios outside of the range of 0.77 and 1.30) were considered to be potential evidence of a clinically significant intestinal transporter interaction. If *MAT* does not significantly change, it can be inferred that either xenobiotic transporters expressed in the intestine are not clinically significant determinants of apixaban disposition or that intestinal transporters are not inhibited or induced in that particular DDI [20].

A comprehensive literature search identified clinical apixaban DDI studies with the perpetrators atenolol [22], cyclosporine [23], diltiazem [24], enoxaparin [25], famotidine [26], ketoconazole [24, 27], naproxen [28], rifampin [29], and tacrolimus [23]. In addition, a study with

activated charcoal [30] and two studies investigating the influence of pharmacogenomic variance with respect to CYP3A5, P-gp and/or BCRP [31, 32] were identified and are critically discussed to compliment the analysis of clinical DDI studies.

Inhibitory or induction-related specificities of each perpetrator were documented to assess potential alteration of CYP3A, P-gp and/or BCRP activity or expression based on a recent compilation of clinically recommended index inhibitors of drug metabolizing enzymes and drug transporters [11]. In addition, the inhibitory potential of perpetrator drugs in the intestine and systemic circulation were investigated by considering the maximum perpetrator concentration in the gut [I_{gut}] or systemic circulation (C_{max}) with respect to each inhibitor's half maximal inhibitory concentration (IC_{50}) for CYP3A4, P-gp and BCRP. Values of [I_{gut}] are estimated by considering perpetrator dose divided by the volume of water with which the perpetrator drug was dosed (and if unreported a standard value of 250 mL was utilized in calculations). Reported values of perpetrator C_{max} were utilized; however if unreported, these values were referenced from the literature for a similar perpetrator dosing scheme. Fraction unbound in plasma ($f_{u,plasma}$) values were also tabulated to further contextualize systemic inhibitory potential based on unbound concentrations and were cited from reference [33] unless otherwise noted. Based on the FDA DDI Guidance, values of [I_{gut}]/IC_{50} > 10 indicate a potentially significant intestinal interaction, and values of C_{max} > 0.1 indicate a potentially significant systemic interaction [10].

The rifampin-apixaban DDI study was conducted following both oral and IV administration [29], therefore the clearance versus bioavailability differentiation methodology for metabolic DDIs [19] was utilized to predict changes in *CL* versus *F*. This analysis was presented in Chapters 3 and 4, and is included again here for reference. Predicted changes in pharmacokinetic

parameters were compared to actual changes based on IV dosing, and provided further insight into the hypothesis that the reported *in vitro* susceptibility to efflux transporters by apixaban may be clinically insignificant. In addition, predictions of changes in *CL* versus *F* were performed for all clinically significant DDIs to characterize the contribution of changes in *F* versus *CL*, and the major site of interaction (intestine versus liver), for each interaction.

Results

Implicating intestinal transporter involvement in apixaban disposition proceeded via examination of changes in apixaban absorption rate in clinical DDIs, based on the *MAT* methodology to identify clinically significant intestinal transporter interactions, as presented in Chapter 4. **Table 5.1** details the inhibitory specificities of the nine perpetrators investigated against CYP3A4, P-gp and BCRP, and summarizes the expected intestinal or systemic inhibitory outcomes based on calculations of $[I_{gut}]$ or C_{max} divided by IC_{50}. Clinically significant alterations in intestinal efflux capacity (based on values of $[I_{gut}]/IC_{50} > 10$) were expected for cyclosporine, diltiazem, ketoconazole, rifampin, and tacrolimus, and not expected or unknown for atenolol, enoxaparin, famotidine, and naproxen. Clinically significant inhibition of systemic efflux transporters based on values of $C_{max}/IC_{50} > 0.1$ were expected for cyclosporine and diltiazem, however, consideration of unbound plasma systemic concentrations ($C_{max,u}$) of these inhibitors does not support systemic inhibitory potential, as unbound perpetrator concentrations are not sufficiently high. Based on multiple dosing of rifampin, clinically significant induction in both intestinal and systemic P-gp is expected.

Clinically insignificant DDI changes in pharmacokinetic parameters are presented in **Table 5.2** (atenolol, cyclosporine, enoxaparin, famotidine, tacrolimus). Clinically significant DDIs are listed in **Table 5.3** (diltiazem, ketoconazole, naproxen, rifampin). No changes in *MAT* values were observed for 10 of the 11 interactions studied, with ratios of interaction to control ranging from 0.92 – 1.12, indicating that intestinal transporters are not clinically significant in these DDIs with a number of potent inhibitors (and one inducer) of P-gp and/or BCRP. These conclusions would be further bolstered if individual patient data were available for analysis, as these results relied on analysis of published average pharmacokinetic profiles. A modest prolongation of *MAT* and t_{max} was observed only for the diltiazem-apixaban interaction [24], with an *MAT* ratio of 1.38 and a t_{max} ratio of 1.33.

Table 5.4 displays the ratios of change in IV and oral apixaban pharmacokinetics following multiple dosing of rifampin [29] that was previously reported in Chapters 3 and 4. By assuming that this interaction is purely metabolic, and based on the recently published clearance versus bioavailability differentiation methodology [19] presented in Chapter 3, the observed 52% reduction in oral apixaban exposure following multiple dosing of rifampin was estimated to be a result of a 1.5-fold increase in *CL* and a 30% reduction in *F*. These estimates were compared to actual changes in *CL* and *F* based on the IV interaction data, indicating that the observed change in *CL* was 1.64-fold yielding a 24% reduction in *F*, supporting the accuracy of our method for predicting the differentiation of changes in clearance from changes in bioavailability for oral metabolic DDIs.

Table 5.1: Inhibitory Potential of Perpetrator Drugs from Apixaban Drug-Drug Interaction Studies for Metabolic Enzymes (CYP3A4) and Xenobiotic Transporters (P-gp and BCRP) Reported to be Clinical Determinants of Apixaban Disposition

Perpetrator Drug	Perpetrator Dose	BDDCS Class	$[I_{gut}]$ [a] (μM)	$f_{u,plasma}$ [b]	C_{max} [c] (μM)	CYP3A4 IC_{50} (μM)	P-gp IC_{50} (μM)	BCRP IC_{50} (μM)	Apixaban-Relevant Inhibitory Potential [d]	References
Atenolol	100 mg PO (Single Dose)	3	1500	0.94	2.25	>100 [34]	Unknown	Unknown	Unknown / Not CYP3A4	[22, 34]
Cyclosporine	100 mg PO (3 Days)	2	333	0.068	0.29 [35], e	1.5 – 20 [36] Clinically Significant [11]	0.74 – 6.18 [37] Clinically Significant [11]	3.2 [38] Clinically Significant [11]	CYP3A4 (I/S) P-gp (I/S) BCRP (I)	[11, 23, 35-38]
Diltiazem	360 mg PO (10 Days)	1	3470	0.18	0.63 [39], f	7.8 [40], 78 [41], 120 [42] Clinically Significant [45]	5.0 – 177 [43] Clinically Significant [45]	>10 [44]	CYP3A4 (I) P-gp (I/S)	[24, 39-45]
Enoxaparin	40 mg PO (Single Dose)	1	35.6 [g]	Unknown	0.61 [46], g	Unknown	Unknown	Unknown	Unknown	[25, 46]
Famotidine	40 mg PO (Single Dose)	3	474	0.84	0.24 [47]	190-390 [48]	Unknown	Unknown	Unknown / Not CYP3A4	[26, 47, 48]
Ketoconazole	400 mg PO (6 Days) [24]	2	3010 [24]	0.017 [49]	0.021 [50]	0.08 [41], 0.12 [41, 42] Clinically Significant [11]	0.65-10.1 [37], 5.6 [51] Clinically Significant [11]	12 [51]	CYP3A4 (I/S) P-gp (I) BCRP (I)	[11, 24, 27, 37, 41, 42, 49-51]
	400 mg PO (1.5 Days) [27]		7530 [27], h							
Naproxen	500 mg PO (Single Dose)	2	8690	0.002	0.293	9-695 [52]	>8000 [3]	>8000 [3], >10 [53]	CYP3A4 (I)	[3, 28, 52, 53]
Rifampin	Rifampin (600 mg PO; 11 Days)	2	3040	0.20	10.3 [54]	Clinically Significant **Inducer** [55]	Clinically Significant **Inducer** [55]	*In vitro* **inducer** [56,57] Clinical relevance has not yet been established [57]	CYP3A4 (I/S) P-gp (I/S) **Inducer**	[29, 54-57]
Tacrolimus	5 mg PO (3 Days)	2	24.9	0.01	0.033 [58], i	0.62 [59]	0.66 [60], 0.84 [61]	10 [53], 3.6 [62]	CYP3A4 (I) P-gp (I)	[23, 53, 58-62]

[a] $[I_{gut}]$ values are calculated as perpetrator dose divided by volume of water utilized in each clinical study. If unreported, the standard volume of 250 mL was assumed

[b] $f_{u,plasma}$ values are referenced from Lombardo et al. [33] unless otherwise noted

[c] C_{max} values are associated with maximum concentration of perpetrator drug reported in original clinical study, however, if unreported the value was referenced from a comparable study with a similar dosing scheme

[d]Apixaban-relevant intestinal (I) and/or systemic (S) inhibitory potential is indicated; $[I_{gut}]/IC_{50} > 10$ indicates intestinal inhibitory potential and $C_{max}/IC_{50} > 0.1$ indicates systemic inhibitory potential, with recognition that unbound plasma concentrations may further diminish systemic inhibitory potential

[e]Referenced C_{max} is associated with a single dose of 100 mg cyclosporine, and likely underpredicts the true C_{max} within this study

[f]Referenced C_{max} is also associated with a steady-state 360 mg PO dose, however, this study utilized an extended release formulation of diltiazem and thus may underpredict the true C_{max} within this study

[g]Utilized average molecular weight of 4500 g/mol to calculate $[I_{gut}]$ and C_{max}; C_{max} is associated with a pharmacodynamic measurement from a 40 mg subcutaneous dose

[h]Differing $[I_{gut}]$ values between studies for the same ketoconazole dose are due to the latter study using only 100 mL to dose PO ketoconazole versus the standard value of 250 mL

[i]Referenced C_{max} is associated with a single dose of 5 mg tacrolimus, and likely underpredicts the true C_{max} within this study

Table 5.2: Clinically Insignificant Changes in Pharmacokinetic Parameters in Drug-Drug Interaction Studies with Apixaban as the Victim Drug

Victim Drug	Perpetrator Drug	Apixaban-Relevant Inhibitory Potential	Population	$\frac{MAT^{DDI}}{MAT^{Con}}$	$\frac{t_{max}^{DDI}}{t_{max}^{Con}}$	$\frac{AUC^{DDI}}{AUC^{Con}}$	$\frac{CL/F^{DDI}}{CL/F^{Con}}$	$\frac{V_{ss}/F^{DDI}}{V_{ss}/F^{Con}}$	$\frac{MRT^{DDI}}{MRT^{Con}}$	$\frac{t_{1/2,z}^{DDI}}{t_{1/2,z}^{Con}}$	Percent AUC Extrapolation (DDI/Con)	Reference	Victim Drug
Apixaban (10 mg PO; Single Dose)	Atenolol (100 mg PO; Single Dose)	Unknown / Not CYP3A4	Healthy Subjects (n=15)[a]	1.07[b]	1.33	0.87	1.15[c]	0.91[b]	0.77[b]	0.84	2%/3%	[22]	Apixaban (10 mg PO; Single Dose)
Apixaban (10 mg PO; Single Dose)	Cyclosporine (100 mg PO; 3 Days)	CYP3A4 (I/S) P-gp (I/S) BCRP (I)	Healthy Males (n=12)[d]	0.98[b]	1.00	1.19	0.79	0.54[b]	0.64[b]	0.56	10%/10%	[23]	Apixaban (10 mg PO; Single Dose)
Apixaban (5 mg PO; Single Dose)	Enoxaparin (40 mg PO; Single Dose; Concurrent Dose)	Unknown	Healthy Subjects (n=20)	1.01[e]	1.00	1.07	0.93[c]	–[e]	–[e]	0.98	3%/3%	[25]	Apixaban (5 mg PO; Single Dose)
Apixaban (5 mg PO; Single Dose	Enoxaparin (40 mg PO; Single Dose; 6 hr after Apixaban)	Unknown	Healthy Subjects (n=20)[f]	0.95[e]	1.00	1.12	0.89[c]	–[e]	–[e]	1.12	3%/3%	[25]	Apixaban (5 mg PO; Single Dose
Apixaban (10 mg PO; Single Dose)	Famotidine (40 mg PO; Single Dose)	Unknown / Not CYP3A4	Healthy Subjects (n=18)	1.03[b]	0.67	1.01	0.99[c]	0.97[b]	0.98[b]	1.20	1%/2%	[26]	Apixaban (10 mg PO; Single Dose)
Apixaban (10 mg PO; Single Dose)	Tacrolimus (5 mg PO; 3 Days)	CYP3A4 (I) P-gp (I)	Healthy Males (n=12)[d]	0.99[b]	1.00	0.77	1.26	0.83[b]	0.66[b]	0.58	9%/10%	[23]	Apixaban (10 mg PO; Single Dose)

Pharmacokinetic values reported in the table are based on published average values, unless otherwise noted

Abbreviations: *AUC*, area under the curve; BCRP, Breast Cancer Resistance Protein; Con, control; *CL/F*, apparent clearance; CYP, cytochrome P450; DDI, drug-drug interaction; *I*, Intestine; *MAT*, mean absorption time; *MRT*, mean residence time; P-gp, P-glycoprotein; *S*, Systemic; t_{max}, time to maximal concentration; $t_{1/2,z}$, terminal half-life; V_{ss}/F, apparent volume of distribution at steady state

[a]Interaction phase was n=14

[b]Ratios are calculated by digitization of published average plasma concentration-time profiles and performing non-compartmental and/or compartmental analysis

[c]*CL/F* was calculated using known dose and reported *AUC*

[d]Subjects were the same for the cyclosporine and tacrolimus DDI studies

[e]Pharmacokinetic curves were not published, thus neither V_{ss} nor *MRT* could be calculated. However, *MAT* was calculated by utilization of the single dose relationship between reported t_{max} and $t_{1/2,z}$, as previously described [20] in Chapter 4

[f]Interaction phase was n=19

Table 5.3: Clinically Significant Changes in Pharmacokinetic Parameters in Drug-Drug Interaction Studies with Apixaban as the Victim Drug

Victim Drug:	Perpetrator Drug:	Relevant Enzyme or Transporter	Population	$\frac{MAT^{DDI}}{MAT^{Con}}$	$\frac{t_{max}^{DDI}}{t_{max}^{Con}}$	$\frac{AUC^{DDI}}{AUC^{Con}}$	$\frac{CL/F^{DDI}}{CL/F^{Con}}$	$\frac{V_{ss}/F^{DDI}}{V_{ss}/F^{Con}}$	$\frac{MRT^{DDI}}{MRT^{Con}}$	$\frac{t_{1/2,z}^{DDI}}{t_{1/2,z}^{Con}}$	Percent AUC Extrapolation (DDI/Con)	Reference
Apixaban (10 mg PO; Single Dose)	Diltiazem (360 mg PO; 10 Days)	CYP3A4 (I) P-gp (I/S)	Healthy Subjects (n=18)	1.38[a]	1.33	1.40[b]	0.73[c]	0.70[a]	1.05[a]	0.95[b]	5%/6%	[24]
Apixaban (10 mg PO; Single Dose)	Ketoconazole (400 mg PO; 6 Days)	CYP3A4 (I/S) P-gp (I) BCRP (I)	Healthy Males (n=18)	1.12[a]	1.00	1.99	0.50[c]	0.56[a]	1.08[a]	1.22	3%/2%	[24]
Apixaban (25 µg PO; Single Dose)	Ketoconazole (400 mg PO; 1.5 Days)	CYP3A4 (I/S) P-gp (I) BCRP (I)	Healthy Subjects (n=18)	0.96[d]	0.88	1.90	0.53	0.69[a]	1.24[a]	1.14	0%/0%[a]	[27]
Apixaban (10 mg PO; Single Dose)	Naproxen (500 mg PO; Single Dose)	CYP3A4 (I)	Healthy Males (n=21)	0.96[a]	1.00	1.54	0.65[c]	0.62[a]	1.14[a]	1.00	2%/2%	[28]
Apixaban (10 mg PO; Single Dose)	Rifampin (600 mg PO; 11 Days)	CYP3A4 (I/S) P-gp (I/S) **Inducer**	Healthy Subjects (n=20)[e]	0.92[a]	1.00	0.48	2.14	1.42[a]	0.65[a]	1.03	10%/9%	[29]

Pharmacokinetic values reported in the table are based on published average values, unless otherwise noted

Abbreviations: *AUC*, area under the curve; BCRP, Breast Cancer Resistance Protein; Con, control; *CL/F*, apparent clearance; CYP, cytochrome P450; DDI, drug-drug interaction; *I*, Intestine; *MAT*, mean absorption time; *MRT*, mean residence time; P-gp, P-glycoprotein; *S*, Systemic; t_{max}, time to maximal concentration; $t_{1/2,z}$, terminal half-life; V_{ss}/F, apparent volume of distribution at steady state

[a]Ratios are calculated by digitization of published average plasma concentration-time profiles and performing non-compartmental and/or compartmental analysis

[b]Control phase was n=17

[c]*CL/F* was calculated using known dose and reported *AUC*

[d]*MAT* was calculated by utilization of the single dose relationship between reported t_{max} and $t_{1/2,z}$, as previously described [20] in Chapter 4

[e]Interaction phase was n=18

Table 5.4: Utilization of the Clearance and Bioavailability Differentiation Methodology to Discriminate Clearance from Bioavailability Changes for Orally Dosed Apixaban (Victim) and Rifampin (Perpetrator)

Victim	Perpetrator	$\frac{AUC^{DDI}}{AUC^{Control}}$	$\frac{V_{ss}/F^{DDI}}{V_{ss}/F^{Control}}$	$\frac{V_{ss}{}^{DDI}}{V_{ss}{}^{Control}}$	$\frac{F^{DDI}}{F^{Control}}$	$\frac{CL/F^{DDI}}{CL/F^{Control}}$	$\frac{CL^{DDI}}{CL^{Control}}$	Reference
Apixaban (IV) (Single Dose)	Rifampin (Multiple Dose)	Observed: 0.61	–	Observed: 0.87	Observed: 0.76	–	Observed: 1.64	[29]
Apixaban (Oral) (Single Dose)	Rifampin (Multiple Dose)	Observed: 0.48	Observed: 1.42[a]	Assumed: 1	Estimated: 0.70	Observed: 2.14	Estimated: 1.50	[29]

Pharmacokinetic values reported in the table are based on published average values, unless otherwise noted
Abbreviations: *AUC*, area under the curve; *CL*, clearance; *CL/F*, apparent clearance; DDI, drug-drug interaction; *F*, bioavailability; V_{ss}, volume of distribution at steady state; V_{ss}/F, apparent volume of distribution at steady state
[a]Ratios are calculated by digitization of published average plasma concentration-time profiles and performing non-compartmental and/or compartmental analysis

Table 5.5: Utilization of the Clearance and Bioavailability Differentiation Methodology to Predict Major Site of Interaction in Clinically Significant Drug-Drug Interactions with Apixaban as the Victim Drug

Victim Drug	Perpetrator Drug	CYP3A4 $[I_{gut}]/IC_{50}$	CYP3A4 C_{max}/IC_{50}	CYP3A4 $C_{max,u}/IC_{50}$	$\frac{AUC^{DDI}}{AUC^{Con}}$ Observed	$\frac{V_{ss}/F^{DDI}}{V_{ss}/F^{Con}}$ Observed	$\frac{F^{DDI}}{F^{Con}}$ Estimated	$\frac{CL/F^{DDI}}{CL/F^{Con}}$ Observed	$\frac{CL^{DDI}}{CL^{Con}}$ Estimated	Primary Site of Interaction	Reference
Apixaban (10 mg PO)	Ketoconazole (400 mg PO; 6 Days)	25,000 - 37,600	0.18 - 0.26	< 0.004	1.99	0.56[a]	1.79	0.50[b]	1.00	Intestine	[24]
Apixaban (25 µg PO)	Ketoconazole (400 mg PO; 1.5 Days)	62,800 - 94,100	0.18 - 0.26	< 0.004	1.90	0.69[a]	1.45	0.53	0.77	Intestine	[27]
Apixaban (10 mg PO)	Naproxen (500 mg PO; Single Dose)	12.5 - 966	< 0.3	< 0.00007	1.54	0.62[a]	1.61	0.65[b]	1.00	Intestine	[28]
Apixaban (10 mg PO)	Diltiazem (360 mg PO; 10 Days)	28.9 - 445	< 0.08	< 0.014	1.40[c]	0.70[a]	1.43	0.73[b]	1.04	Intestine	[24]

Abbreviations: *AUC*, area under the curve; BCRP, Breast Cancer Resistance Protein; Con, control; *CL*, clearance; *CL*/*F*, apparent clearance; CYP, cytochrome P450; DDI, drug-drug interaction; *F*, bioavailability; I, Intestine; P-gp, P-glycoprotein; *S*, Systemic; V_{ss}, volume of distribution at steady state; V_{ss}/F, apparent volume of distribution at steady state

[a]Ratios are calculated by digitization of published average plasma concentration-time profiles and performing non-compartmental and/or compartmental analysis

[b]*CL*/*F* was calculated using known dose and reported *AUC*

[c]Control phase was n=17

Although confirming IV data were not available for the remaining four clinically significant DDIs, **Table 5.5** displays the predicted changes in *CL* versus *F* for these interactions with the assumption that all interactions are purely metabolic, based on the recently described *CL* versus *F* discrimination methodology [19] in Chapter 3. Predicted changes in systemic *CL* were minimal, ranging from 0.77 – 1.04, while predicted changes in *F* ranged from 1.43 – 1.79. Additionally, estimates of $[I_{gut}]/IC_{50}$, C_{max}/IC_{50}, and $C_{max,u}/IC_{50}$ were calculated, suggesting that all four interactions are predicted to be primarily intestinal, rather than systemic.

A clinical study was identified in which activated charcoal was dosed both 2 hr and 6 hr post apixaban oral dosing [30]. Although no change in C_{max} or t_{max} was observed, *AUC* and $t_{1/2,z}$ both decreased. For the 2 hr and 6 hr dose, *AUC* decreased to 0.49 and 0.71, respectively, while $t_{1/2,z}$ decreased to 0.40 and 0.37, respectively.

Two pharmacogenomic studies were identified in which differences in apixaban disposition were investigated with respect to CYP3A5, P-gp and/or BCRP [31, 32]. The first study investigated apixaban disposition in patients with atrial fibrillation and acute stroke with respect to gene polymorphisms in *CYP3A5* and *ABCB1* (P-gp), concluding that these polymorphisms do not affect the pharmacokinetics of apixaban [31]. The second study investigated dose-normalized apixaban plasma trough concentrations in 70 measurements from 44 patients with atrial fibrillation [32]. The investigators concluded that P-gp pharmacogenomics did not impact plasma trough concentrations, however, patients exhibiting either *ABCG2* (BCRP) or *CYP3A5* gene polymorphisms had higher plasma trough concentrations.

Discussion

Discerning involvement of transporters versus metabolic enzymes is challenging, particularly because the susceptibility of drug to efflux or uptake transporters *in vitro* does not always translate to clinically significant *in vivo* involvement [4]. Further, following oral dosing DDIs, separating changes in *CL* or V_{ss} from *F*, as well as consideration of the impact of both *CL* and V_{ss} on *MRT* and half-life, makes discerning clinically significant transporter involvement a difficult task. Based on the recognition that significant intestinal transporter interactions will result in discernable changes in *MAT* (and therefore t_{max}) [20], it is possible to implicate intestinal transporters in oral DDI studies, with no change indicating that intestinal transporters are not relevant (Chapter 4). Apixaban t_{max} occurs approximately 3-4 hours after oral dosing [1, 63], a value large enough to sensitively detect changes in absorption rate under standard pharmacokinetic sampling schemes [20].

No change in apixaban absorption rate was observed in 10 of 11 oral DDI studies with *MAT* ratios ranging from 0.92 – 1.12 (**Table 5.2** and **Table 5.3**), which included perpetrator drugs with significant potential to inhibit P-gp and BCRP based on *in vitro* data (**Table 5.1**). These results are consistent with the BDDCS class 1 designation of apixaban (high permeability, high solubility), which proposes that such drugs' high solubility characteristics allows very high concentrations of drug to passively diffuse, greatly overwhelming any transporter-mediated effects at clinically relevant concentrations [4]. It is noteworthy that the ketoconazole-apixaban interaction was conducted at both a clinically relevant dose (10 mg) and a microdose (25 μg), and thus it may be expected that for the lower dose, transporter effects can no longer be overwhelmed due to lower overall concentrations. However, in both studies no changes in *MAT* or t_{max} were observed, and

the degree of changes in exposure and clearance were almost identical between both studies, indicating at both apixaban concentrations the interaction was primarily due to a process for which soluble concentrations are irrelevant; i.e., CYP3A4 inhibition. Although these results are striking, conclusions would be further strengthened if it were possible to examine patient data in order to calculate changes in *MAT* and t_{max} for each individual.

The diltiazem-apixaban DDI resulted in a 1.38-fold change in *MAT* and a 1.33-fold change in t_{max}, both values that are very close to our cutoff of 1.30 but suggesting a potentially significant intestinal transporter interaction. If this result was truly reflective of inhibition of P-gp, then it would be expected that other P-gp inhibitors, in particular more potent inhibitors, should also show similar changes in absorption rate. The diltiazem estimate of $[I_{gut}]/IC_{50}$ for P-gp ranges from 19.6 to 694 and is not markedly different from estimates for cyclosporine (53.9 – 450), ketoconazole (298 – 4,630 and 746 – 11,600), and tacrolimus (29.6 – 37.7). Ketoconazole also significantly inhibits intestinal BCRP, with $[I_{gut}]/IC_{50}$ estimates of 251 and 628 for both studies.

It is possible that non-transporter mediated changes in absorption rate may be responsible for these results, such as changes in pH or gastric emptying by the perpetrator drug diltiazem. However, apixaban does not contain ionizable groups (**Figure 5.1**), and thus potential changes in gastric pH by diltiazem should not alter apixaban solubility or absorption, and this hypothesis was nicely confirmed in the famotidine study, where changes in gastric pH had no effect on apixaban pharmacokinetics [26]. Further, changes in gastric emptying by diltiazem are not expected [64], therefore perhaps this outcome is related to limitations associated with utilizing published average pharmacokinetic profiles, as such graphical representations do not necessarily represent any single subject within the study. The study authors indicate diltiazem

had no effect on t_{max} [24], however since we only had access to published median t_{max} values our calculated t_{max} ratio was 1.33. Thus, we again highlight that conclusions from utilization of the *MAT* methodology discussed in Chapter 4 will be strengthened if absorption rate is calculated for each individual in the study. It should also be recognized that t_{max} is influenced by both absorption rate and elimination rate parameters, as highlighted in Chapter 4, and we have recently published the single dose and steady-state mathematical relationships for reference [20]. Therefore, implicating intestinal transporter involvement based on t_{max} ratios alone may mislead an investigator, such as in the atenolol or famotidine results where t_{max} ratios are 1.33 and 0.67, respectively, while the respective *MAT* ratios of 1.07 and 1.03 show no change in absorption rate.

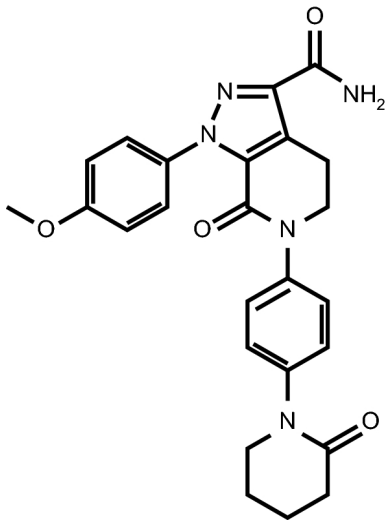

Figure 5.1. Chemical structure of apixaban

As intestinal efflux transporter involvement is unlikely to contribute to apixaban bioavailability, we further investigate the potential involvement of systemic P-gp/BCRP inhibition

to affect apixaban disposition. Examination of the inhibitory potential of perpetrators associated with clinically insignificant DDIs (**Table 5.2**) reveals that only cyclosporine had the potential to inhibit systemic P-gp with a calculated C_{max}/IC_{50} value of > 0.39 and a $C_{max,u}/IC_{50}$ value of > 0.027 (based on values presented in **Table 5.1**), yet no change in apixaban exposure was observed. Of the clinically significant inhibitory DDIs, only diltiazem was expected to achieve systemic concentrations capable of inhibiting P-gp, with similar C_{max}/IC_{50} values of > 0.17 and $C_{max,u}/IC_{50}$ of > 0.023, highlighting when compared to cyclosporine that the observed diltiazem *AUC* ratio of 1.4 is likely not due to inhibition of P-gp. Further, significant transporter interactions are expected to result in marked changes in V_{ss} of victim drugs [7, 8], however changes in V_{ss} in the IV rifampin-apixaban DDI were minimal (ratio 0.87) (**Table 5.4**). Based on Chapter 2, purely metabolic DDIs do not affect the V_{ss} of victim drug [5, 6], thus following oral dosing it is possible to estimate the relative change in *CL* versus *F* by attributing the observed change in V_{ss}/F to *F* alone [19], as described in Chapter 3. **Table 5.4** demonstrates that utilization of this methodology for the oral interaction data results in remarkably accurate predictions of *CL* versus *F* change, further supporting that for an interaction with a potent inducer of CYP3A4 and P-gp, apixaban is primarily susceptible to alterations in metabolic enzymes rather than transporters.

Examination of the clinically significant DDIs listed in **Table 5.3** show that in general, changes in CL/F were similar in magnitude to V_{ss}/F, resulting in unchanged *MRT* and $t_{1/2,z}$, suggesting that these significant DDIs are primarily due to changes in *F.* **Table 5.5** utilizes the *CL* versus *F* differentiation methodology to predict the extent of change in *CL* and *F* to understand if the observed exposure changes are primarily due to an intestinal or systemic effect. Based on this analysis, predicted changes in systemic *CL* were minimal (0.77 – 1.04) whereas predicted

changes in *F* ranged from 1.43 – 1.79. These results suggest that these significant exposure changes are primarily driven by intestinal interactions, and taken together with the unchanged absorption rates associated with these interactions, we conclude intestinal CYP3A4 is responsible for all significant apixaban DDIs. This conclusion is further rationalized by examining the intestinal versus systemic CYP3A4 inhibitory potential listed in **Table 5.5**, as all four perpetrators have $[I_{gut}]/IC_{50}$ values greater than 10, however, $C_{max,u}/IC_{50}$ is only greater than 0.1 for diltiazem.

It is noteworthy that the cyclosporine and tacrolimus DDI studies did not result in clinically significant changes in exposure [23], given their potential to inhibit intestinal CYP3A4. It is possible that since the aim of this DDI study was to examine the impact of clinically relevant systemic cyclosporine and tacrolimus concentrations achieved in transplant patients on apixaban disposition, the oral dosing of these perpetrators was not necessarily at the same time as apixaban dosing. This aspect was not clearly described within the methods, however the study design scheme published within that article [23] does indicate there was some amount of time between dosing of perpetrator and apixaban. Thus, we hypothesize the true intestinal perpetrator concentrations may be much lower than we report in **Table 5.1**.

The impact of activated charcoal was also investigated, where activated charcoal was dosed during the absorption phase of apixaban (2 hr after dosing) and after apixaban absorption was complete (6 hr after dosing) [30]. Activated charcoal is often used in situations of drug overdose, as drug is adsorbed on to activated charcoal in the intestine thus reducing extent of absorption. Activated charcoal studies can also be utilized to investigate the potential of a drug to undergo enterohepatic recycling, as reabsorption of drug is prevented after biliary excretion into the intestine. Between the 2 hr and 6 hr doses of activated charcoal, *AUC* decreased with

ratios of 0.49 and 0.71, respectively, while $t_{1/2,z}$ decreased similarly with ratios of 0.40 and 0.37, respectively. The differential changes in *AUC* with respect to dosing time support the expected outcome that a larger decrease in *F* would be observed when activated charcoal was dosed during the apixaban absorption phase. The modest reduction in exposure associated with the 6 hr dose of activated charcoal (*AUC* ratio of 0.71) is not likely due to prevention of enterohepatic recirculation by activated charcoal, as biliary excretion is a minor elimination pathway [65] and none of the pharmacokinetic profiles in any investigated study displayed the characteristic secondary peaks commonly associated with enterohepatic recirculation. Thus, the study authors hypothesize that apixaban undergoes enteroenteric recycling (recycling between systemic circulation and intestinal lumen via passive diffusion) that is prevented when apixaban is adsorbed on to activated charcoal. This may explain the observed similar reduction in $t_{1/2,z}$ for both the 2 hr and 6 hr doses, as there may be an increase in extent of direct apixaban elimination into the feces via the intestine when activated charcoal is present. We agree that further mechanistic studies are warranted, however, these results underscore the potential bidirectional ability of apixaban to cross intestinal membranes between gut lumen and systemic circulation via passive diffusion, further countering the hypothesis that apixaban is susceptible to the action of transporters.

We identified two pharmacogenomic studies in which CYP3A5, P-gp and/or BCRP pharmacogenomics were investigated. The first study concluded that differences in CYP3A5 and P-gp pharmacogenomics do not affect the pharmacokinetics of apixaban [31]. The second study investigated BCRP pharmacogenomics in addition to CYP3A5 and P-gp. Pharmacokinetic parameters were not assessed, however, investigators associated pharmacogenomics with dose-

normalized trough concentration measurements taken 10 – 14 hr post apixaban dosing, for 70 measurements from 40 patients. The investigators concluded that BCRP and CYP3A5 pharmacogenomics, but not P-gp pharmacogenomics, impacted dose-normalized trough concentrations. However, it is unclear if these results accounted for the differences in sampling time between individuals in each group, or even with respect to multiple samples from the same individual. Thus, we reserve any conclusions related to apixaban pharmacogenomics and suggest further research is warranted.

Conclusions

Throughout the literature [66-69], and even in the apixaban FDA label [1], authors routinely cite the clinically significant DDI studies listed in **Table 5.3** as evidence that P-gp and/or BCRP is a clinically significant determinant of apixaban disposition, confirming results of *in vitro* transporter studies [2, 3]. However, rational examination of these clinical studies using basic pharmacokinetic theory simply does not support the clinical significance of efflux transporters in apixaban disposition. These conclusions are not limited to the involvement of intestinal efflux transporters (based on changes in absorption time) for P-gp and BCRP, there is also little evidence that these transporters are clinically significant determinants of systemic clearance. Inhibition or induction of intestinal CYP3A4 can account for exposure changes of apixaban in all clinically significant DDIs, and lack of intestinal CYP3A4 inhibition can explain all studies with no exposure changes, regardless of the potential for these perpetrators to inhibit intestinal or systemic efflux transporters.

References

1. ELIQUIS (apixaban) [package insert]. Princeton, NJ: Bristol-Myers Squibb Company; 2012.
2. Jacqueroux E, Mercier C, Margelidon-Cozzolino V, Hodin S, Bertoletti L, Delavenne X. In vitro assessment of P-gp and BCRP transporter-mediated drug-drug interactions of riociguat with direct oral anticoagulants. *Fundam Clin Pharmacol*. 2020;34(1):109-119.
3. Zhang D, He K, Herbst JJ, Kolb J, Shou W, Wang L, Balimane PV, Han Y-H, Gan J, Frost CE, Humphreys WG. Characterization of efflux transporters involved in distribution and disposition of apixaban. *Drug Metab Dispos*. 2013;41(4):827-835.
4. Wu C-Y, Benet LZ. Predicting drug disposition via application of BCS: transport / absorption / elimination interplay and development of a biopharmaceutics drug disposition classification system. *Pharm Res*. 2005;22(1):11-23.
5. Benet LZ, Bowman CM, Koleske ML, Rinaldi CL, Sodhi JK. Understanding drug-drug interaction and pharmacogenomic changes in pharmacokinetics for metabolized drugs. *J Pharmacokinet Pharmacodyn*. 2019;46(2):155-163.
6. Sodhi JK, Huang CH, Benet LZ. Volume of distribution is unaffected by metabolic drug-drug interactions. *Clin Pharmacokinet*. 2020; [E-pub ahead of print, July 28, 2020].
7. Benet LZ, Bowman CM, Sodhi JK. How transporters have changed basic pharmacokinetic understanding. *AAPS J*. 2019;21(6):103.
8. Grover A, Benet LZ. Effects of drug transporters on volume of distribution. *AAPS J*. 2009;11(2):250-261.

9. Benet LZ, Galeazzi RL. Noncompartmental determinations of the steady-state volume of distribution. *J Pharm Sci*. 1979;68(8):1071-1074.
10. U.S. Food and Drug Administration, Center for Drug Evaluation and Research. In vitro drug interaction studies – cytochrome P450 enzyme- and transporter- mediated drug interactions guidance for industry. Silver Spring, MD; 2020.
11. Tornio A, Filppula AM, Niemi M, Backman JT. Clinical studies on drug-drug interactions involving metabolism and transport: methodology, pitfalls and interpretation. *Clin Pharmacol Ther*. 2019;105(6):1345-1361.
12. Benet LZ, Bowman CM, Liu S, Sodhi JK. The extended clearance concept following oral and intravenous dosing: theory and critical analyses. *Pharm Res*. 2018;35(12):242.
13. Cheong J, Halladay JS, Plise E, Sodhi JK, Salphati L. The effects of drug metabolizing enzymes inhibitors on hepatic efflux and uptake transporters. *Drug Metab Lett*. 2017;11(2):111-118.
14. Kimoto E, Mathialagan S, Tylaska L, Niosi M, Lin J, Carlo AA, Tess DA, Varma MVS. Organic anion transporter 2-mediated hepatic uptake contributes to the clearance of high-permeability-low-molecular-weight acid and zwitterion drugs: evaluation using 25 drugs. *J Pharmacol Exp Ther*. 2018;367(2):322-334.
15. Sato T, Mishima E, Mano N, Abe T, Yamaguchi H. Potential drug interactions mediated by renal organic anion transporter OATP4C1. *J Pharmacol Exp Ther*. 2017;362(2):271-277.

16. Zamek-Gliszczynski MJ, Taub ME, Chothe PP, Chu X, Giacomini KM, Kim RB, Ray AS, Stocker SL, Unadkat JD, Wittwer MB, Xia C, Yee S-W, Zhang L, Zhang Y, International Transporter Consortium. Transporters in drug development: 2018 ITC recommendations for transporters of emerging clinical importance. *Clin Pharmacol Ther*. 2018;104(5):890-899.
17. Alluri RV, Li R, Varma MVS. Transporter-enzyme interplay and the hepatic drug clearance: what have we learned so far? *Expert Opin Drug Metab Toxicol*. 2020;16(5):387-401.
18. Varma MV, El-Kattan AF. Transporter-enzyme interplay: deconvoluting effects of hepatic transporters and enzymes on drug disposition using static and dynamic mechanistic models. *J Clin Pharmacol*. 2016;56:S99-S109.
19. Sodhi JK, Benet LZ. A simple methodology to differentiate changes in bioavailability from changes in clearance following oral dosing of metabolized drugs. *Clin Pharmacol Ther*. 2020;108(2):306-315.
20. Sodhi JK, Benet LZ. The necessity of using changes in absorption time to implicate intestinal transporter involvement in oral drug-drug interactions. *AAPS J*. 2020;22(5):111.
21. Lau YY, Huang Y, Frassetto L, Benet LZ. Effect of OATP1B1 transporter inhibition on the pharmacokinetics of atorvastatin in healthy volunteers. *Clin Pharmacol Ther*. 2007;81(2),194-204.

22. Frost C, Song Y, Yu Z, Wang J, Lee LS, Schuster A, Pollack A, LaCreta F. The effect of apixaban on the pharmacokinetics of digoxin and atenolol in healthy subjects. *Clin Pharmacol*. 2017;9:19-28.
23. Bashir B, Stickle DF, Chervoneva I, Kraft WK. Drug-drug interaction study of apixaban with cyclosporine and tacrolimus in healthy volunteers. *Clin Transl Sci*. 2018;11(6):590-596.
24. Frost CE, Byon W, Song Y, Wang J, Schuster AE, Boyd RA, Zhang D, Yu Z, Dias C, Shenker A, LaCreta F. Effect of ketoconazole and diltiazem on the pharmacokinetics of apixaban, an oral direct factor Xa inhibitor. *Br J Clin Pharmacol*. 2015;79(5):838-846.
25. Barrett YC, Wang J, Song Y, Pursley J, Wastall P, Wright R, LaCreta F, Frost C. A randomized assessment of the pharmacokinetic, pharmacodynamic and safety interaction between apixaban and enoxaparin in healthy subjects. *Thromb Haemost*. 2012;107(5):916-924.
26. Upreti VV, Song Y, Wang J, Byon W, Boyd RA, Pursley JM, LaCreta F, Frost CE. Effect of famotidine on the pharmacokinetics of apixaban, an oral direct factor Xa inhibitor. *Clin Pharmacol*. 2013;5:59-66.
27. Mikus G, Foerster KI, Schaumaeker M, Lehmann M-L, Burhenne J, Haefeli WE. Microdosed cocktail of three oral factor Xa inhibitors to evaluate drug-drug interactions with potential perpetrator drugs. *Clin Pharmacokinet*. 2019;58(9):1155-1163.

28. Frost C, Shenker A, Gandhi MD, Pursley J, Barrett YC, Wang J, Zhang D, Byon W, Boyd RA, LaCreta F. Evaluation of the effect of naproxen on the pharmacokinetics and pharmacodynamics of apixaban. *Br J Clin Pharmacol*. 2014;78(4):877-885.
29. Vakkalagadda B, Frost C, Byon W, Boyd RA, Wang J, Zhang D, Yu Z, Dias C, Shenker A, LaCreta F. Effect of rifampin on the pharmacokinetics of apixaban, an oral direct inhibitor of factor Xa. *Am J Cardiovasc Drugs*. 2016;16(2):119-127.
30. Wang X, Mondal S, Wang J, Tirucherai G, Zhang D, Boyd RA, Frost C. Effect of activated charcoal on apixaban pharmacokinetics in healthy subjects. *Am J Cardiovasc Drugs*. 2014;14(2):147-154.
31. Kryukov AV, Sychev DA, Andreev DA, Ryzhikova KA, Grishina EA, Ryabova AV, Loskutnikov MA, Smirnov VV, Konova OD, Matsneva IA, Bochkov PO. Influence of ABCB1 and CYP3A5 gene polymorphisms on pharmacokinetics of apixaban in patients with atrial fibrillation and acute stroke. *Pharmgenomics Pers Med*. 2018;11:43-49.
32. Ueshima S, Hira D, Fujii R, Kimura Y, Tomitsuka C, Yamane T, Tabuchi Y, Ozawa T, Itoh H, Horie M, Terada T, Katsura T. Impact of ABCB1, ABCG2 and CYP3A5 polymorphisms on plasma trough concentrations of apixaban in Japanese patients with atrial fibrillation. *Pharmacogenet Genomics*. 2017;27(9):329-336.
33. Lombardo F, Berellini G, Obach RS. Trend analysis of a database of intravenous pharmacokinetic parameters in humans for 1352 drug compounds. *Drug Metab Dispos*. 2018;46(11):1466-1477.

34. Maréchal J-D, Yu J, Brown S, Kapelioukh I, Rankin EM, Wolf CR, Roberts GCK, Paine MJI, Sutcliffe MJ. In silico and in vitro screening for inhibition of cytochrome P450 CYP3A4 by comedications commonly used by patients with cancer. *Drug Metab Dispos*. 2006;34(4):534-538.

35. Hulskotte E, Gupta S, Xuan F, van Zutven M, O'Mara E, Feng H-P, Wagner J, Butterton J. Pharmacokinetic interaction between the hepatitis C virus protease inhibitor boceprevir and cyclosporine and tacrolimus in healthy volunteers. *Hepatology*. 2012;56(5):1622-1630.

36. Donato MT, Jiménez N, Castell JV, Gómez-Lechón MJ. Fluorescence-based assays for screening nine cytochrome P450 (P450) activities in intact cells expressing individual human P450 enzymes. *Drug Metab Dispos*. 2004;32(7);699-706.

37. Rautio J, Humphreys JE, Webster LO, Balakrishnan A, Keogh JP, Kunta JR, Serabjit-Singh CJ, Polli JW. In vitro p-glycoprotein inhibition assays for assessment of clinical drug interaction potential of new drug candidates: a recommendation for probe substrates. *Drug Metab Dispos*. 2006;34(5):786-792.

38. Miyata H, Takada T, Toyoda Y, Matsuo H, Ichida K, Suzuki H. Identification of febuxostat as a new strong ABCG2 inhibitor: potential applications and risks in clinical situations. *Front Pharmacol*. 2016;7:518.

39. Patel CG, Li L, Girgis S, Kornhauser DM, Frevert EU, Boulton DW. Two-way pharmacokinetic interaction studies between saxagliptin and cytochrome P450 substrates or inhibitors: simvastatin, diltiazem extended-release, and ketoconazole. *Clin Pharmacol*. 2011,3:13-25.

40. Burt HJ, Galetin A, Houston JB. IC50-based approaches as an alternative method for assessment of time-dependent inhibition of CYP3A4. *Xenobiotica*. 2010;40(5):331-343.

41. Ma B, Preuksaritanont T, Lin JH. Drug interactions with calcium channel blockers: possible involvement of metabolite-intermediate complexation with CYP3A. *Drug Metab Dispos*. 2000;28(2):125-130.

42. Wang J-S, Wen X, Backman JT, Taavitsainen P, Neuvonen PJ, Kivistö KT. Midazolam alpha-hydroxylation by human liver microsomes in vitro: inhibition by calcium channel blockers, itraconazole, and ketoconazole. *Pharmacol Toxicol*. 1999;85(4):157-161.

43. Ellens H, Deng S, Coleman J, Bentz J, Taub ME, Ragueneau-Majlessi I, Chung SP, Herédi-Szabó K, Neuhoff S, Palm J, Balimane P, Zhang L, Jamei M, Hanna I, O'Connor M, Bednarczyk D, Forsgard M, Chu X, Funk C, Guo A, Hillgren KM, Li L, Pak AY, Perloff ES, Rajaraman G, Salphati L, Taur J-S, Weitz D, Wortelboer HM, Xia CQ, Xiao G, Yamagata T, Lee CA. Application of receiver operating characteristic analysis to refine the prediction of potential digoxin drug interactions. *Drug Metab Dispos*. 2013;41(7):1367-1374.

44. Zhang Y, Gupta A, Wang H, Zhou L, Vethanayagam RR, Unadkat JD, Mao Q. BCRP transports dipyridamole and is inhibited by calcium channel blockers. *Pharm Res*. 2005;22(12):2023-2034.

45. Isoherranen N, Lutz JD, Chung SP, Hachad H, Levy RH, Ragueneau-Majlessi I. Importance of multi-P450 inhibition in drug-drug interactions: evidence of incidence, inhibition magnitude, and prediction from in vitro data. *Chem Res Toxicol*. 2012;25(11):2285-2300.
46. Frydman AM, Bara L, Le Roux Y, Woler M, Chauliac F, Samama MM. The antithrombotic activity and pharmacokinetics of enoxaparine, a low molecular weight heparin in humans given single subcutaneous doses of 20 to 80 mg. *J Clin Pharmacol*. 1988;28(7):609-618.
47. Lin JH, Chremos AN, Kanovsky SM, Schwartz S, Yeh KC, Kann J. Effects of antacids and food on absorption of famotidine. *Br J Clin Pharmacol*. 1987;24(4):551-553.
48. Moody DE, Liu F, Fang WB. In vitro inhibition of methadone and oxycodone cytochrome P450-dependent metabolism: reversible inhibition by H2-receptor agonists and proton-pump inhibitors. *J Anal Toxicol*. 2013:37(8):476-485.
49. Brown HS, Galetin A, Hallifax D, Houston JB. Prediction of in vivo drug-drug interactions from in vitro data: factors affecting prototypic drug-drug interactions involving CYP2C9, CYP2D6 and CYP3A4. Clin Pharmacokinet. 2006;45(10):1035-1050.
50. Badri PS, Dutta S, Wang H, Podsadecki TJ, Polepally AR, Khatri A, Zha J, Chiu Y-L, Awni WM, Menon RM. Drug interactions with the direct-acting antiviral combination of ombitasvir and paritaprevir-ritonavir. *Antimocrob Agents Chemother*. 2015;60(1):105-114.

51. Vermeer LMM, Isringhausen CD, Ogilvie BW, Buckley DB. Evaluation of ketoconazole and its alternative clinical CYP3A4/5 inhibitors as inhibitors of drug transporters: the in vitro effects of ketoconazole, ritonavir, clarithromycin, and itraconazole on 13 clinically relevant drug transporters. *Drug Metab Dispos*. 2016;44(3):453-459.
52. Kajbaf M, Longhi R, Montanari D, Vinco F, Rigo M, Fontana S, Read KD. A comparative study of the CYP450 inhibition potential of marketed drugs using two fluorescence based assay platforms routinely used in the pharmaceutical industry. *Drug Metab Lett*. 2011:5(1),30-39.
53. Saito H, Hirano H, Nakagawa H, Fukami T, Oosumi K, Murakami K, Kimura H, Kouchi T, Konomi M, Tao E, Tsujikawa N, Tarui S, Nagakura M, Osumi M, Ishikawa T. A new strategy of high-speed screening and quantitative structure activity relationship analysis to evaluate human ATP-binding cassette transporter ABCG2-drug interactions. *J Pharmacol Exp Ther*. 2006;317(3):1114-1124.
54. Polk RE, Brophy DF, Israel DS, Patron R, Sadler BM, Chittick GE, Symonds WT, Lou Y, Kristoff D, Stein DS. Pharmacokinetic interaction between amprenavir and rifabutin or rifampin in healthy males. *Antimicrob Agents Chemother*. 2001;45(2):502-508.
55. Niemi M, Backman JT, Fromm MF, Neuvonen PJ, Kivistö KT. Pharmacokinetic interactions with rifampicin. *Clin Pharmacokinet*. 2003;42(9):819-850.
56. Lemmen J, Tozakidis IEP, Galla H-J. Pregnane X receptor upregulates ABC-transporter Abcg2 and Abcb1 at the blood-brain barrier. *Brain Res*. 2013;1491:1-13.

57. Goreczyca L, Aleksunes LM. Transcription factor-mediated regulation of the BCRP/ABCG2 efflux transporter: a review across tissues and species. *Expert Opin Drug Metab Toxicol*. 2020;16(3):239-253.

58. Bekersky I, Dressler D, Colburn W, Mekki Q. Bioequivalaence of 1 and 5 mg tacrolimus capsules using a replicate study design. *J Clin Pharmacol*. 1999;39:1032-1037.

59. Amundsen R, Åsberg A, Ohm IK, Christensen H. Cyclosporine A- and tacrolimus-mediated inhibition of CYP3A4 and CYP3A5 in vitro. *Drug Metab Dispos*. 2012:40(4):655-661.

60. Kishimoto W, Ishiguro N, Ludwig-Schwellinger E, Ebner T, Schaefer O. In vitro predictability of drug-drug interaction likelihood of p-glycoprotein-mediated efflux of dabigatran etexilate based on $[I]_2/IC_{50}$ threshold. *Drug Metab Dispos*. 2014;42(2):257-263.

61. Patil AG, D'Souza R, Dixit N, Damre A. Validation of quinidine as a probe substrate for the in vitro P-gp inhibition assay in Caco-2 cell monolayer. *Eur J Drug Metab Pharmacokinet*. 2011;36(3):115-119.

62. Gupta A, Dai Y, Vethanayagam RR, Hebert MF, Thummel KE, Unadkat JD, Ross DD, Mao Q. Cyclosporine A, tacrolimus and sirolimus are potent inhibitors of the human breast cancer resistance protein (ABCG2) and reverse resistance to mitoxantrone and topotecan. *Cancer Chemother Pharmacol*. 2006;58(3):374-383.

63. Frost C, Nepal S, Wang J, Schuster A, Byon W, Boyd RA, Yu Z, Shenker A, Barrett YC, Mosqueda-Garcia R, LeCreta F. Safety, pharmacokinetics and pharmacodynamics of multiple oral doses of apixaban, a factor Xa inhibitor, in healthy subjects. *Br J Clin Pharmacol*. 2013;76(5):776-786.
64. Yavorski RT, Hallgren SE, Blue PW. Effects of verapamil and diltiazem on gastric emptying in normal subjects. *Dig Dis Sci*. 1991;36(9):1274-1276.
65. Raghavan N, Frost CE, Yu Z, He K, Zhang H, Humphreys WG, Pinto D, Chen S, Bonacorsi S, Wong PC, Zhang D. Apixaban metabolism and pharmacokinetics after oral administration to humans. *Drug Metab Dispos*. 2009;37(1):74-81.
66. Byon W, Garonzik S, Boyd RA, Frost CE. Apixaban: A clinical pharmacokinetic and pharmacodynamic review. *Clin Pharmacokinet*. 2019;58(10):1265-1279.
67. Prom R, Spinler SA. The role of apixaban for venous and arterial thromboembolic disease. *Ann Pharmacother*. 2011;45(10):1262-1283.
68. Budovich A, Zargarova O, Nogid A. Role of apixaban (eliquis) in the treatment and prevention of thromboembolic disease. *Pharm Ther*. 2013;38(4):206-31.
69. Gong IY, Kim RB. Important of pharmacokinetic profile and variability as determinants of dose and response to dabigatran, rivaroxaban, and apixaban. *Can J Cardiol*. 2013;29:S24-S33.

CHAPTER 6: CHALLENGING THE RELEVANCE OF UNBOUND TISSUE-TO-BLOOD PARTITION COEFFICIENT (Kp_{uu}) ON PREDICTION OF DRUG-DRUG INTERACTIONS*

Abstract

The purpose of this work is to examine the theoretical and practical utility of the liver-to-blood partition coefficient (Kp_{uu}) for predicting drug-drug interactions, and to compare the Kp_{uu}-approach to the extended clearance concept AUC_R-approach. To address this, the Kp_{uu} relationship was derived from first principles. Theoretical simulations investigated the impact of changes in a single hepatic-disposition process on unbound systemic exposure ($AUC_{B,u}$) and unbound hepatic exposure ($AUC_{H,u}$) versus Kp_{uu}. Practical aspects regarding Kp_{uu} utilization were examined by predicting the magnitude of DDI between ketoconazole and midazolam employing published ketoconazole Kp_{uu} values. The theoretical examination found that the Kp_{uu} hepatic-disposition relationship is based on the well-stirred model. Simulations emphasize that changes in influx and efflux intrinsic clearances will result in Kp_{uu} changes, however $AUC_{H,u}$ remains unchanged**.** Although incorporation of Kp_{uu} is believed to improve DDI-predictions, utilizing published ketoconazole Kp_{uu} values resulted in prediction errors for a midazolam DDI. In conclusion, there is limited benefit in using Kp_{uu} for drug-drug interaction predictions as the AUC_R-based approach can reasonably predict drug-drug interactions without measurement of intracellular drug concentrations, a difficult task that is hindered by experimental variability. Further, Kp_{uu} changes can mislead as they may not correlate with changes in $AUC_{B,u}$ or $AUC_{H,u}$.

* Modified from the publication: Sodhi JK, Liu S, Benet LZ. Challenging the relevance of unbound tissue-to-blood partition coefficient (Kp_{uu}) on prediction of drug-drug interactions. *Pharm Res*. 2020;37:73.

The well-stirred model basis of Kp_{uu} when applied to hepatic-disposition implies that nuances of intracellular drug distribution are not considered by the Kp_{uu} model.

Introduction

It is generally accepted that estimation of tissue- or target-specific unbound drug concentration is imperative to accurately assess *in vivo* pharmacological efficacy, drug-drug interaction (DDI) potential and toxicological effects of therapeutic drugs [1]. However, unbound systemic drug concentrations have historically been used as a surrogate to estimate potential pharmacokinetic or pharmacodynamic drug effects in accordance with the free drug theory [2], largely due to the difficulty in accurately determining intracellular drug concentrations. The free drug theory assumes a rapid equilibrium between unbound drug concentration in the blood and the tissues, i.e., that unbound blood concentration is equal to unbound tissue concentration ($C_{B,u}$ = $C_{H,u}$). Here, we consider the liver as our target organ. However, this assumption may not be valid for substrates of active cellular transport, since one may assume that active uptake would result in increased intracellular unbound drug accumulation, whereas efflux would decrease tissue-specific unbound drug concentration. Therefore, differential concentrations of unbound drug in the blood versus tissue are often anticipated in the *in vivo* scenario, and are often considered crucial in predictions related to drug disposition.

The unbound liver-to-blood partition coefficient (Kp_{uu}) has been developed to provide estimates of unbound intracellular drug concentrations based on the extended clearance model [3]. The value of Kp_{uu} is governed by active and passive drug passage into and out of the liver, as well as by hepatic elimination (metabolism and biliary excretion) and is based on a single unbound drug driving-force concentration in the liver, as depicted in panel A of **Figure 6.1**. As we have recently reviewed [4, 5] and others in the field have recognized [6-12], the assumption that a single liver concentration drives the various processes of basolateral efflux, biliary

elimination and metabolism implies that the extended clearance model is a well-stirred model construct. Here we derive Kp_{uu} to demonstrate that Kp_{uu} is also a well-stirred model concept when attempting to predict hepatic elimination and question the relevance of Kp_{uu} determinations for predicting drug-drug interactions.

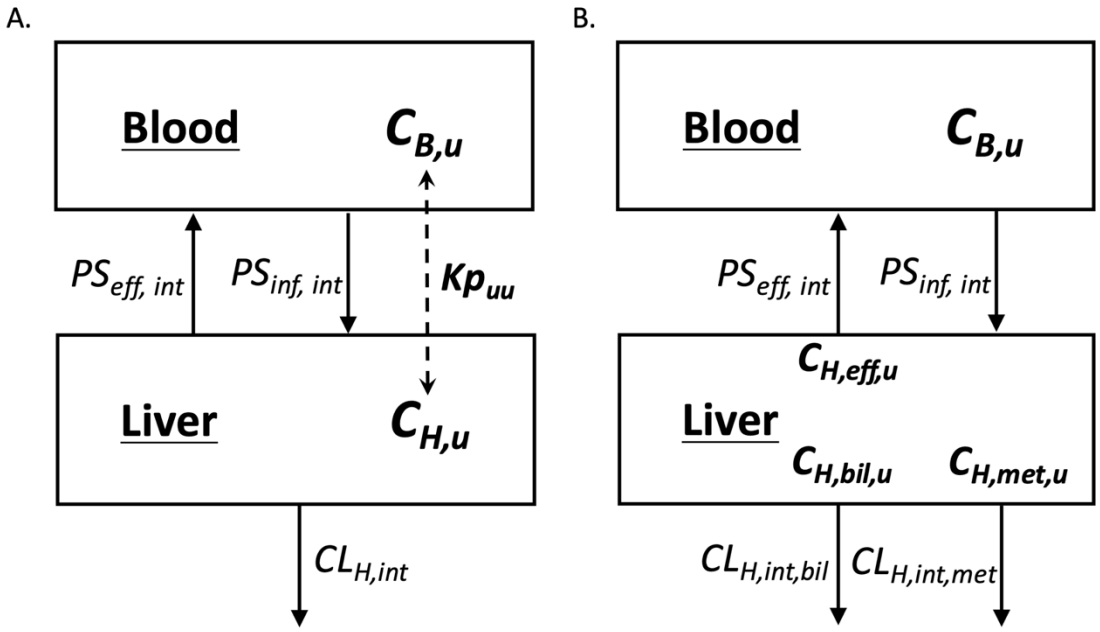

Figure 6.1: Schematic representation of liver-to-blood partition coefficient (Kp_{uu}) that relates unbound concentration of drug in the blood ($C_{B,u}$) to unbound concentration of drug in the liver ($C_{H,u}$). Differential concentrations are determined by the active and passive transporter influx and efflux intrinsic clearances ($PS_{int,inf}$ and $PS_{int,eff}$) as well as intrinsic hepatic clearance ($CL_{H,int}$), which represents the irreversible loss of drug by metabolism and biliary excretion. The average unbound concentration in the liver driving these processes is depicted in (A) and the individual driving force concentrations are depicted in (B).

Methods

The derivation of Kp_{uu} was conducted based on mass balance principles, with consideration of the amount of drug within the liver with respect to time under steady state

conditions due to active plus passive influx and efflux intrinsic membrane passage clearances ($PS_{inf,int}$, $PS_{eff,int}$), intrinsic metabolic plus biliary elimination ($CL_{H,int}$), and fraction unbound of drug in the blood ($f_{u,B}$) and within the liver ($f_{u,H}$). The resulting Kp_{uu} relationship was compared with previously derived [4] relationships of systemic and organ exposure ($AUC_{B,u}$ and $AUC_{H,u}$) following oral dosing, which include considerations of oral bioavailability as indicated by the fraction of oral dose that is absorbed (F_{abs}) and the fraction that escapes gut elimination (F_G).

To illustrate the relevance of Kp_{uu} on predictions of drug-drug interactions, simulations were conducted to explore the impact of up to a 10-fold increase or decrease in an individual disposition process ($PS_{inf,int}$, $PS_{eff,int}$, $CL_{H,int}$ or $F_{abs}{\cdot}F_G$) on Kp_{uu}, $AUC_{B,u}$ and $AUC_{H,u}$ using the derived relationships presented here.

Kp_{uu} is commonly employed to estimate intracellular concentrations of perpetrator drugs to predict the inhibitory potential on hepatic disposition processes, such as metabolic or biliary elimination. Here, a metabolic drug interaction between IV midazolam (victim drug) and ketoconazole (perpetrator) [13] was selected to investigate if predictions of changes in *AUC* were improved by addition of Kp_{uu} to estimate intracellular ketoconazole concentrations. Predicted ratios of midazolam systemic exposure in the ketoconazole versus control phases (AUC_R) were calculated using the FDA recommended basic model for reversible inhibition [14]:

$$AUC_R = 1 + \frac{[I_{max,u}]}{K_i}$$

where $I_{max,u}$ is the maximal unbound plasma concentration of the inhibitor drug ketoconazole and K_i is the unbound inhibition constant of ketoconazole on cytochrome P450 (CYP) 3A4-

mediated midazolam metabolism. The K_i value was calculated by averaging reported inhibition constants of ketoconazole on CYP3A4-mediated formation of 1-hydroxymidazolam, and was found to be 0.061 µM as summarized by Greenblatt et al. [15]. The value for $I_{max,u}$ was calculated by multiplying ketoconazole $f_{u,plasma}$ by the observed maximum ketoconazole plasma concentration in the clinical study investigated [13]. The ketoconazole $f_{u,plasma}$ utilized was 0.029 [16] and I_{max} was estimated to be 3.0 µg/ml (5.6 µM) from visual inspection of published IV plasma concentration time profiles [13]. Measured human ketoconazole Kp_{uu} values from the literature [7, 17, 18], as well as simulated Kp_{uu} values between 0.1 and 10, were utilized to adjust $I_{max,u}$ (i.e., $[I_{max,u}] \cdot Kp_{uu}$) to account for intracellular ketoconazole concentrations in contact with hepatic CYP3A4 in prediction of the magnitude of the ketoconazole-midazolam drug-drug interaction. The ketoconazole Kp_{uu} values identified from the literature and the methodologies employed for Kp_{uu} determination are listed as follows: 0.32 (extended clearance method) [18]; 0.58 (extended clearance method) [7]; 0.72 (homogenization method) [18]; 0.97 (temperature method) [18]; 1.04 (temperature method) [17]; 3.18 (homogenization method) [17]; and 4.67 (log D 7.4 method) [18].

Results and Discussion

The Unbound Liver-to-Blood Partition Coefficient is Only Consistent with the Well-Stirred Model of Hepatic Elimination when Correlated with Hepatic Elimination Parameters

The liver model in **Figure 6.1** Panel B depicts the various hepatic processes that govern liver-to-blood drug partitioning, with the reasonable consideration that the driving-force hepatic

concentration for basolateral efflux ($C_{H,eff}$) may not necessarily be equal to the apical concentration driving biliary elimination ($C_{H,bil}$) nor the average hepatic concentration driving metabolic elimination ($C_{H,met}$). Solving for the change in total hepatic drug amount (A_H) with time (i.e. the mass balance relationship) gives the following relationship:

$$\frac{dA_H}{dt} = PS_{inf,int} \cdot f_{u,B} \cdot C_B - PS_{eff,int} \cdot f_{u,H} \cdot C_{H,eff} - CL_{H,int,met} \cdot f_{u,H} \cdot C_{H,met} - CL_{H,int,bil} \cdot f_{u,H} \cdot C_{H,bil}$$

where PS_{int} values represent the total of both intrinsic active and passive basolateral influx (*inf*) and efflux (*eff*) into and out of the liver, $f_{u,B}$ is the unbound fraction of drug in the blood, $f_{u,H}$ is the unbound fraction of drug within the liver, $CL_{H,int,met}$ is the intrinsic metabolic clearance, $CL_{H,int,bil}$ is the intrinsic biliary secretion clearance, C_B is the total concentration of drug in the blood, and C_H is the total drug concentrations in the liver driving basolateral efflux (*eff*), apical biliary elimination (*bil*), and metabolism (*met*).

Although differentiating the various concentrations driving their respective hepatic processes may be a reasonable assumption (as depicted in **Figure 6.1** Panel B), there are currently no reliable analytical methods available to differentiate these various intracellular concentrations. Further, the utility of this model is limited when attempting to calculate a single partition coefficient to predict clinically relevant outcomes, especially when multiple processes determine hepatic concentration. But by adopting the well-stirred model of hepatic disposition, it follows that the hepatocyte is a 'well-stirred' compartment and that a single hepatic concentration (C_H) drives all intracellular processes. This scenario is depicted as **Figure 5.1** Panel A, has been previously elucidated [5], and is given by the following relationship:

$$\frac{dA_H}{dt} = PS_{inf,int} \cdot f_{u,B} \cdot C_B - \left(CL_{H,int} + PS_{eff,int}\right) \cdot f_{u,H} \cdot C_H$$

where $CL_{H,int}$ is the sum of the intrinsic biliary secretion and intrinsic metabolism clearances.

At steady state, the change in total drug amount over time inside the liver ($\frac{dA_H}{dt}$) is equal to zero, therefore the above relationship can be solved for the ratio of unbound concentration of drug in the liver to that in the blood ($C_{H,u}/C_{B,u}$), in other words, Kp_{uu}.

$$Kp_{uu} = \frac{f_{u,H} \cdot C_H}{f_{u,B} \cdot C_B} = \frac{C_{H,u}}{C_{B,u}} = \frac{PS_{inf,int}}{PS_{eff,int} + CL_{H,int}}$$

This relationship is widely utilized throughout the industry to predict relevant unbound liver concentrations at steady-state [3, 6, 12, 18-21].

The Kp_{uu} relationship is a well-stirred model concept when related to liver transport or elimination processes since it is based on the mass balance relationship where C_H is the single liver concentration that drives biliary elimination, metabolic clearance, and efflux of drug back into the blood. Only in the well-stirred model does a single concentration drive all hepatic processes at steady state; therefore, Kp_{uu} when expressed in terms of elimination parameters is not consistent with alternate hepatic disposition models, such as the parallel tube or axial dispersion models, where the concentrations at the basolateral and apical hepatocyte membranes driving efflux and biliary elimination, respectively, as well as the average concentration driving metabolism, are all assumed to be different concentrations (**Figure 5.1**

Panel A). Recognition that Kp_{uu} is based on the well-stirred model has been noted previously by the International Transporter Consortium [1] and as we have recently reviewed [4, 5], it is well-recognized throughout the field that inclusion of transporters in calculations of hepatic elimination are only consistent with the well-stirred model. Therefore, utilization of Kp_{uu} must be accompanied with appreciation that the apparent Kp_{uu} value is a mere estimation of degree of partitioning based on a useful but simplified model of whole-hepatocyte cytosolic drug concentration. This limitation, amongst others, will be discussed in further detail subsequently.

Questioning the Utility of Kp_{uu} for Drug-Drug Interaction or Pharmacogenomic Variance Predictions

Estimation of Kp_{uu} is often utilized in attempts to improve pharmacokinetic or pharmacodynamic predictions, as cytosolic unbound drug concentrations are more relevant than systemic concentrations for predictions of tissue-specific potency or toxicity and drug disposition (such as metabolic or biliary elimination). The International Transporter Consortium has outlined these useful applications of Kp_{uu} in a 2013 review article and the authors conclude that "The intracellular concentration of unbound form of a drug is an important parameter for predicting drug efficacy, toxicity, and DDIs" [1]. We agree that determination of Kp_{uu} is undoubtedly relevant for predicting drug potency or toxicity, as pharmacodynamic effects are driven by unbound intracellular drug concentrations, however the aspects related to the importance of Kp_{uu} in drug-drug interaction prediction should be further clarified.

To examine the utility of Kp_{uu} in DDI predictions, we take the integral of the concentrations over all time for the numerator and denominator of the two middle terms in the equation directly above for the Kp_{uu} relationship

$$Kp_{uu} = \frac{f_{u,H} \cdot AUC_H}{f_{u,B} \cdot AUC_B} = \frac{AUC_{H,u}}{AUC_{B,u}} = \frac{PS_{inf,int}}{PS_{eff,int} + CL_{H,int}}$$

where AUC_u is the area under the concentration time curve of unbound drug at the respective sites following either an oral or IV dose.

As we have recently demonstrated [4] and others in the field have previously recognized, following oral dosing the equations describing systemic and hepatic AUC_u are given by:

$$\frac{AUC_{B,u}}{Dose_{oral}} = \frac{F_{abs} \cdot F_G \cdot (CL_{H,int} + PS_{eff,int})}{PS_{inf,int} \cdot CL_{H,int}}$$

$$\frac{AUC_{H,u}}{Dose_{oral}} = \frac{F_{abs} \cdot F_G}{CL_{H,int}}$$

where F_{abs} is the fraction of the dose absorbed intact and F_G is the fraction of the dose that escapes intestinal elimination. As expected, dividing the dose-normalized $AUC_{H,u}$ relationship by the dose-normalized $AUC_{B,u}$ relationship results in the Kp_{uu} relationship. The same Kp_{uu} relationship would be derived utilizing the more complicated equations for $AUC_{H,u}$ and $AUC_{B,u}$ following IV dosing from reference [4].

These relationships describing systemic and hepatic AUC_u indicates that unbound AUC_u in the liver and blood following oral dosing are not a function of protein binding, therefore any changes in protein binding (either hepatic or systemic) will have little clinical relevance on

pharmacodynamic outcomes such as efficacy and toxicity [22]. According to these equations, hepatic DDIs will only occur if the perpetrator drug affects F_{abs}, F_G, $CL_{H,int}$, $PS_{inf,int}$ or $PS_{eff,int}$. Therefore, knowledge of intracellular unbound concentrations via measurements of $f_{u,B}$, $f_{u,H}$ or Kp_{uu} will not provide any relevant information regarding predictions of clinically significant changes in systemic or organ drug exposure resulting from DDIs or pharmacogenomics variance. Such changes are simply a multiple of how $CL_{H,int}$, $PS_{inf,int,}$ $PS_{eff,int}$, F_{abs} and F_G change for an orally dosed victim drug, and knowledge of Kp_{uu} is unnecessary to make that prediction. Therefore, we emphasize that evaluation of AUC_R (*AUC* ratios expressed as $AUC_{interaction}/AUC_{control}$) is a more useful approach than evaluating rate determining steps, β or Kp_{uu} in predictions of DDIs.

Recently, we have critically assessed the pharmacokinetic changes expected for transporter substrates [5] and the impact of changes in $CL_{H,int}$ and F_G on the pharmacokinetics of metabolized victim drugs [23] in drug-drug and pharmacogenomic interactions utilizing this extended clearance concept AUC_R-based approach. Utilization of the $AUC_{H,u}$ and $AUC_{B,u}$ relationships provides a clearer understanding of the effect of perpetrator drugs on the magnitude of DDIs than Kp_{uu}-based analysis. For hepatic uptake transporter substrates, a perpetrator drug that markedly inhibits or induces relevant uptake transporters will require a human DDI study to quantitate the effect on systemic concentrations (independent of whether the drug is eliminated by metabolism or not), however, no clinically relevant intrahepatic interaction will be expected. For drugs that are eliminated by metabolism, a perpetrator that significantly inhibits or induces metabolism will require a human DDI study to quantitate the systemic concentration effect, with recognition that both hepatic and intestinal metabolism may be affected. Intrahepatic concentrations will also be affected, therefore DDI studies for

metabolic interactions should also measure changes in organ-specific pharmacodynamic outcomes (such as efficacy and toxicity) as changes in both $CL_{H,int}$ and F_G will influence intrahepatic concentrations. For drugs that are eliminated into the bile, perpetrator drugs with the potential to inhibit apical biliary efflux transporters within the hepatocyte may result in clinically significant systemic concentration changes requiring a human DDI study, as well as potential intrahepatic concentration changes requiring consideration of potential pharmacodynamic changes. Inhibition of basolateral efflux ($PS_{eff,int}$) can impact both the systemic and intrahepatic concentrations of all drugs, regardless of their major route of elimination. In summary, changes in intracellular unbound concentrations as a result of drug-drug or pharmacogenomic interactions can reasonably be predicted based on the AUC_R-based approach without knowing Kp_{uu} or $f_{u,H}$.

An excellent example of quantitative drug-drug interaction predictions of OATP1B1 substrates based on the extended clearance AUC_R values approach was conducted by Varma et al. [24]. In that study, Kp_{uu} was not used in predictions of DDI, rather, the theoretical changes in Kp_{uu} were derived using the above-presented Kp_{uu} relationship and by considering predicted changes in the individual clearance and transport parameters (under the assumption that $PS_{eff,int}$ was only comprised of passive processes) and these changes were compared to observed AUC_R values. The analysis categorizes interactions in four groups based on direction of change in AUC_R versus Kp_{uu}: (a) increased systemic exposure and increased Kp_{uu}, (b) increased systemic exposure but decreased Kp_{uu}, (c) decreased systemic exposure and decreased Kp_{uu}, and (d) decreased systemic exposure but increased Kp_{uu}, highlighting that changes in Kp_{uu} are not always in the same direction as systemic exposure. For perpetrators that inhibit hepatic active uptake (i.e.,

active portion of $PS_{inf,int}$) via OATP1B such as cyclosporine and rifampin (single dose), the expected increase in AUC_R of victim OATP substrates is observed based on examination of the $AUC_{B,u}$ relationship. Consideration of the $AUC_{H,u}$ relationship would result in understanding that intrahepatic exposure remains unchanged when uptake is inhibited, which is important since efficacy of the statins (prototypical OATP1B substrates) relies on unbound intrahepatic concentrations to drive efficacy. However, if the Kp_{uu} relationship had been utilized, inhibition of $PS_{inf,int}$ would predict a decreased unbound liver-to-blood drug concentrations of the victim drug, which may potentially mislead the investigator into thinking that unbound intracellular exposure has decreased, when in reality the reduced Kp_{uu} value is a result of the increase in systemic unbound concentrations and that this change is not relevant for statin's effects. Varma et al. [24] acknowledge this point by indicating that "these results have potential implications for clinical practice – particularly using statins. Arguably, dose adjustments based on plasma exposure during comedication may avoid systemic adverse events such as myopathy and rhabdomyolysis, but could lead to lack of clinical efficacy due to reduced hepatic concentrations".

To further illustrate the impact of changes in a single disposition process (such as $PS_{inf,int}$ as discussed by Varma et al. [24]) on observed $AUC_{B,u}$, $AUC_{H,u}$ and Kp_{uu} values, simulations were conducted to vary a single parameter by 10-fold in each direction (**Figure 6.2**). Changes in $CL_{H,int}$, $PS_{inf,int}$, $PS_{eff,int}$, or $F_{abs}{\cdot}F_G$ were examined (x-axis) and resulting fold-changes in observed $AUC_{B,u}$, $AUC_{H,u}$ and Kp_{uu} are depicted (y-axis). Changes in $PS_{inf,int}$ (**Figure 6.2** Panel B) or $PS_{eff,int}$ (**Figure 6.2** Panel C) result in no change in unbound liver exposure (blue lines), however, unbound systemic exposure (red lines) and Kp_{uu} (green lines) are observed to change inversely. Changes in $F_{abs}{\cdot}F_G$ (**Figure 6.2** Panel D) result in no change in Kp_{uu} due to proportional changes in both systemic and

liver unbound exposure. Increases in $CL_{H,int}$ (**Figure 6.2** Panel A) result in decreases in all three parameters to different degrees, with an observed linear impact on unbound liver exposure (blue line). These simulations exemplify why utilization of Kp_{uu} may mislead and why examination of systemic and hepatic AUC_u ratios should preferentially be utilized.

We further emphasize that these AUC_u relationships describe unbound drug exposure, and that multiplying both sides of these equations by $f_{u,B}$ or $f_{u,H}$, respectively, results in the relationships for total *AUC*:

$$\frac{AUC_B}{Dose_{oral}} = \frac{f_{u,B} \cdot F_{abs} \cdot F_G \cdot (CL_{H,int} + PS_{eff,int})}{PS_{inf,int} \cdot CL_{H,int}}$$

$$\frac{AUC_H}{Dose_{oral}} = \frac{f_{u,H} \cdot F_{abs} \cdot F_G}{CL_{H,int}}$$

Examination of these relationships further emphasizes that changes in protein binding will definitely impact total drug concentrations, however, these changes will not alter unbound systemic or hepatic concentrations that ultimately drive efficacy and toxicity. The nuanced importance of this concept can best be illustrated when considering drug level monitoring, where a change in protein binding would result in altered total blood concentrations and may ultimately influence a clinician to make a dose adjustment. However, consideration of the unbound exposure relationships reveal that unbound exposure had not changed and such dose adjustments could lead to lack of efficacy or safety.

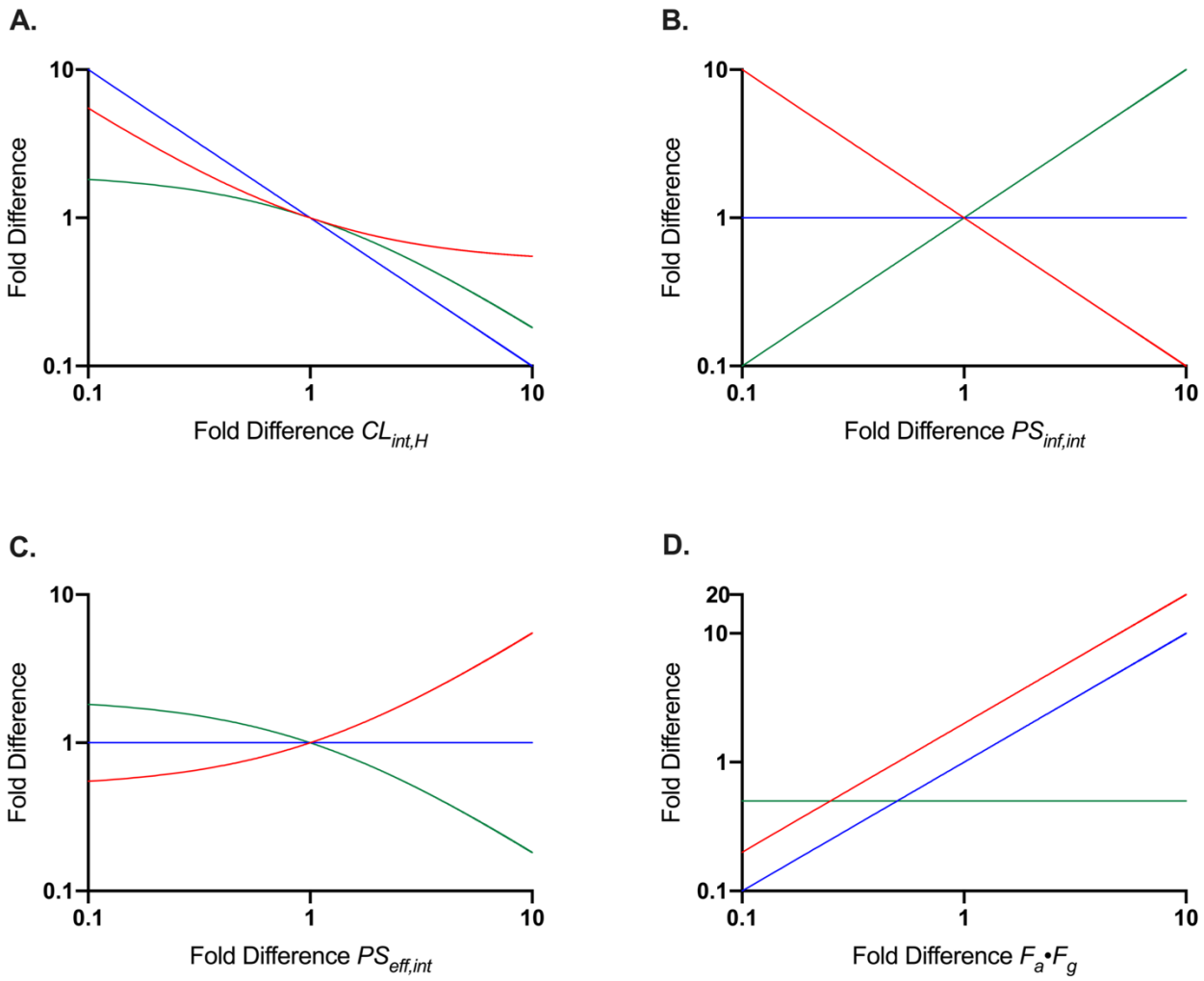

Figure 6.2: Expected fold difference outcomes for systemic unbound exposure ($AUC_{B,u}$), hepatic unbound exposure ($AUC_{H,u}$) and Kp_{uu} based on changes in (A) $CL_{int,H}$, (B) $PS_{inf,int}$, (C) $PS_{eff,int}$ or (D) $F_a \cdot F_g$. Resulting changes in $AUC_{B,u}$ are indicated by the red lines, changes in $AUC_{H,u}$ are indicated by the blue lines, and changes in Kp_{uu} are indicated by the green lines.

The Appropriate Role of Kp_{uu} in Predicting PK/PD and Drug-Drug Interactions

As mentioned above, Kp_{uu} is useful in predicting pharmacodynamic (PD) drug effects driven entirely by unbound intracellular drug concentrations, such as drug efficacy or toxicity associated with a specific organ [21,25-27]. This is particularly relevant for statins, as drug

efficacy is a function of intrahepatic concentrations, however systemic or muscle exposure may drive undesirable myopathy side effects. Evaluation of Kp_{uu} may also be useful when estimating free liver concentrations based on readily measurable plasma concentrations in a clinical study. Thus, an *in vitro* measurement of Kp_{uu} has the potential to allow for estimations of drug exposure within the organ, a concentration that is extremely difficult to measure, which can help inform potential for pharmacological and adverse effects.

Determination of Kp_{uu} may also be helpful in improving predictions of pharmacokinetic drug disposition (i.e. in prediction of hepatic drug elimination). Recently, Riccardi et al. [28] demonstrated improved clearance predictions for transporter and enzyme substrates involving *in vitro* hepatocyte clearance determinations in the presence of 4% bovine serum albumin, to account for protein-facilitated uptake mechanisms, as recently described by Bowman and Benet [29]. A modified version of Kp_{uu} that accounts for unbound drug partitioning between the liver tissue and the liver plasma was utilized in the mathematical model and was estimated with consideration of measured partitioning between the hepatocytes and the protein-augmented buffer, resulting in improved clearance predictions.

With respect to drug interaction prediction, Kp_{uu} can be utilized in improving predictions of inhibitory potential of an intracellular perpetrator drug, but only in regards to processes driven by intracellular concentrations, i.e. metabolic elimination ($CL_{int,H}$), biliary elimination ($CL_{int,bil}$) and basolateral efflux ($PS_{int,eff}$), since active uptake processes ($PS_{int,inf}$) into the liver would be driven by systemic perpetrator concentrations (**Figure 6.1**). Predictions of inhibitory potential of perpetrator drugs are routinely performed and according to the FDA Draft Guidance [14] the change in systemic exposure of victim drug as a result of a perpetrator can estimated by the AUC_R

relationship presented in the Methods, reflecting a basic interaction with a reversible inhibitor of a single hepatic disposition process. More complex models involving time-dependent inhibitors or inhibition of multiple pathways are commonly integrated in physiologically-based pharmacokinetic (PBPK) modeling approaches, and are essentially based on integration of individual specific models for each process into the $AUC_{H,u}$ and $AUC_{B,u}$ relationships to predict overall *AUC* changes in complex drug-drug interactions [24, 30, 31]. Determinations of Kp_{uu} are theoretically valuable in accounting for the true unbound concentration of an intracellular inhibitor in order to more accurately predict drug interaction potential, but the uncertainty of Kp_{uu} measurements via the different procedures employed belies the usefulness of this approach as we show below.

Recently, Iwasaki et al. [17] introduced Kp_{uu} into their PBPK models to potentially improve the predictability of twenty-two CYP-mediated DDIs. The authors determined Kp_{uu} by three methods (temperature, homogenization and *in vivo* rat studies) and incorporated these values into their predictive models; model outcomes of these simulations were compared to that of simulations conducted without consideration of Kp_{uu} (i.e., Kp_{uu} = 1). These authors concluded that the accuracy of DDI predictions improved upon inclusion of Kp_{uu}, however, although root mean square error (RMSE) showed a moderate improvement (5.12 versus 2.31-3.91), there was no change in average fold error (AFE) (1.45 versus 1.36-1.43) nor in percent within 2-fold (86.4% versus 81.8-100%). The purported improvement of DDI predictions based on RMSE values appears to rely entirely on one interaction (itraconazole-triazolam; AUC_R = 27.1) for which drug interaction potential was underpredicted. It is telling that the experimental determinations of Kp_{uu} for itraconazole in that report vary greatly between methodologies utilized, with values

ranging from 4.16 to 22.6. Aspects related to variability in the Kp_{uu} value due to the intricate methodologies required will be discussed in further detail subsequently.

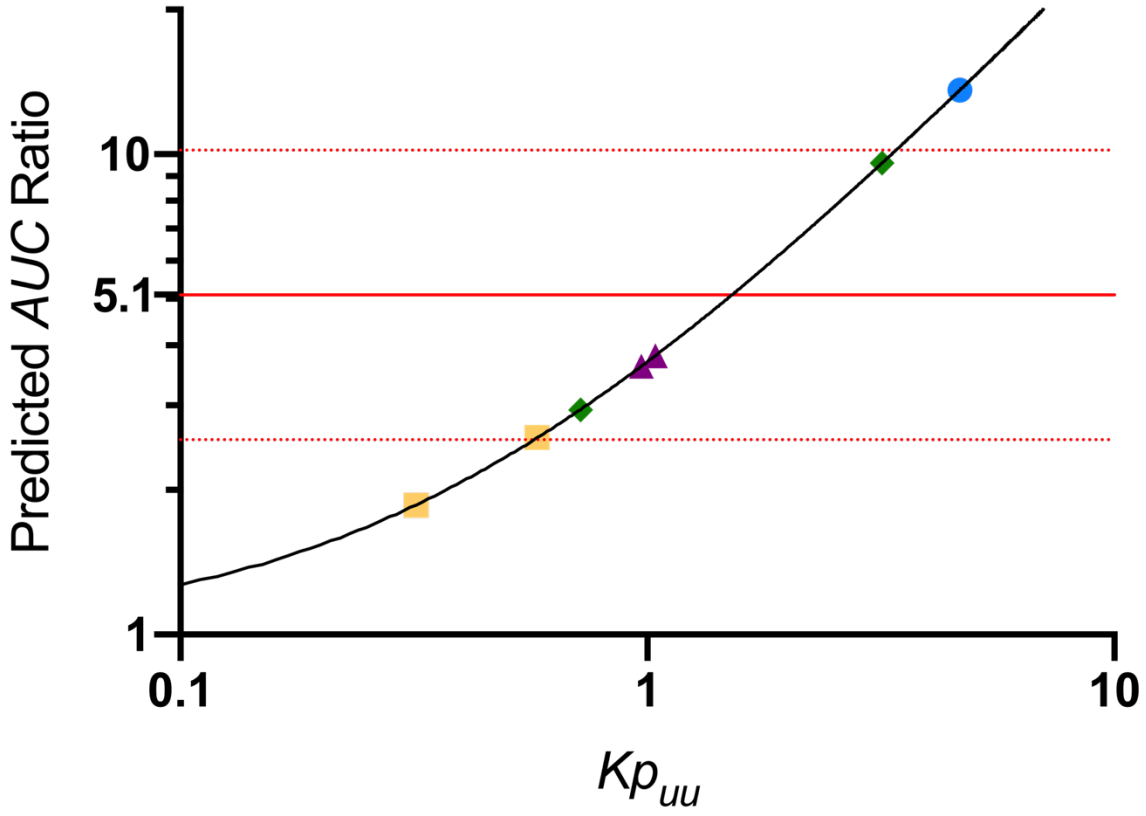

Figure 6.3. Predicted magnitude of metabolic drug-drug interaction between ketoconazole (perpetrator) and midazolam (victim) based on Tsunoda et al. [13]. The ratio of *AUC* for the interaction phase divided by the control phase is plotted on the y-axis. The observed clinical *AUC* ratio of 5.1 is indicated by the horizontal red line (red dotted lines indicate two-fold differences from this value). Predictive midazolam *AUC* ratios for simulations incorporating Kp_{uu} values (ranging from 0.1 to 10) that would be observed for reversible CYP3A4 inhibition by ketoconazole are indicated by the black line. Experimental measures of Kp_{uu} from the literature are presented as symbols on this line: purple triangles, temperature method; green diamonds, homogenization method; blue circle, Log D method; yellow squares, extended clearance method.

To investigate if predictions of AUC_R for a simple metabolic interaction could be improved with implementation of Kp_{uu} to assess relevant inhibitory concentrations, the CYP3A4-mediated interaction between IV midazolam (victim drug) and ketoconazole (perpetrator) [13] was predicted utilizing the AUC_R relationship presented in the Methods. Maximum unbound concentration ($I_{max,u}$) of ketoconazole was determined to be 0.16 µM and average unbound inhibitory constant (K_i) was 0.061 µM, resulting in a predicted AUC_R of 3.6, as compared to the observed ratio of 5.1 as indicated by the solid red line in **Figure 6.3**. Published values of ketoconazole Kp_{uu} were utilized to attempt to improve prediction of unbound intracellular ketoconazole concentrations in contact with CYP3A4 and these values were supplemented by simulations of Kp_{uu} ranging from 0.1 to 10, as indicated by the solid black line. To achieve a predicted AUC_R of 5.1, a Kp_{uu} value of 1.5 is necessary, however the reported literature Kp_{uu} values ranged almost 15-fold, from 0.32 – 4.67. Thus, depending on the methodology employed, drastically different predictions are achieved. Further, a 4.4-fold difference in Kp_{uu} value for the homogenization method was observed between labs (0.72 [18] vs. 3.18 [17]), highlighting the large degree of inter-lab variability associated with these measurements.

Limitations in the Utility of Kp_{uu} Values

Although utilization of Kp_{uu} values should theoretically improve the optimization and development of novel therapeutics, significant limitations related to Kp_{uu} methodology result in limited benefits of its implementation, including (1) its basis upon the well-stirred model, which ignores the nuances of intracellular-drug distribution, (2) labor-intensive determination

methodologies that are (3) prone to a high degree of variability in outcome with respect to experimental methodology employed and inter-lab variability.

First, the simplification of driving-force concentrations may result in noteworthy limitations in the utility of Kp_{uu}. If subcellular drug localization is not uniform, Kp_{uu} may over- or under-estimate true unbound drug concentrations relevant for the process-of-interest. For instance, discerning any differences between potential inhibition of hepatic metabolism, basolateral transport and apical transport processes poses a challenge when only the average intracellular concentration is known. Further, Kp_{uu} cannot account for the effects of subcellular drug accumulation, which may occur due to pH or electrochemical differences between cytosol and organelles (particularly in lysosomes and mitochondria). If drug accumulates in subcellular compartments, measurement of apparent Kp_{uu} would result in an overestimate of true intracellular cytosolic drug concentration and confound predictions of hepatic disposition of processes associated with unbound cytosolic drug concentrations.

The impact of subsequent subcellular drug partitioning on the apparent Kp_{uu} value has been investigated by a number of groups, with particular focus on lysosomal trapping, which is known to affect basic compounds (**Table 6.1**) [18, 32]. For basic drugs, that is diltiazem, erythromycin, imatinib, propranolol, and verapamil, a significant decrease in the apparent Kp_{uu} value was observed when lysosomal trapping was inhibited by chloroquine. The largest Kp_{uu} decrease was observed for imatinib (5.3-fold reduction) when lysosomal trapping was inhibited, highlighting that traditional measurements of apparent Kp_{uu} would have significantly overpredicted cytosolic unbound drug concentration by approximately 5-fold. Data summarized in **Table 6.1** support that this trend is not as apparent for acidic drugs (such as diclofenac,

indomethacin and simvastatin acid). The value of Kp_{uu} for verapamil varied greatly between reports (5.7 versus 0.7), highlighting the issues surrounding inter-lab variability.

Table 6.1: Published Kp_{uu} Values with Respect to Subcellular Partitioning

Drug	Charge Class	Kp_{uu}	Kp_{uu} + Chloroquine	Chloroquine Conc. (μM)	Fold Difference in Kp_{uu}	Method [Reference]
Diclofenac	Acid	2.6	2.2	0.5	0.85	Homogenization Method[a]; [32]
			2.6	5	1.0	
			2.7	50	1.0	
Indomethacin	Acid	1.3	1.4	0.5	1.1	Homogenization Method[a]; [32]
			1.6	5	1.2	
			1.5	50	1.2	
Simvastatin Acid	Acid	0.70	1.3	0.5	1.9	Homogenization Method[a]; [32]
			1.6	5	2.3	
			1.1	50	1.6	
Diltiazem	Basic	2.9	1.9	0.5	0.66	Homogenization Method[a]; [32]
			1.2	5	0.41	
			0.63	50	0.22	
Erythromycin	Basic	11.5	3.36	0.5	0.29	Temperature Method; [18]
		0.11	0.06	0.5	0.55	Homogenization Method; [18]
Imatinib	Basic	2.71	0.56	0.5	0.21	Temperature Method; [18]
		1.30	0.25	0.5	0.19	Homogenization Method; [18]
Propranolol	Basic	4.7	3.3	0.5	0.70	Homogenization Method[a]; [32]
			1.6	5	0.34	
			1.4	50	0.30	
Verapamil	Basic	5.7	5.3	0.5	0.93	Homogenization Method[a]; [32]
			3.7	5	0.65	
			1.8	50	0.32	
Verapamil	Basic	0.73	1.05	0.5	1.4	Temperature Method; [18]
		0.67	0.41	0.5	0.61	Homogenization Method; [18]

[a]Values were digitized from Figure 5 of Mateus et al. [32]

Further in the Riede et al. report [18], erythromycin Kp_{uu} values varied 100-fold between determination methodologies (homogenization method (0.11) versus temperature method (11.5)) within the same lab, demonstrating the need for reliable and consistent methodologies for Kp_{uu} determination. In summary, these studies highlight that subcellular drug accumulation may result in inflated apparent Kp_{uu} values, resulting in an overestimation of true unbound intracellular cytosolic drug concentrations, as well as potential underestimation of subcellular accumulation, which may be relevant for certain pharmacological targets, such as for respiratory indications with targets located in the lung [26]. Until significant advancements in experimental and analytical methodology to detect the nuances of subcellular drug distribution, utilization of Kp_{uu} in pharmacokinetic or pharmacodynamic predictions should be accompanied with recognition of the inherent limitations of the simple but useful single-concentration well-stirred model assumption.

We emphasize that measurement of Kp_{uu} is not a trivial task, either involving (1) determination of total drug partitioning (Kp) that is further corrected by measures or predictions of incubational and hepatic binding ($f_{u,inc}$ and $f_{u,H}$, respectively) or by (2) measurement of individual hepatic disposition intrinsic clearances for incorporation into the Kp_{uu} equation, which must be conducted under multiple experimental conditions to isolate each process. Therefore, it is to be expected that experimental outcome may be plagued with variability issues. In a subsequent publication, we will evaluate the reliability of human *in vitro* Kp_{uu} measurements with respect to inter- and intra-lab variability, experimental methodology, and with consideration of the theoretical Kp_{uu} values expected for transport substrates (versus drugs with no clinical significant transporter involvement for which values are expected to be close to or less than 1).

As demonstrated here for a limited dataset, our evaluation will report significant variability in measurements for the same drug across different methodologies and by different labs.

Conclusions

Although Kp_{uu} may be useful in improving predictions of pharmacodynamics, there is limited benefit of utilization of Kp_{uu} in improving drug-drug interaction predictions. In DDI predictions of victim drug, dependence on extended clearance concept-based AUC_R equations is a more reasonable approach, as changes in Kp_{uu} can potentially mislead an investigator to incorrectly conclude that the Kp_{uu} change has resulted in altered intrahepatic concentrations, an aspect crucial for tissue-specific efficacy or toxicity. Further, utilization of the AUC_R equations in DDI prediction can reasonably predict the magnitude of DDIs and does not require any measurement of Kp_{uu} or $f_{u,H}$, potentially difficult tasks plagued with a high degree of variability between laboratories and between methodologies. The appropriate use of Kp_{uu} is in improving predictions related to pharmacodynamics (i.e. efficacy and toxicity), drug disposition (hepatic clearance or biliary elimination) or in characterizing the inhibitory potential of perpetrator drugs for processes driven by intracellular unbound drug concentrations. Consideration that Kp_{uu} is based on a well-stirred model interpretation of hepatic elimination must be taken into account, as nuances of intracellular drug distribution are not considered by the Kp_{uu} model. Finally, a significant degree of variability in Kp_{uu} values has been suggested in the literature and therefore utilization of this difficult-to-measure theoretical value may result in a large prediction error depending on the particular methodology used. This necessitates the development of reliable

and consistent experimental Kp_{uu} determination methodologies to support its role in improving predictive models related to drug disposition.

References

1. Chu X, Korzekwa K, Elsby R, Fenner K, Galetin A, Lai Y, Matsson P, Moss A, Nagar S, Rosania GR, Bai JPF, Polli JW, Sugiyama Y, Brouwer KLR, International Transporter Consortium. Intracellular drug concentrations and transporters: measurement, modeling, and implications for the liver. *Clin Pharmacol Ther*. 2013;94(1):126-141.
2. Trainor GL. The importance of plasma protein binding in drug discovery. *Expert Opin Drug Discov*. 2007;2(1):51-64.
3. Camenisch G, Riede J, Kunze A, Huwyler J, Poller B, Umehara K. The extended clearance model and its use for the interpretation of hepatobiliary elimination data. *ADMET & DMPK*. 2015;3(1):1-14.
4. Benet LZ, Bowman CM, Liu S, Sodhi JK. The extended clearance concept following oral and intravenous dosing; theory and critical analysis. *Pharm Res*. 2018;35(12):242.
5. Benet LZ, Bowman CM, Sodhi JK. How transporters have changed basic pharmacokinetic understanding. *AAPS J*. 2019;21(6):103.
6. Barton HA, Lai Y, Goosen TC, Jones HM, El-Kattan AF, Gosset JR, Lin J, Varma MV. Model-based approaches to predict drug-drug interactions associated with hepatic uptake transporters: preclinical, clinical and beyond. *Expert Opin Drug Metab Toxicol*. 2013;9(4):459-472.
7. Camenisch G, Umehara K. Predicting human hepatic clearance from in vitro drug metabolism and transport data: a scientific and pharmaceutical perspective for assessing drug-drug interactions. *Biopharm Drug Dispos*. 2012;33(4):179-194.

8. El-Kattan AF, Varma MVS. Navigating transporter sciences in pharmacokinetics characterization using the extended clearance classification system. *Drug Metab Dispos*. 2018;46(5):729-739.
9. Patilea-Vrana G, Unadkat JD. Transport vs. metabolism: what determines the pharmacokinetics and pharmacodynamics of drugs? Insights from the extended clearance model. *Clin Pharmacol Ther*. 2016;100(5):413-418.
10. Sirianni GL, Pang KS. Organ clearance concepts: new perspectives on old principles. *J Pharmacokinet Biopharm*. 1997;25(4):449-470.
11. Varma MV, Steyn SJ, Allerton C, El-Kattan AF. Predicting clearance mechanism in drug discovery: extended clearance classification system (ECCS). *Pharm Res*. 2015;32(12):3785-3802.
12. Webborn PJH, Parker AJ, Denton RL, Riley RJ. In vitro-in vivo extrapolation of hepatic clearance involving active uptake: theoretical and experimental aspects. *Xenobiotica*. 2007;37(10-11):1090-1109.
13. Tsunoda SM, Velez RL, von Moltke LL, Greenblatt DJ. Differentiation of intestinal and hepatic cytochrome P450 3A activity with use of midazolam as an in vivo probe: effect of ketoconazole. *Clin Pharmacol Ther*. 1999;66(5):461-471.
14. U.S. Food and Drug Administration, Center for Drug Evaluation and Research. In vitro metabolism- and transporter-mediated drug-drug interaction studies: guidance for industry. Silver Spring, MD; 2017.

15. Greenblatt DJ, Venkatakrishnan K, Harmatz JS, Parent SJ, von Moltke LL. Sources of variability in ketoconazole inhibition of human cytochrome P450 3A in vitro. *Xenobiotica*. 2010;40(10):713-720.
16. Martínez-Jordá R, Rodriguez-Sasiain JM, Suárez E, Calvo R. Serum binding of ketoconazole in health and disease. *Int J Clin Pharmacol Res*. 1989;10(5):271-276.
17. Iwasaki S, Kosugi Y, Zhu AZX, Nakagawa S, Sano N, Funami M, Kosaka M, Furuta A, Hirabayashi H, Amano N. Application of unbound liver-to-plasma concentration ratio to quantitative projection of cytochrome P450-mediated drug-drug interactions using physiologically based pharmacokinetic modelling approach. *Xenobiotica*. 2019;49(11):1251-1259.
18. Riede J, Camenisch G, Huwyler J, Poller B. Current in vitro methods to determine hepatic Kp_{uu}: a comparison of their usefulness and limitations. *J Pharm Sci*. 2017;106(9):2805-2814.
19. Li Z, Di L, Maurer TS. Theoretical considerations for direct translation of unbound liver-to-plasma partition coefficient from in vitro to in vivo. *AAPS J*. 2019;21(3):43.
20. Nordell P, Winiwarter S, Hilgendorf C. Resolving the distribution-metabolism interplay of eight OATP substrates in the standard clearance assay with suspended human cryopreserved hepatocytes. *Mol Pharmaceut*. 2013;10(12):4443-4451.
21. Riede J, Poller B, Huwyler J, Camenisch G. Assessing the risk of drug-induced cholestasis using unbound intrahepatic concentrations. *Drug Metab Dispos*. 2017;45(5):523-531.

22. Benet LZ, Hoener B-a. Changes in plasma protein binding have little clinical relevance. *Clin Pharmacol Ther*. 2002;71(3):115-121.

23. Benet LZ, Bowman CM, Koleske ML, Rinaldi CL, Sodhi JK. Understanding drug-drug interaction and pharmacogenomic changes in pharmacokinetics for metabolized drugs. *J Pharmacokinet Pharmacodyn*. 2019;46(2):155-163.

24. Varma MV, Bi YA, Kimoto E, Lin J. Quantitative prediction of transporter- and enzyme-mediated clinical drug-drug interactions of organic anion-transporting polypeptide 1B1 substrates using a mechanistic net-effect model. *J Pharmacol Exp Ther*. 2014;351(1):214-223.

25. Loryan I, Sinha V, Mackie C, Van Peer A, Drinkenburg W, Vermeulen A, Morrison D, Monshouwer M, Heald D, Hammarlund-Udenaes. Mechanistic understanding of brain drug disposition to optimize the selection of potential neurotherapetuics in drug discovery. *Pharm Res*. 2014;31(8):2203-2219.

26. Ufuk A, Assmus F, Francis L, Plumb J, Damian V, Gertz M, Houston JB, Galetin A. In vitro and in silico tools to assess extent of cellular uptake and lysosomal sequestration of respiratory drugs in human alveolar macrophages. *Mol Pharmaceut*. 2017;14(4):1033-1046.

27. Tsmandouras N, Dickinson G, Guo Y, Hall S, Rostami-Hodjegan A, Galetin A, Aarons L. Development and application of a mechanistic pharmacokinetic model for simvastatin and its active metabolite simvastatin acid using an integrated population PBPK approach. *Pharm Res*. 2015;32(6):1864-1883.

28. Riccardi KA, Tess DA, Lin J, Patel R, Ryu S, Atkinson K, Di L, Li R. A novel unified approach to predict human hepatic clearance for both enzyme- and transporter-mediated mechanisms using suspended human hepatocytes. *Drug Metab Dispos*. 2019;47(5):484-492.
29. Bowman CM, Benet LZ. An examination of protein binding and protein-facilitated uptake relating to in vitro-in vivo extrapolation. *Eur J Pharm Sci*. 2018;123:502-514.
30. Gertz M, Cartwright CM, Hobbs MJ, Kenworthy KE, Rowland M, Houston JB, Galetin A. Cyclosporine inhibition of hepatic and intestinal CYP3A4, uptake and efflux transporters: application of PBPK modeling in the assessment of drug-drug interaction potential. *Pharm Res*. 2013;30(3):761-780.
31. Rowland Yeo K, Walsky RL, Jamei M, Rostami-Hodjegan A, Tucker GT. Prediction of time-dependent CYP3A4 drug-drug interactions by physiologically based pharmacokinetic modelling: impact of inactivation parameters and enzyme turnover. Eur J Pharm Sci. 2011;43(3):160-173.
32. Mateus A, Matsson P, Artursson P. Rapid measurement of intracellular unbound drug concentrations. Mol Pharmaceut. 2013;10(6):2467-2478.

CHAPTER 7: ARE THERE ANY EXPERIMENTAL PERFUSION DATA THAT PREFERENTIALLY SUPPORT THE DISPERSION AND PARALLEL TUBE MODELS OVER THE WELL-STIRRED MODEL OF ORGAN ELIMINATION?*

Abstract

In reviewing previously published isolated perfused rat liver studies, we find no experimental data for high clearance metabolized drugs that reasonably or unambiguously support preference for the dispersion and parallel tube models versus the well-stirred model of organ elimination when only entering and exiting drug concentrations are available. It is likely that the investigators cited here may have been influenced by: 1) the unphysiologic aspects of the well-stirred model, which may have led them to undervalue the studies that directly test the various hepatic disposition models for high clearance drugs (for which model differences are the greatest); 2) experimental assumptions made in the last century that are no longer valid today, related to the predictability of *in vivo* outcomes from *in vitro* measures of drug elimination and the influence of albumin in hepatic drug uptake; and 3) a lack of critical review of previously reported experimental studies, resulting in inappropriate interpretation of the available experimental data. The number of papers investigating the theoretical aspects of the dispersion, parallel tube and well-stirred models of hepatic elimination greatly outnumber the papers that actually examine the experimental evidence available to substantiate these models. When all experimental studies that measure organ elimination using entering and exiting drug

* Modified from the publication: Sodhi JK, Wang H-J, Benet LZ. Are there any experimental perfusion data that preferentially support the dispersion and parallel-tube models over the well-stirred model of organ elimination? *Drug Metab Dispos.* 2020;48(7):537-543.

concentrations at steady state are critically reviewed, the simple but unphysiologic well-stirred model is the only model that can describe all trustworthy published available data.

Introduction

Forty-eight years ago, Rowland [1] defined steady-state organ clearance (here hepatic, CL_H) as the fraction of the entering drug blood concentration (C_{in}) that is eliminated by the organ multiplied by organ blood flow (Q_H), with the ratio of concentration terms designated as the extraction ratio (*ER*). This relationship will be referred to subsequently as Equation 1.

$$CL_H = Q_H \cdot \frac{C_{in} - C_{out}}{C_{in}} = Q_H \cdot \left(1 - \frac{C_{out}}{C_{in}}\right) = Q_H \cdot ER$$

This simple but useful relationship allowed for clearance measurements based only on knowledge of entering and exiting concentrations and organ blood flow. In 2018, Benet et al. maintained that Eq. 1 was only consistent with the well-stirred model of hepatic elimination, since the amount lost at steady-state, $Q_H \bullet (C_{in} - C_{out})$, was divided by the drug concentration entering the liver (C_{in}) to obtain CL_H, and no other concentrations within the liver were considered in the clearance determination [2]. These are solely characteristics of the well-stirred model. In a Commentary accompanying that paper [3], Rowland and Pang write that Eq. 1 is model independent and "simply express[es] proportionality between observed rate of elimination and a reference concentration", and as they had earlier indicated [4] that "by definition" organ clearance is given by Eq. 1.

In the present chapter, we do not further discuss the theoretical differences of Benet et al. [2] versus Rowland and Pang [3] with respect to Eq. 1, rather we objectively review and critically evaluate the experimental data available when Eq. 1 is used to calculate organ clearance. If there is truth to the assertion that Eq. 1 is model independent there should be

experimental data supporting preference for the dispersion or parallel tube models versus the well-stirred model when Eq. 1 is used to calculate organ clearance. There are numerous papers related to the theoretical basis of alternate models of hepatic elimination (which we agree are more physiologically-relevant than the well-stirred model), and even more papers by hundreds of authors throughout the field where such models are utilized, including by widely employed PBPK programs. However, there are very few experimental papers that directly test the differences between the theoretical organ disposition models, as we review here. Let us be clear. We agree that the well-stirred model (also called the venous equilibration model) is unphysiologic. We agree that there is zonal distribution of the metabolic activity of enzymatic processes within the liver. We agree that there is dispersion within the liver that is neither zero nor infinite. The purpose of this paper is to examine for the first time all of the experimental data when only entering and exiting concentrations for an organ of elimination are available, with respect to which model is consistent with the Eq. 1 definition of hepatic elimination.

Methods

Literature Search

Previously published isolated perfused rat liver (IPRL) studies were identified from the literature as it is possible to directly distinguish the models of hepatic elimination with such isolated organ studies, and because such IPRL studies were commonly utilized and cited by the field as support of one hepatic disposition model versus another. A schematic of a typical single-pass IPRL study is presented as **Figure 7.1**. Since the well-stirred model, dispersion model, and parallel tube model quantitatively predict similar clearance values for low and moderately

extracted drugs, analysis focused only on high extraction ratio substrates (*ER* > 0.7) where the models can maximally be discriminated from one another. The literature search resulted in identification of only four publications that performed IPRL studies for high clearance drugs (lidocaine [4, 5], meperidine [5] and propranolol [6, 7]) in which model differentiation was possible. Four additional studies were identified for two high clearance non-drug substances (galactose [8] and taurocholate [9-11]) and five studies for which the low clearance drugs, diazepam and diclofenac, were manipulated to behave like a high clearance drug by altering protein binding [10, 12-15]. All discussed publications are listed in **Table 7.1**. These studies were critically examined with respect to the degree of discrepancy that the experimental data had with predictions from each hepatic disposition model, with the purpose of potentially identifying experimental data that cannot be described by the well-stirred model.

In evaluating the validity of results of steady-state IPRL studies, it is important to ensure that the viability of the IPRL is maintained throughout the experimentation period. Key points to consider include (1) length of perfusion times, with preference for shorter duration times, (2) ensuring elimination follows first-order kinetics at concentrations tested, (3) flows should be optimized as to not damage to liver at very high flow rates and ensure the vasculature is fully perfused, which may be an issue for flow rates that are too low and (4) adequate oxygenation of the system. For the purposes of model discrimination, the selected drugs should be high *ER* and perfusion rate limited.

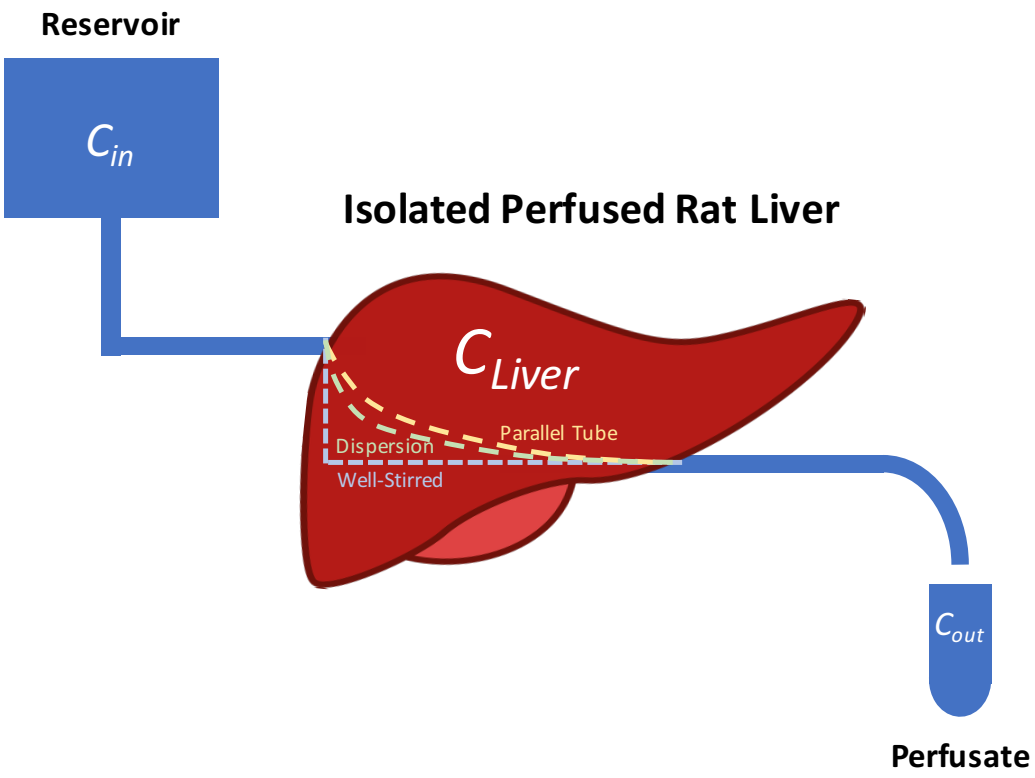

Figure 7.1: Schematic representation of an isolated perfused rat liver (IPRL) study and its utility in evaluating hepatic disposition models. By using a known entering drug concentration (C_{in}) and measuring the exiting drug concentration (C_{out}), it is possible to evaluate the various hepatic disposition models by predicting the C_{out} associated with each model (and comparing this value with measured C_{out}). Perturbations in protein binding or perfusate flow are often utilized to evaluate which model is most predictive of such changes. Depicted in the figure are the two boundary hepatic disposition models: (1) the well-stirred model (which assumes instantaneous and non-incremental metabolism) and (2) the parallel-tube model (which assumes log-linear decline of drug concentrations). The dispersion model falls between these two boundaries, as the loss of drug depends on the specific degree of dispersion assumed by the model.

Model Discrimination

Investigators conducted IPRL studies with known C_{in} values and measured C_{out} values under different experimental conditions that alter experimental flow (Q) or protein binding (f_u). Experimental results were reported as ER, availability ($F = \frac{C_{out}}{C_{in}}$), or the ratio of observed C_{out}

values under different experimental conditions. Investigators then compared these observed outcome measurements with the predicted value expected for the well-stirred model versus the values expected for the alternate parallel tube and dispersion models. In all of these studies, clearance was calculated by Eq. 1 under the assumption that Eq. 1 is model independent. It should be noted that if Eq. 1 is not model independent, then the expected values for the parallel tube and dispersion models reported by these investigators would be incorrect. However, here we accept these comparisons and the model independent assumption of Eq. 1 to objectively evaluate the available experimental data under the same assumptions made by the investigators.

In Vitro to In Vivo Extrapolation (IVIVE) Approach

An alternate indirect approach to test model discrimination was previously proposed by Roberts and Rowland [16] and further presented by Iwatsubo et al. [17], in which in vitro measures of intrinsic clearance (CL_{int}) were scaled up to predictions of in vivo CL_{int} following physiologically-based IVIVE techniques for a number of drugs with published IPRL data. These IVIVE-predicted in vivo CL_{int} values were then utilized to calculate an efficiency number (R_N) ($R_N = f_u \bullet CL_{int} / Q_H$) based on IPRL experimental conditions and plotted against experimentally observed hepatic availability (F), which was calculated using Eq. 1 and the extraction ratio/bioavailability relationship ($ER = 1 - F$). Finally, these values were compared with the hepatic availability values expected for the various hepatic disposition models.

Table 7.1: Summary of Isolated Perfused Rat Liver (IPRL) Studies for High Clearance Substrates

Test Compound	Category	Condition Altered	Reference
Lidocaine	Drug	Q_H (1.6-fold)	Pang and Rowland, 1977 [4]
Lidocaine	Drug	Q_H (1.5-fold)	Ahmad et al., 1983 [5]
Meperidine (Pethidine)	Drug	Q_H (1.5-fold)	Ahmad et al., 1983 [5]
Propranolol	Drug	f_u (2.7-fold)	Jones et al., 1984 [6]
Propranolol	Drug	f_u (5.7-fold)	Jones et al., 1985 [7]
Galactose	Non-Drug Substrate	Q_H (1-4 to 1.8-fold)	Keiding and Chiarantini, 1978 [8]
Taurocholate	Non-Drug Substrate	f_u (Single pass: 11.1-fold)	Smallwood et al., 1988 [9]
Taurocholate	Non-Drug Substrate	f_u (Recirculating; 18-fold)	Smallwood et al., 1988 [9]
Taurocholate	Non-Drug Substance	f_u (14.6-fold)	Ching et al., 1989 [10]
Taurocholate	Non-Drug Substrate	f_u (7.4-fold)	Roberts et al., 1990 [11]
Taurocholate	Non-Drug Substrate	Q_H (3.7-fold)	Roberts et al., 1990 [11]
Diazepam[a]	Drug	f_u (13.2-fold)	Ching et al., 1989 [10]
Diazepam[a]	Drug	f_u (1.3-fold)	Rowland et al., 1984 [12]
Diazepam[a]	Drug	f_u (2.7-fold)	Diaz-Garcia et al., 1992 [14]
Diazepam[a]	Drug	Q_H (2.0-fold)	Diaz-Garcia et al., 1992 [14]
Diazepam[a]	Drug	f_u (1.4-fold)	Wang and Benet, 2019 [15]
Diclofenac[a]	Drug	f_u (333-fold)	Hussein et al., 1993 [13]

Abbreviations: f_u, fraction unbound (protein binding); Q_H, hepatic flow
[a]Low clearance drug manipulated to be high clearance in absence of plasma proteins

Results

Isolated Perfused Rat Liver (IPRL) Studies of High Clearance Drugs

The various hepatic disposition models diverge from one another as clearance value increases, therefore high clearance (extraction ratio) compounds are the most appropriate for testing model discrimination. There are only four published isolated rat perfusion (IPRL) studies that evaluate these models for high extraction ratio drugs [4-7]. All four of those studies, including two from the Rowland laboratory, conclude that the data are consistent with the well-stirred model, not alternate hepatic clearance models.

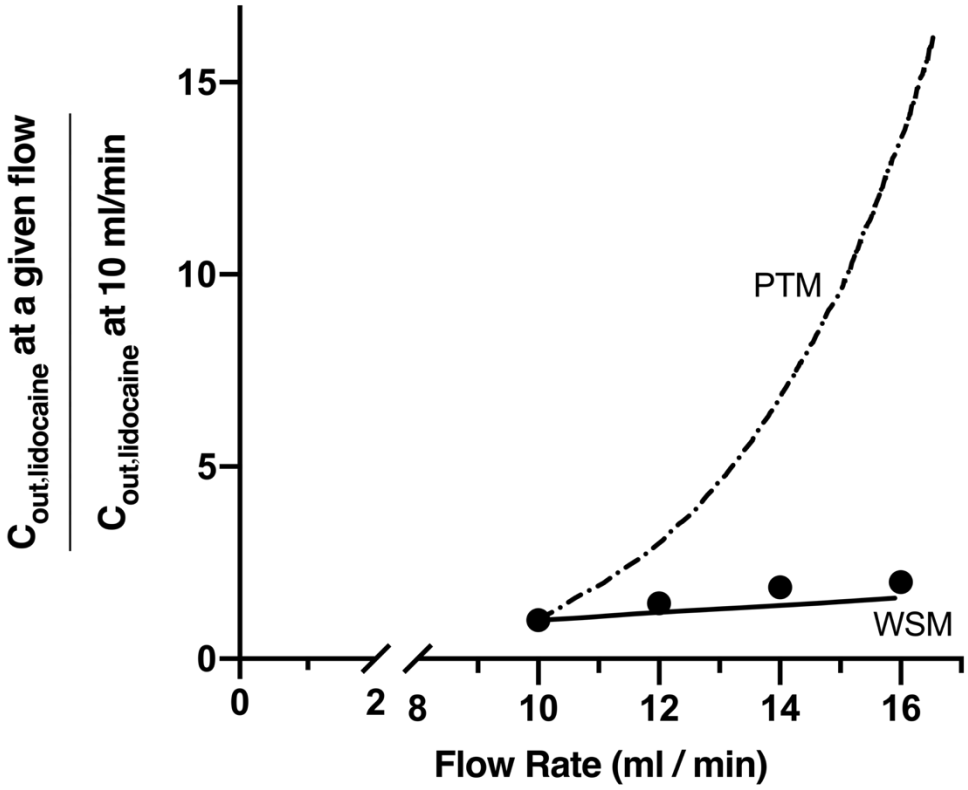

Figure 7.2: Experimental lidocaine isolated perfused rat liver (IPRL) results and models of hepatic elimination from Pang and Rowland [4]. The well-stirred model (WSM) appears as a solid line and the parallel-tube model (PTM) appears as a dashed line.

In the first of the two Rowland publications, Pang and Rowland [4] evaluated the effect of changing organ blood flow on the extraction ratio of lidocaine as depicted in **Figure 7.2**. The title of the paper indicates the results: "Experimental evidence for acceptance of the well-stirred model over the parallel tube model using lidocaine in the perfused rat liver in situ preparation". In the second Rowland publication, Ahmad et al. also evaluated the effect of changing blood flow on the extraction ratio of lidocaine and meperidine (pethidine), displaying figures that markedly differentiate the experimental outcome between the well-stirred model and the parallel tube model for both drugs [5]. The concluding sentence of the abstract of that paper states, "The experimental findings indicate that the well-stirred model more accurately predicts the elimination of highly cleared drugs with perturbation of flow than does the parallel tube model."

Two additional studies were published by Jones et al. [6, 7] that evaluated the effect of changing protein binding on the extraction ratio of propranolol. The advantage of altering protein binding (as opposed to flow) is that it is possible to vary binding over a much larger range than flow can be varied, due to liver integrity issues resulting from flow rates that are too high or too low. In the Jones et al. (1984) study, a 2.7-fold change in propranolol protein binding was achieved when albumin concentration was varied [6]. The following year Jones et al. (1985) reported an average 5.7-fold change in protein binding when α_1-acid glycoprotein (AAG) was the binding protein examined [7]. In contrast, in the Rowland studies, flow was only able to be varied by 1.6-fold [4] and 1.5-fold [5]. Results for both Jones et al. studies show clear preference for the well-stirred model [6, 7]. At the beginning of the concluding paragraph of the Jones et al. (1984) paper, they state, "Although there may be no simple anatomical explanation for the applicability of one or other model, it is clear that the venous equilibration model precisely describes the

hepatic elimination of propranolol. Operationally, the liver is behaving as a well mixed compartment, however 'unphysiological' this may seem" [6]. In the first sentence of the concluding paragraph of Jones et al. (1985) they warn that "the *a priori* thinking which rules out the venous equilibrium model on the grounds of physiological 'irrelevance' deserves careful reappraisal" [7]. In the final sentence, Jones et al. [7] quote Cobelli et al. "it would seem unjustified to contravene the 'principle of parsimony' by invoking a more complex model when the simpler model will do" [18].

The four studies above are the only published IPRL studies for high clearance drugs, and they are all consistent with the well-stirred model as acknowledged by the authors.

Isolated Perfused Rat Liver (IPRL) Studies of Non-Drug Substrates

Non-drug substances have also been studied in IPRL experiments. A frequently cited study is that of Keiding and Chiarantini [8] who examined galactose elimination in recirculating rat liver perfusions, versus the single pass perfusions utilized in the studies discussed above. Although this paper, which concludes that sinusoidal perfusion (the parallel tube model) is consistent with the experimental data, is frequently cited, it appears the field has accepted the conclusion without examination of the experimental data. Galactose had been previously demonstrated to be a high clearance substrate by Goresky et al. [19] where it is reported that "the extraction is almost complete, i.e., the hepatic venous blood is almost completely cleared of galactose" at the galactose concentrations tested by Keiding and Chiarantini [8]. However, the experimental results of the Keiding and Chiarantini [8] study are not consistent with galactose being a high clearance substance as would be expected for galactose. At flow rates of 10-11 ml/min, the

lowest C_{out}/C_{in} values of the 10 experiments reported are 0.32 and 0.34 (experiment 9), corresponding to *ER* values of 0.68 and 0.66. However, the average *ER* value for the 20 measurements in the 10 experiments was 0.46 ± 0.11 (SD). For the 6-7 ml/min infusions the lowest C_{out}/C_{in} is 0.12 (*ER* = 0.88) but values are as high as 0.45 (*ER* = 0.55), and in fact, only 3 of all 10 experiments support galactose being a high clearance drug (*ER* > 0.7) at the 6-7 ml/min infusion. The average *ER* of all 10 experiments was 0.68 ± 0.10 (SD).

Of further concern with the Keiding and Chiarantini [8] report is that when comparing clearance from the 10-11 ml/min to the 6-7 ml/min conditions, for four of the 10 experiments clearance is higher at the lower blood flow of 6-7 ml/min (experiments 1, 2, 3 and 5). No model of hepatic elimination is consistent with this outcome. Perhaps these unacceptable results are a function of suboptimal experimental conditions, as the authors mention that measured galactose concentrations were not corrected for perfusate volume changes due to evaporation, since they reason that the degree of evaporation in the recirculating system was approximately equal to the volume of galactose infusate (22 ml). Further, no studies were conducted to confirm that galactose elimination was in a linear range at the concentrations tested. Finally, based on the average rat liver weight of 6.87 g, a flow rate of 6 ml/min corresponds to an average flow rate of 0.87 ml/min/g, which is likely too low to fully perfuse the livers.

The second high-clearance compound investigated in IPRL studies is taurocholate. Smallwood et al. investigated taurocholate in the IPRL with changing fraction unbound in both recirculating and single-pass perfusion studies [9]. In both experimental designs, the experimental data were fit equally well by the well-stirred and the dispersion models, and in fact these two models could not be differentiated from one another (represented by the same line in

their Figure 2) due to a very high average fitted dispersion numbers of 5.0×10^7 (single-pass) and 13.3 (recirculating). The authors acknowledge that when the dispersion number is sufficiently large (approaches infinity) the dispersion model approaches the well-stirred model (infinite mixing) and that their observed dispersion numbers were "sufficiently large that the dispersion model has 'collapsed' into the venous equilibrium model extreme." Yet they conclude, "Moreover, perhaps it is time to relinquish the venous equilibration model, which, though operationally accurate, is conceptually flawed," which highlights the hesitation of the field to accept a model that best fits the data simply because of its limited physiological relevance.

A reviewer of our published manuscript on this topic has questioned the trustworthiness of the Smallwood et al. report [9], as the authors used total radioactivity as a measure of taurocholate (which forms a sulfate), and because experimental details related to the duration of these experiments were not clearly stated (although they can be deduced and appear to be a reasonable length of time). Additionally, rat liver weights are not reported, therefore it is not possible to assess the viability of the preparation for a continued high flow rate of 32 ml/min, which typically should not exceed 3 ml/min/g liver weight. However, reported rat liver weights from other IPRL studies cited here and in the literature range from 5.51 – 15.4 g for rats weighing 200 – 400 g. Therefore, a flow rate of 32 ml/min could be reasonably sustained for rat livers weighing approximately 10.5 g, which is quite likely in this study given that the rats weigh between 250 to 300 g. Smallwood and coworkers [10] repeated their single-pass IPRL studies with taurocholate one year later, and again found that in each of their six replicates the well-stirred model best describes taurocholate elimination, since "dispersion number was greater than 10^{15} in all experiments and was therefore taken as infinite."

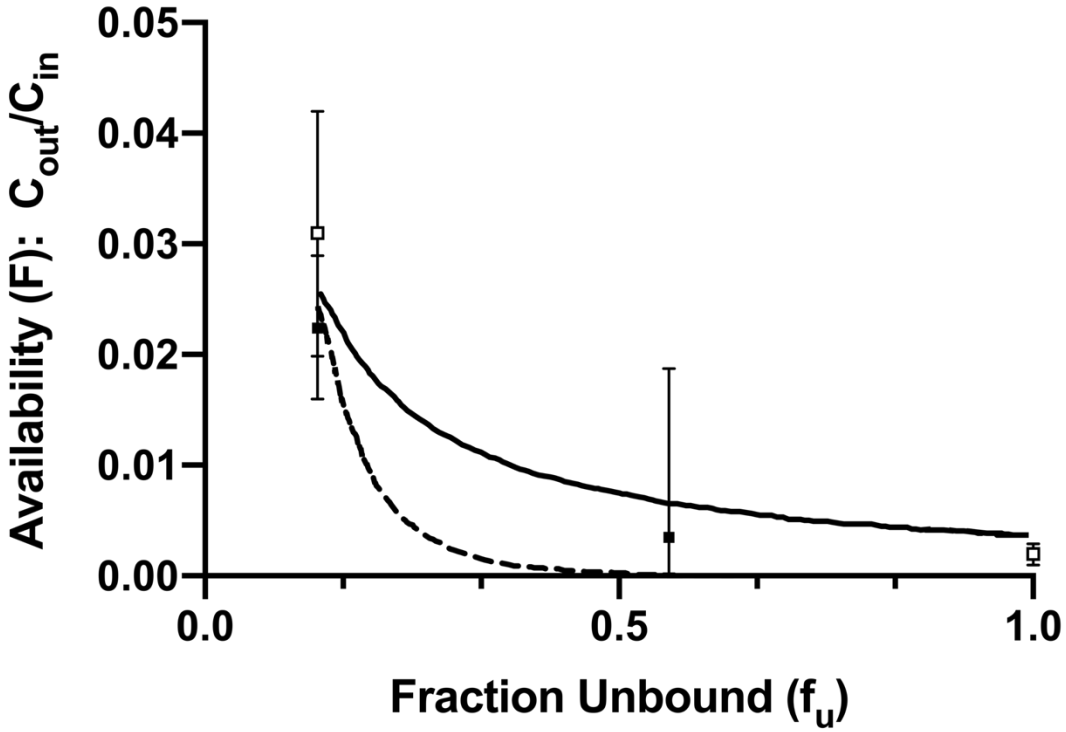

Figure 7.3: Hepatic availability (*F*) predictions of the well-stirred and dispersion models of taurocholate availability with changes in fraction unbound in the perfusate for two different experiments reported by Roberts et al. [11]. The well-stirred model is represented by the upper solid line and the dispersion model is represented by the lower dashed line. Observed hepatic availability values (mean ± SD) are depicted for experiments containing 5% albumin (f_u = 0.14), 0.5% albumin (f_u = 0.56), or 0% albumin (f_u = 1.0) and are experimentally calculated by C_{out}/C_{in}.

Roberts et al. also investigated taurocholate elimination in IPRL studies by varying both protein binding and flow [11]. **Figure 7.3** depicts experimental data from two different experiments from this publication in which protein binding is altered by experiments containing 0%, 0.5% or 5% albumin (at a flow rate of 10 ml/min) versus the hypothetical well-stirred and dispersion models. In this figure, two values are from the experiments designed to alter protein binding (0.5% versus 5% albumin) at a flow of 10 ml/min, and two values are from the 10 ml/min experiments designed to alter flow, which were run at both 0% and 5% albumin. From **Figure**

7.3, it is difficult to suggest a preference of one model versus another, especially given the large standard deviations for the potentially discriminating data points with the moderate protein binding value. The authors comment on the inadequacy of the fit to the well-stirred model but make no direct comparison with the dispersion model until the final sentence of the manuscript where they excuse its insufficiency by indicating that "alterations in albumin content results in availabilities that require an albumin-mediated transport system to be used in conjunction with the dispersion model."

Roberts et al. [11] further purport to show preference for the dispersion model over the well-stirred model when blood flow changes, although no model comparison figure is provided. The authors state, "The well-stirred model is unphysiological…if the well-stirred model were applied to the flow data in Table V, availabilities of 0.007 (observed 0.048 ± 0.061 SD) and 0.12 (observed 0.18 ± 0.08 SD) would be predicted from 0 and 5% albumin at 37 ml/min using 10 ml/min data. With the correction for volume changes, the predicted availabilities are 0.004 and 0.059. Thus, the well-stirred model does not account for the data obtained in this study." The standard deviations listed above were not in the original text but have been added by us. The authors again do not directly evaluate the fit of experimental data with variable flow to the dispersion model as they do for the well-stirred model.

Isolated Perfused Rat Liver (IPRL) Studies of Diazepam and Diclofenac

There are three experimental IPRL clearance studies with the low hepatic clearance drug diazepam and one with diclofenac from the last century, where the drug has been manipulated to be high clearance in the absence of plasma proteins [10, 12-14]. One study demonstrates

preference of diazepam for the parallel tube model [12] and the other three studies demonstrate preference of diazepam [10, 14] and diclofenac [13] for the axial dispersion model versus the well-stirred model. In the case of the Hussein et al. diclofenac study [13], the authors admit that "the improvement [of the dispersion model] over the well-stirred model was statistically significant in four of the eight preparations only," highlighting the variability associated with their results, as well as that the reported success of the dispersion model was due to the fact that it was approximating the well-stirred model in half of their replicates. A similar degree of variability in model preference was also observed in the Ching et al. [10] diazepam study, where for six replicates that support the dispersion model, three were fit with dispersion numbers of approximately zero (the parallel-tube model) and one was fit with a dispersion number of infinity (the well-stirred model).

Further, it should be highlighted that except for zero addition of protein to the perfusion solution, no other experimental results in these studies can adequately differentiate organ hepatic clearance models in all four of these publications. Additionally, the high degree of variability associated with the zero protein experiments for these highly protein bound drugs is noteworthy. Wang and Benet [15] very recently repeated these diazepam IRPL studies at zero protein concentration but also at very low albumin concentrations (0.025 and 0.05%) with the intent of including more than a single model-discriminating experimental data point as well as potential mitigation of the variability associated with zero protein addition conditions. Results confirmed that at zero albumin concentration, data were consistent with the parallel tube model as reported by Rowland et al. [12]. The results exhibited high variability, as also was seen in the

previous Rowland laboratory studies. However, at 0.025% and 0.05% albumin the results were preferentially consistent with the well-stirred model.

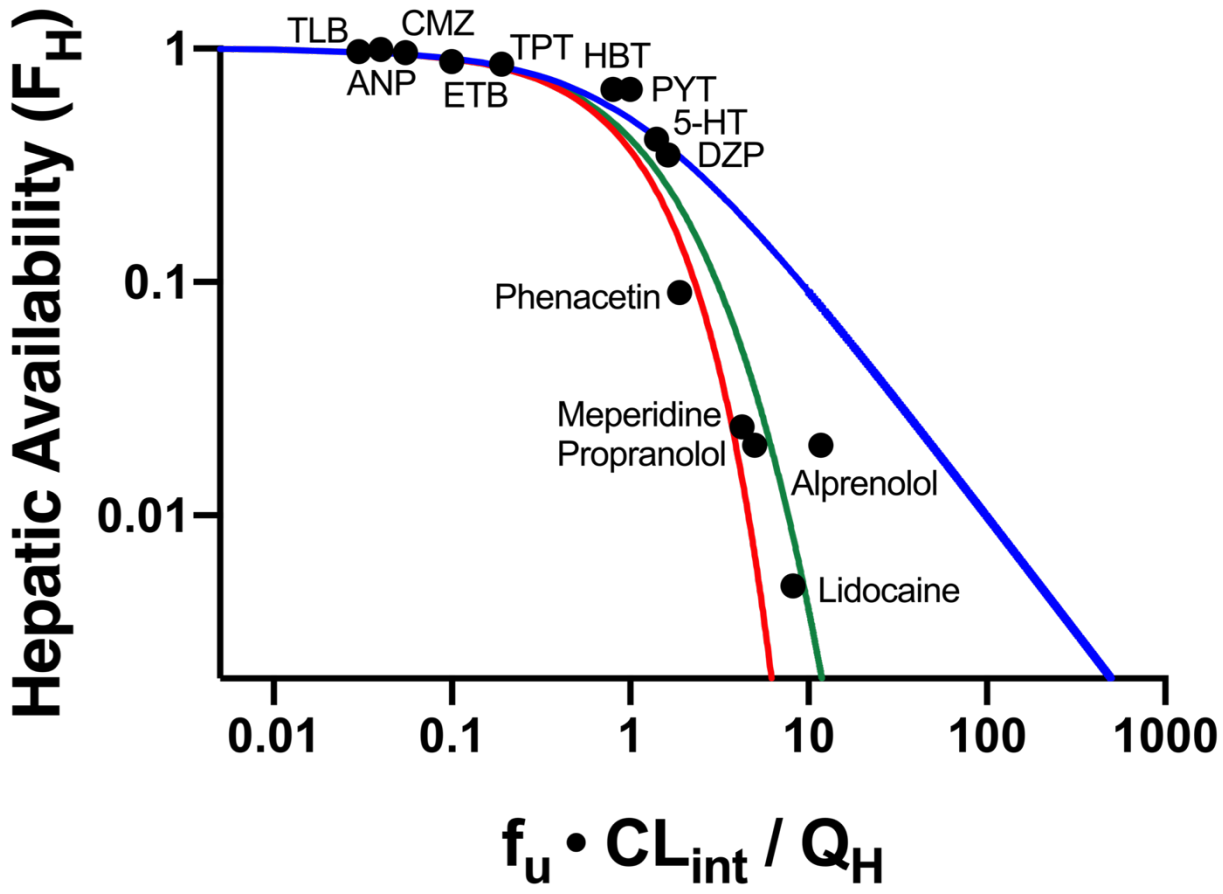

Figure 7.4: Plots of F_H vs $f_u \cdot CL_{int}/Q_H$ including the theoretical well-stirred, parallel tube and dispersion model relationships based on data from Roberts and Rowland [16] and Iwatsubo et al. [17]. Data points assuming no error in IVIVE prediction are depicted. The five high extraction ratio compounds included in this analysis (alprenolol, lidocaine, meperidine, phenacetin and propranolol) are labeled. Additional compounds (low and moderate extraction ratio) are labeled with the following abbreviations: 5-HT, 5-hydroxytryptamine; ANP, antipyrine; CMZ, carbamazepine; DZP, diazepam; ETB, ethoxybenzamide; HBT, hexobarbitone; PYT, phenytoin; TLB, tolbutamide; TPT, thiopental. Blue, green and red lines depict the well-stirred, dispersion and parallel tube model relationships, respectively.

In Vitro to In Vivo Extrapolation (IVIVE) Approaches

An alternate indirect methodologic approach to evaluate previously published IPRL data was proposed by Roberts and Rowland [16] to support the dispersion model. In that analysis, in vitro measures of CL_{int} have been used following IVIVE techniques to predict in vivo CL_{int} for drugs with published IPRL data. The predictions of in vivo CL_{int} were further utilized to calculate an efficiency number ($R_N = f_u \bullet CL_{int} / Q_H$) based on experimental conditions of Q_H and f_u from the IPRL studies and these values were plotted against experimentally observed hepatic availability (F) from the same IPRL studies. For ten drugs the predictive R_N values were determined and for high extraction ratio compounds (alprenolol, lidocaine, meperidine, phenacetin and propranolol) the results appear to be best described by the dispersion model (**Figure 7.4**). This analysis was further presented subsequently by Iwatsubo et al. [17] and included four additional drugs from the literature, which have also been incorporated in **Figure 7.4**.

The outcome for this indirect approach in support of the dispersion model is unexpected since for three of the five high clearance compounds included in this analysis, there are published IPRL experimental studies directly testing model preference, showing that the data only fit the well-stirred model: changing blood flow for lidocaine [4, 5] and meperidine [5]; changing protein binding for propranolol [6, 7]. How can this difference be explained? In contrast to Roberts and Rowland [16], Iwatsubo et al. [17] emphasize that the indirect IVIVE analysis is dependent on the assumption that in vitro determination of CL_{int} will accurately predict in vivo CL_{int} and CL_H. Iwatsubo et al. argued in 1996 that this was a valid assumption and that any difference between predicted and observed clearance was negligible. They provide the data available in 1996 to support this contention. But with time, it has been recognized by these authors that this

assumption is incorrect [20] and as Rowland and Pang [3] note "IVIVE tends to underpredict the estimated in vivo hepatic clearance (Halifax et al. [21]) for poorly understood reasons." Bowman and Benet [22] recently reported that of 19 drugs shown clinically in humans to be high *ER*, only 1 (5.5%) of 18 from human hepatocyte CL_{int} measurements and only 3 (15.8%) of 19 from human microsomal CL_{int} measurements were correctly predicted to be high *ER*. For studies of high in vivo *ER* drugs in rats, only 2 (22.2%) of 9 were predicted to be high *ER* by rat hepatocytes and only 2 (25%) of 8 were predicted to be high *ER* by rat microsomes, supporting observations by the field that the IVIVE underprediction is not a species-specific phenomenon.

For the high clearance compounds included in **Figure 7.4**, the supplemental table to Wood et al. [23] shows that the CL_{int} under-prediction for lidocaine in human hepatocytes is 11-fold and for microsomes 32-fold; the alprenolol under-prediction in human hepatocytes is 2.6-fold and for microsomes 3.4-fold; the propranolol under-prediction in human hepatocytes 6.7-fold and for microsomes 18-fold; the phenacetin under prediction in human hepatocytes is 28.6-fold and for microsomes 20.2-fold. Values for meperidine are not reported. To be fair, however, the previous analyses [16, 17] are for rats and no rat values are given in Wood et al. [23] for lidocaine, alprenolol, meperidine and phenacetin. For propranolol in rat hepatocytes, Wood et al. [23] report a 1.9-fold under-prediction, but for microsomes a 3.2-over-prediction. In **Figure 7.5** Panel E, we again present the original published relationship between *F* and the three models of hepatic organ elimination assuming that IVIVE predictions are valid [16, 17]. In **Figure 7.5** Panels A-D, we present the results that would be obtained accounting for the IVIVE under-predictions for all drugs, (including the values presented above for high clearance compounds) by utilizing published IVIVE discrepancy values from human hepatocytes (**Figure 7.5** Panel A), human

microsomes (**Figure 7.5** Panel B), rat hepatocytes (**Figure 7.5** Panel C) and rat microsomes (**Figure 7.5** Panel D) based on Wood et al. [23]. The IVIVE underprediction corrections result in a rightward shift in the data closer to the well-stirred model fit, and this trend is particularly striking for human microsomes (**Figure 7.5** Panel B). It is obvious today that in vitro CL_{int} markedly underpredicts in vivo CL_{int} and the Roberts and Rowland [16] and Iwatsubo et al. [17] analyses today might be very different then that published last century. Therefore, an IVIVE-based approach to model discrimination cannot reliably be trusted without consideration of the degree of underprediction expected for the drugs studied.

Vascular Dispersion and Axial Tissue Diffusion

Rivory et al. (1992) attempted to explain "the paradoxical ability of the venous-equilibration model to describe the steady-state kinetics of lipophilic drugs such as lidocaine, meperidine and propranolol" versus more physiological relevant models. The authors attempt to validate the complex but physiologically-relevant Tissue-Diffusion model in a 43-page paper with 35 equations, and propose that "vascular dispersion is of major importance to the availability of poorly diffusible compounds, whereas axial tissue diffusion becomes increasingly dominant for highly diffusive and partitioned substances." Reanalysis of a number of the above IPRL experiments [4-6] result in figures that essentially demonstrate that the Tissue-Diffusion model can also accommodate the data by approximating the well-stirred model fits.

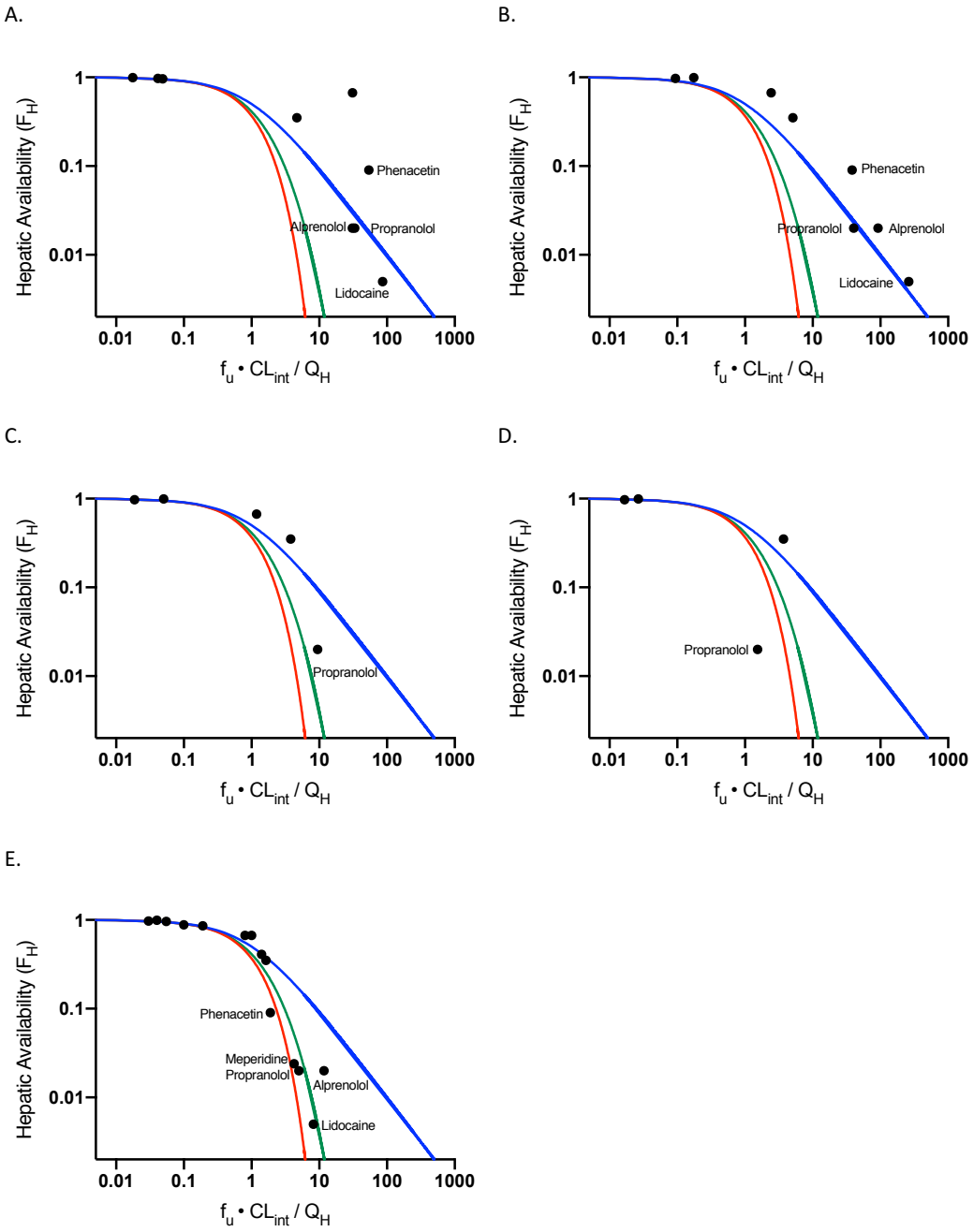

Figure 7.5: **Plots of F_H vs $f_u \cdot CL_{int}/Q_H$ based on data from Roberts and Rowland [16] and Iwatsubo et al. [17] that have been corrected for in vitro to in vivo underprediction error**. Original data is corrected for degree of observed in vitro to in vivo extrapolation (IVIVE) error in humans and rats as reported by Wood et al. [23] based on *in vitro* data from (A) human hepatocyte, (B) human microsomes, (C) rat hepatocytes, and (D) rat microsomes. Original data points assuming no error in IVIVE prediction are depicted in E. The five high extraction ratio compounds included in this analysis (alprenolol, lidocaine, meperidine, phenacetin and propranolol) are labeled in each figure. Blue, green and red lines depict the well-stirred, dispersion and parallel tube model relationships, respectively.

Discussion

Although alternate models to the well-stirred model for hepatic drug elimination have been examined since 1977, we find no comprehensive review of the concordance of these models with experimental IPRL results. The evaluation of high *ER* compounds in model-discrimination is critical, as each hepatic disposition model diverges from one another for high clearance compounds. Surprisingly, there are only four IPRL studies that have directly evaluated these models for high *ER* drugs [4-7]. In all four of these studies, data are preferentially consistent with the well-stirred model; a fact acknowledged by the authors in each publication.

High clearance non-drug substrates have also been evaluated in IPRL studies for galactose and taurocholate. The frequently cited Keiding and Chiarantini galactose IPRL study concluded that the parallel-tube model is preferentially consistent with the experimental data [8], however, critical examination of their experimental results calls their conclusion into question. Although galactose is known to be a high clearance compound [19, 25], galactose did not have a high *ER* in any experiment run at 10-11 ml/min (with an average *ER* of 0.46 ± 0.11). At the 6-7 ml/min infusions, galactose was only observed to be a high *ER* compound in 3 of 10 replicates. But of utmost concern, clearance was observed to increase as flow was decreased from 10-11 ml/ml to 6-7 ml/min in 4 of 10 experiments. This outcome violates hepatic physiology and no model of hepatic disposition is consistent with this outcome. The validity of the Keiding and Chiarantini publication [8] in support of the parallel tube model is highly questionable and these data should not be further cited in the literature as supporting an alternate model of hepatic elimination.

A second high clearance non-drug substance, taurocholate, was investigated by Smallwood et al. under conditions of altered protein binding [9]. In both single-pass and

recirculating perfusion studies, their dispersion model fits had collapsed into the well-stirred model with very high average fitted dispersion numbers (5.0 x 10^7 (single-pass) and 13.3 (recirculating)), as evidenced by both models being represented by the same line in their Figure 2. Although they acknowledge that when dispersion number approaches infinity, the dispersion model simply approximates the well-stirred model, they hesitate to accept the conclusion that the well-stirred model is adequate due to its limited physiological relevance. Ching et al. repeated the taurocholate single-pass IPRL studies, again finding that the well-stirred model best fits the observed data [10]. Taurocholate was also investigated by Roberts et al. in IPRL experiments that varied protein binding and flow [11]; resulting data are plagued with high variability precluding the ability to conclude model preference. Their experimental data from studies that altered protein binding are depicted in **Figure 7.3** and clearly no conclusion can be drawn given the huge variability associated with the model-discriminating protein binding measurements. No figure is presented for experiments that altered flow. Although authors consistently describe the inadequacy of the well-stirred model fits, no direct comparisons nor statistical analyses are provided regarding the dispersion model fits.

Four studies were identified where low *ER* drugs were manipulated to be high clearance in the absence of plasma proteins; one study indicates preference of diazepam for the parallel-tube model [12] and the other three indicate preference of diazepam [10, 14] and diclofenac [13] for the dispersion model. The conclusions of these studies hinged on the experimental measurements conducted without plasma proteins that were plagued with a high degree of variability, resulting in inconsistencies in model preference for each replicate. For instance, the diclofenac study [13] reported that the success of the dispersion model over the well-stirred

model was only statistically significant in four of eight experiments, highlighting that the purported success of the dispersion model was simply due to its approximation of the well-stirred model in half of their replicates. Significant variability in model preference was also observed in the Ching et al. [10] diazepam study; for six experiments reported to prefer the dispersion model, three were fit with dispersion numbers of zero (parallel-tube model) and one was fit with a dispersion number of infinity (the well-stirred model). In all these studies, the only model discriminating conditions are those with zero protein in the perfusion media and the high degree of variability associated with this condition is particularly noteworthy. For these reasons, we repeated these diazepam IPRL studies with additional low albumin concentrations (0.025 and 0.05%) to include more than a single model-discriminating experimental data point [15]. These results confirmed the high degree of variability associated with the experimental measurement with zero protein in the perfusate. However, for the two additional very low albumin concentrations, results were preferentially consistent with the well-stirred model. Recent studies in the Poulin, Sugiyama and Benet laboratories with hepatocytes report markedly improved IVIVE predictability in the presence of albumin than in its absence [26-28]. This could also explain the differences seen by Roberts et al. [11] with zero protein concentration for taurocholate. Therefore, although our diazepam IPRL results (in the absence of protein in the perfusion media) support the high variability and outcomes observed by Rowland and coworkers, such results cannot be reasonably interpreted as supporting preference for any model.

Previous indirect model-discrimination approaches presented by Roberts and Rowland [16] and Iwatsubo et al. [17] are reproduced in **Figure 7.4**, but are dependent on the assumption that IVIVE of hepatic clearance is accurate. Based on the contemporary understanding that in

vitro measures of drug metabolism inexplicably and significantly underpredict in vivo drug clearance [21], it is reasonable that the IVIVE-based predictions of in vivo CL_{int} used in determination of R_N (x-axis) are underpredictions. Accounting for average IVIVE underprediction error (as recently reported [23]) for the drugs included in this analysis clearly demonstrates the rightward shift of data points towards the well-stirred model relationship (**Figure 7.5**).

Conclusions

Thus, in response to the title of this chapter, we find no experimental data that reasonably or unambiguously supports preference for the dispersion or parallel-tube models versus the well-stirred model of organ elimination when only entering and exiting drug concentrations are available, except for the studies of highly bound diazepam and diclofenac only at zero protein concentration. However, there are data that unambiguously show that C_{out}/C_{in} measurements with changing blood flow and protein binding can only be fit by the well-stirred model. This outcome is unexpected if Eq. 1 is assumed to be model-independent, as it would be expected that data would sometimes support the well-stirred model (infinite mixing), sometimes the parallel-tube model (zero mixing) and sometimes neither of these models.

We propose a simple reason why success is not consistent for more "physiological" hepatic models (compared to the well-stirred model) based on our contention of the model-dependence of Eq. 1. That is, experimental data for steady-state IPRL studies for high clearance drugs are consistent with Eq. 1, the well-stirred model relationship. When alternate hepatic disposition models approximate the boundary condition of the well-stirred model, successful fitting of the data is observed. Other explanations previously proposed to support alternate

methodologies and models are flawed in assuming IVIVE is accurate and that perfusion studies in the absence of albumin yield exaggerated outcomes compared to even the smallest presence of protein. In our recent studies of diazepam, we confirmed the high variability associated with zero protein addition, however at two additional model-differentiating low albumin concentrations, the data were best described by the well-stirred model [15].

It is difficult to understand why the four IPRL studies that directly test model preference for highly cleared drugs that support the well-stirred model are undervalued by the field. Perhaps the investigators were influenced by the unphysiologic aspects of the well-stirred model, by assumptions made last century that are no longer valid today, and by lack of critical review of previously reported studies, resulting in inappropriate interpretation of the available experimental data. We emphasize the frequently cited quote of 1965 Nobel Prize physicist Richard Feynman "It doesn't matter how beautiful your theory is, it doesn't matter how smart you are. If it doesn't agree with experiment, it's wrong" [29]. We agree that the dispersion model is more physiologic than the well-stirred model and believe that it is more beautiful. We know that it is impossible for the well-stirred model to capture the complexities of liver physiology, including heterogeneity in enzymatic expression and dispersive flow throughout the liver. But, when experimental studies are limited to measurements for the entering and exiting drug concentrations of the elimination organ at steady state and Eq. 1, only the well-stirred model analysis is possible. The results summarized here do not indicate that the well-stirred model is an accurate representation of true hepatic elimination, it simply highlights that the well-stirred model is the best we can do when Eq. 1 is utilized to calculate clearance. With recent advancement of experimental and analytical techniques that can allow us to measure dynamic

intracellular hepatic concentrations, with respect to time as well as location within the organ, there is significant potential for our field to drastically improve the current oversimplified models of organ disposition.

References

1. Rowland M. Influence of route of administration on drug availability. *J Pharm Sci.* 1972;61(1):70-74.
2. Benet LZ, Liu S, Wolfe AR. The universally unrecognized assumption in predicting drug clearance and organ extraction ratio. *Clin Pharmacol Ther*. 2018;103(3):521-525.
3. Rowland M and Pang KS. Commentary on "The universally unrecognized assumption in predicting drug clearance and organ extraction ratio". *Clin Pharmacol Ther*. 2018;103(3):386-388.
4. Pang KS and Rowland M. Hepatic clearance of drugs. II. Experimental evidence for acceptance of the "well-stirred" model over the "parallel-tube" model using lidocaine in the perfused rat liver in situ preparation. *J Pharmacokinet Biopharm.* 1977;5(6):655-680.
5. Ahmad AB, Bennett PN and Rowland M. Models of hepatic drug clearance: discrimination between the 'well stirred' and 'parallel-tube' models. *J Pharm Pharmacol*. 1983:35(4)**:**219-224.
6. Jones DB, Morgan DJ, Mihaly GW, Webster LK and Smallwood RA. Discrimination between the venous equilibrium and sinusoidal models of hepatic drug elimination in the isolated perfused rat liver by perturbation of propranolol protein binding. *J Pharmacol Exp Ther*. 1984;229(2):522-526.

7. Jones DB, Ching MS, Smallwood RA, and Morgan DJ. A carrier-protein receptor is not a prerequisite for avid hepatic elimination of highly bound compounds: a study of propranolol elimination by the isolated perfused rat liver. *Hepatology*. 1985;5(4):590-593.
8. Keiding S and Chiarantini E. Effect of sinusoidal perfusion on galactose elimination kinetics in perfused rat liver. *J Pharmacol Exp Ther*. 1988;205(2):465-470.
9. Smallwood RH, Mogan DJ, Mihaly W, Jones DB and Smallwood RA. Effect of protein binding on elimination of taurocholate by isolated perfused rat liver: comparison of venous equilibrium, undistributed and distributed sinusoidal, and dispersion models. *J Pharmacokinet Biopharm*. 1988;16(4):377-396.
10. Ching MS, Morgan DJ and Smallwood RA. Models of hepatic elimination: implications from studies of the simultaneous elimination of taurocholate and diazepam by isolated rat liver under varying conditions of binding. *J Pharmacol Exp Ther*. 1989;250(3)**:**1048-1054.
11. Roberts MS, Fraser S, Wagner A and McLeod L. Residence time distributions of solute in the perfused rat liver using a dispersion model of hepatic elimination: 1. Effect of changes in perfusate flow and albumin concentration on sucrose and taurocholate. *J Pharmacokinet Biopharm*. 1990;18(3):209-234.
12. Rowland M, Leitch D, Fleming G and Smith B. Protein binding and hepatic clearance: discrimination between models of hepatic clearance with diazepam, a drug of high intrinsic clearance, in the isolated perfused rat liver preparation. *J Pharmacokinet Biopharm*. 1984;12(2):129-147.

13. Hussein Z, Evans AM and Rowland M. Pysiologic models of hepatic drug clearance: influence of altered protein binding on the elimination of diclofenac in the isolated perfused rat liver. *J Pharm Sci*. 1993;82(9):880-885.
14. Diaz-Garcia JM, Evans AM and Rowland M. Application of the axial dispersion model of hepatic drug elimination to the kinetics of diazepam in the isolated perfused rat liver. *J Pharmacokinet Biopharm*. 1992;20(2):171-193.
15. Wang H-J and Benet LZ. Protein binding and hepatic clearance: Re-examining the discrimination between models of hepatic clearance with diazepam in the isolated perfused rat liver preparation. *Drug Metab Dispos.* 2019;47(12):1397-1402.
16. Roberts MS and Rowland M. Correlation between in-vitro microsomal enzyme activity and whole organ hepatic elimination kinetics: analysis with a dispersion model. *J Pharmacol*. 1986;48(3)**:**177-181.
17. Iwatsubo T, Hirota N, Ooie T, Suzuki H and Sugiyama Y. Prediction of in vivo drug disposition from in vitro data based on physiological pharmacokinetics. *Biopharm Drug Dispos*. 1996;17(4):273-310.
18. Cobelli C, Carson ER, Finkelstein L and Leaning MS. Validation of simple and complex models in physiology and medicine. *Am J Physiol*. 1984;246:R259-R266.
19. Goresky CA, Bach GG and Nadeau BE. On the uptake of materials by the intact liver: the transport and net removal of galactose. *J Clin Invest*. 1973:52(5): 991-1009.
20. Chiba M, Ishii Y and Sugiyama Y. Prediction of hepatic clearance in human from in vitro data for successful drug development. *AAPS J.* 2009;11(2)**:**262-276.

21. Hallifax D, Foster JA and Houston JB. Prediction of human metabolic clearance from in vitro systems: retrospective analysis and prospective view. *Pharm Res*. 2010;27(10)**:**2150-2161.
22. Bowman CM and Benet LZ. In vitro-in vivo extrapolation and hepatic clearance-dependent underprediction. *J Pharm Sci*. 2019;108(7):2500-2504.
23. Wood FL, Houston JB and Hallifax D. Clearance prediction methodology needs fundamental improvement: trends common to rat and human hepatocytes/microsomes and implications for experimental methodology. *Drug Metab Dispos*. 2017;45(11):1178-1188.
24. Rivory LP, Roberts MS and Pond SM. Axial tissue diffusion can account for the disparity between current models of hepatic elimination for lipophilic drugs. *J Pharmacokinet Biopharm*. 1992;20(1)**:**19-61.
25. Henderson JM, Kutner MH and Bain RP. First-order clearance of plasma galactose: the effect of liver disease. Gastroenterology. 1982;83(5):1090-1096.
26. Bowman CM, Benet LZ. An examination of protein binding and protein-facilitated uptake relating to in vitro-in vivo extrapolation. *Eur J Pharm Sci*. 2018;123:502-514.
27. Kim SJ, Lee KR, Miyauchi S and Sugiyama Y. Extrapolation of in vivo hepatic clearance from in vitro uptake clearance by suspended human hepatocytes for anionic drugs with high binding to human albumin: Improvement of in vitro-to-in vivo extrapolation by considering the "albumin-mediated" hepatic uptake mechanism on the basis of the "facilitated-dissociation model". *Drug Metab Dispos*. 2019;47(2):94-103.

28. Poulin P and Haddad S. Extrapolation of the hepatic clearance of drugs in the absence of albumin in vitro to that in the presence of albumin in vivo: comparative assessment of 2 extrapolation models based on the albumin-mediated hepatic uptake theory and limitations and mechanistic insights. *J Pharm Sci*. 2018;107(7): 1791-1797.
29. Feynman RP. The Character of Physical Law, Chapter 7, p. 156, The M.I.T. Press, Cambridge, Massachusetts and London, England; 1965.

CHAPTER 8. CONCLUSIONS

The important influence of xenbiotic transporters in drug disposition is widely recognized, as transporters can be responsible for drug clearance (i.e renal or biliary elimination), drug distribution throughout the body by allowing or restricting drug access to various tissues, and following oral dosing can influence bioavailability by restricting or facilitating the intestinal absorption of xenobiotics. It is universally agreed that there are significant challenges associated with prediction of transporter-mediated drug disposition. Due to the lack of specific and clinically-validated tool compounds (index substrates, inhibitors, and inducers) for the major xenobiotic transporters, there are still significant challenges in not only properly interpreting *in vitro* transporter studies, but also in translating those results to the *in vivo* scenario. The same issues associated with non-specific inhibitors and substrates persists into the clinic, where often it is difficult to validate if a purported transporter-mediated interaction based on *in vitro* interaction potential is indeed clinically relevant. As the field continues to identify additional xenobiotic transporters of potential clinical relevance, the issue of non-specific tool compounds is further compounded.

It is of concern that it is common for clinical investigations to conclude that a particular transporter is clinically significant based only on an *in vitro* interaction potential in tandem with an observed change in drug exposure. Further, following oral dosing it is rare for investigators to characterize the bioavailability versus systemic clearance changes, as they both contribute to overall exposure change. These issues necessitate significant advancement of the clinical pharmacokinetic theory surrounding the validation of clinically significant involvement of

xenobiotic transporters. This led to the development of the methodologies discovered in this dissertation research, in order to provide a framework to recognize transporter involvement in clinical drug-drug interaction studies, strongly founded in basic pharmacokinetic theory.

In Chapter 2 we demonstrated that in strictly metabolic interactions for drugs dosed intravenously, volume of distribution does not change. This results in intuitive changes in mean residence time and half-life that are equal in direction but opposite in magnitude of clearance changes. The results of this analysis are in contrast to significant transporter interactions that have the potential to result in large changes in volume of distribution, which can also be associated with changes in clearance and half-life that are in the same direction (i.e. reduction in clearance associated with a shorter half-life). Thus, the recognition that volume of distribution has the potential to change in significant transporter interactions is further strengthened as a clinical tool since it was extensively validated that volume does not change for metabolic interactions. Further, comparing the direction of change in clearance versus half-life or mean residence time can further discern a metabolic interaction from one that may involve transporters.

In Chapter 3 we developed a methodology that can allow for differentiation of clearance changes from bioavailability changes in oral metabolic drug-drug interactions, two parameters that are considered indistinguishable from one another following oral dosing. Based on the findings of Chapter 2 that volume of distribution is unchanged in strictly metabolic interactions, it was recognized that following oral dosing changes in apparent volume of distribution at steady state will reflect changes in bioavailability alone. Thus, the estimated change in bioavailability can be utilized to predict changes in systemic clearance from measurements of apparent

clearance. This methodology can further be utilized to identify the major site of interaction (i.e. intestinal versus systemic). These findings provide powerful tools for clinical pharmacologists and drug investigators to make predictions on the contribution of oral bioavailability in drug interactions, as it has been believed by the field for decades that this could not accurately be determined without performing an IV interaction study to confirm the extent of clearance changes.

In Chapter 4 we developed another powerful methodology to identify intestinal transporter involvement in oral drug-drug interactions. This methodology is based on the recognition that clinically relevant intestinal transporter interactions will result in altered rate of absorption of victim drugs, thus examination of changes in mean absorption time should always be incorporated when implicating intestinally-expressed transporters in a drug-drug interaction. This methodology is particularly useful since for orally dosed drugs, the contribution of intestinal interactions to overall exposure changes can be significant and is often overlooked. Further, this simple but robust methodology will not only allow investigators to implicate transporters in complex drug-drug interactions, it will also allow clinical validation of additional transporter inhibitors due to the current lack of specific inhibitors, allow further investigation of the potential for transporter induction, characterize emerging intestinal transporters, and provide the field with the tools necessary to solve transporter-related debates, such as the localization and/or direction of OATP2B1 within the enterocyte.

In Chapter 5 we integrate all of the above-mentioned methodologies and concepts in investigation of the purported complex drug-drug interactions involving the victim drug apixaban. Throughout the literature and even in the apixaban FDA label, intestinally expressed

efflux transporters are implicated as a significant determinant of apixaban disposition. However, rational examination of all available apixaban clinical studies using the proposed framework does not support the clinical significance of efflux transporters in apixaban disposition. Not only were no changes in mean absorption time observed for perpetrator drugs with the significant potential to inhibit such transporters (Chapter 4), minimal change in volume of distribution was observed following intravenous dosing (Chapter 2), confirming that transporters are not clinically significant determinants of disposition intestinally nor systemically. Utilization of the clearance versus bioavailability differentiation methodology revealed that all clinically significant interactions could reasonably be explained by intestinal CYP3A4 interactions, and all clinically insignificant interactions could be explained by a lack of CYP3A4 inhibition potential by perpetrators. This chapter demonstrates in detail the practical application of all of the methodologies developed in this dissertation towards the identification of transporter drug-drug interactions, and highlights the powerful conclusions that can be made based on a firm understanding of simple pharmacokinetic theory.

In Chapter 6 we derive the liver-to-blood partition coefficient (Kp_{uu}) from first principles and discuss the theoretical and practical utility of Kp_{uu}-based predictions of drug-drug interactions. Although Kp_{uu} may be useful in improving predictions of pharmacodynamics, there is limited benefit of utilization of Kp_{uu} in improving drug-drug interaction predictions. Utilization of the extended clearance concept-based AUC_R equations is a more reasonable approach as changes in Kp_{uu} can potentially mislead an investigator to incorrectly conclude that the Kp_{uu} change has resulted in altered intrahepatic concentrations, an aspect crucial for tissue-specific efficacy or toxicity. Further, utilization of the AUC_R equations in DDI prediction can reasonably

predict the magnitude of DDIs and does not require any measurement of Kp_{uu} or $f_{u,H}$, potentially difficult tasks plagued with a high degree of variability between laboratories and between methodologies. Consideration that Kp_{uu} is based on a well-stirred model interpretation of hepatic elimination must be taken into account, as nuances of intracellular drug distribution are not considered by the Kp_{uu} model. Finally, a significant degree of variability in Kp_{uu} values has been suggested in the literature and therefore utilization of this difficult-to-measure theoretical value may result in a large prediction error depending on the particular methodology used.

Finally, Chapter 7 critically evaluates all published experimental IPRL data that were conducted to identify which hepatic disposition model can best describe liver metabolism. The premise of this study was based on the recent recognition by our laboratory that when clearance calculations are based on extraction ratio, the well-stirred model has inherently been assumed. Here we hypothesized that if this were true, all experimental data should prefer the well-stirred model, and if we were incorrect, then there should be experimental evidence in the literature that supports alternate models of hepatic disposition. Based on this analysis, we found no experimental data that reasonably or unambiguously supports preference for the dispersion or parallel-tube models versus the well-stirred model of organ elimination, rather, we found a number of studies that unambiguously support the well-stirred model and cannot be fit by the other models. Further, all four IPRL studies that directly test model preference for highly cleared drugs only support the well-stirred model, and this fact is acknowledged by the original authors. It is difficult to understand why these results are undervalued, but perhaps it is due to the simple and unphysiologic nature of the well-stirred model that results in the reluctance to admit it can most adequately describe clearance when extraction ratio is utilized in calculations.

This thesis significantly advances the clinical pharmacokinetic methodologies required to analyze complex drug-drug interaction studies. It further points out the importance of understanding the utility and limitations of experimental systems, as well as the inherent assumptions of the pharmacokinetic equations utilized to translate such results, in the successful translation of *in vitro* or *in situ* experimental information to a prediction of *in vivo* drug disposition. For instance, the simple recognition by our laboratory that extraction ratio is a well-stirred model derivative is challenged by highly respected leaders in our field, that have obviously invested decades believing its model independence. However, persistence in a preferred 'belief' is contrary to the spirit of science. Theories and models can be complex and beautiful or simple and succinct; however, it is the experimental data that determines their success. And, it is our responsibility as scientists to follow the data alone towards advancing the success of our field.

Publishing Agreement

It is the policy of the University to encourage open access and broad distribution of all theses, dissertations, and manuscripts. The Graduate Division will facilitate the distribution of UCSF theses, dissertations, and manuscripts to the UCSF Library for open access and distribution. UCSF will make such theses, dissertations, and manuscripts accessible to the public and will take reasonable steps to preserve these works in perpetuity.

I hereby grant the non-exclusive, perpetual right to The Regents of the University of California to reproduce, publicly display, distribute, preserve, and publish copies of my thesis, dissertation, or manuscript in any form or media, now existing or later derived, including access online for teaching, research, and public service purposes.

DocuSigned by:
Jasleen Sodhi
D3562F4EDFD04CA...
Author Signature

12/13/2020
Date